Published for SISSA by Springer

Received: *February 27, 2024*
Accepted: *May 5, 2024*
Published: *May 23, 2024*

# Search for new particles in final states with a boosted top quark and missing transverse momentum in proton-proton collisions at $\sqrt{s} = 13$ TeV with the ATLAS detector

## The ATLAS collaboration

*E-mail:* atlas.publications@cern.ch

Abstract: A search for events with one top quark and missing transverse momentum in the final state is presented. The fully hadronic decay of the top quark is explored by selecting events with a reconstructed boosted top-quark topology produced in association with large missing transverse momentum. The analysis uses 139 fb$^{-1}$ of proton-proton collision data at a centre-of-mass energy of $\sqrt{s} = 13$ TeV recorded during 2015-2018 by the ATLAS detector at the Large Hadron Collider. The results are interpreted in the context of simplified models for Dark Matter particle production and the single production of a vector-like $T$ quark. Without significant excess relative to the Standard Model expectations, 95% confidence-level upper limits on the corresponding cross-sections are obtained. The production of Dark Matter particles in association with a single top quark is excluded for masses of a scalar (vector) mediator up to 4.3 (2.3) TeV, assuming $m_\chi = 1$ GeV and the model couplings $\lambda_q = 0.6$ and $\lambda_\chi = 0.4$ ($a = 0.5$ and $g_\chi = 1$). The production of a single vector-like $T$ quark is excluded for masses below 1.8 TeV assuming a coupling to the top quark $\kappa_T = 0.5$ and a branching ratio for $T \to Zt$ of 25%.

Keywords: Hadron-Hadron Scattering

ArXiv ePrint: 2402.16561

Open Access, © The Authors.
Article funded by SCOAP$^3$.

https://doi.org/10.1007/JHEP05(2024)263

JHEP05(2024)263

## Contents


**1 Introduction** **1**

**2 Signal phenomenology** **3**
2.1 Dark Matter production in association with top quarks 4
2.2 Production of a single vector-like $T$ quark 4

**3 ATLAS detector** **5**

**4 Data and simulated samples** **6**

**5 Event reconstruction and object selection** **9**

**6 Event selection and background estimate** **10**
6.1 Signal region definition 11
6.2 Background estimate 14

**7 Systematic uncertainties** **14**

**8 Results** **17**

**9 Conclusions** **27**

**The ATLAS collaboration** **38**


## 1 Introduction

Despite its success in predicting the phenomenology of fundamental particle physics, the Standard Model (SM) is still far from being considered a complete description of nature at the smallest length scales due to experimental observations such as the evidence for Dark Matter (DM) [1–3] and theoretical arguments, one of these being the hierarchy problem in the Higgs sector [4]. The top quark, being the heaviest fundamental particle in the SM, plays an important role in the resolution of these questions in the context of many Beyond the Standard Model (BSM) extensions. This paper focuses on the *mono-top* experimental signature and presents a search for an excess of events relative to the SM prediction in which a single top quark is produced together with significant missing transverse momentum ($E_{\mathrm{T}}^{\mathrm{miss}}$). Data from proton-proton ($pp$) collisions at the Large Hadron Collider (LHC) corresponding to an integrated luminosity of 139 $\mathrm{fb}^{-1}$ at a centre-of-mass energy of $\sqrt{s} = 13$ TeV are used. The *mono-top* signature can arise from the production of DM in association with a top quark, where the DM candidate is identified as missing transverse momentum in the detector [5–8], or from the production of a single new vector-like $T$ quark [9–11], when $T$ decays into a top quark and a $Z$ boson, with the $Z$ boson decaying into neutrinos.



JHEP05(2024)263

Strong evidence of non-luminous gravitating matter, commonly known as DM, arises from measurements of astrophysical phenomena such as the cosmic microwave background and gravitational lensing. Through its gravitational interactions, it is suggested that DM constitutes up to five times the ordinary matter contained in the universe [12, 13]. Its nature remains however unknown and is one of the major questions in physics. Assuming that DM is a weakly interacting massive particle [14], these particles may be produced in $pp$ collisions at the LHC via new mediator particles that couple both to SM and DM particles. While such candidates are not expected to interact significantly with the detector, the momentum imbalance of SM particles produced in association with the unobserved DM particles could allow these processes to be detected.

The ATLAS and CMS Collaborations have carried out several searches for DM production in association with jets [15, 16], photons [17, 18], vector bosons [19–22], Higgs bosons [23, 24, 24, 25] and pairs of $b$-quarks [26, 27] and top quarks [28–33]. Searches for same-charge top-quark pairs also probe the production of DM mediator particles [34].

The *mono-top* signature targeted in this paper has already been explored by the CDF Collaboration in $p\bar{p}$ collisions at $\sqrt{s} = 1.96$ TeV [35] and more recently by both the ATLAS and CMS Collaborations in $pp$ collisions at $\sqrt{s} = 8$ TeV [36, 37] and $\sqrt{s} = 13$ TeV [38, 39]. BSM models that predict a *mono-top* signature are typically characterised by the violation of the baryon number or by the inclusion of flavour-changing neutral currents (FCNC) [6]. To consistently explore all the possible scenarios, an effective model is usually considered in which new mediators connect the SM particles and the DM candidates, encompassing all the tree-level production mechanisms of *mono-top* events [5, 6]. Two mechanisms are expected depending on the nature of the mediator particle. One case consists of the production of a new scalar mediator $\phi$ decaying into a top quark and a DM candidate $\chi$. The latest analyses exclude such production for masses of the mediator particle below 3.5 TeV. The second mechanism is characterised by the production of a vector mediator $V$ that couples with SM particles via an FCNC interaction and decays into DM particles $\chi$. Masses of the mediator $V$ below 2 TeV are excluded by the latest analyses targeting this model. This analysis focuses on the high mass region beyond the excluded phase space.

Vector-like quarks (VLQ) are colour-triplet spin-1/2 fermions in which the left- and right-handed components have the same properties under transformations of the $\mathrm{SU}(2)_L \times \mathrm{U}(1)_Y$ electroweak symmetry group. Such particles are predicted in many BSM extensions, such as Little Higgs [40, 41] and Composite Higgs [42, 43] models, to cancel out the quadratically divergent contributions to the Higgs boson mass caused by radiative corrections from the SM particles. They are expected to mix with SM quarks and modify their Yukawa couplings depending on the specific VLQ model [44, 45]. To preserve the gauge invariance, only a limited set of possible representations exist [45, 46]. In this document, only the production of a single $2/3e$-charged vector-like $T$ quark in the weak-isospin singlet is considered. Even though the coupling of $T$ with quarks from the first two generations is not excluded [47, 48], it is common to assume $T$ quarks couple only with the third-generation quarks [9].

Vector-like quarks can be produced singly via the electroweak interaction or in pairs via the strong interaction in $pp$ collisions. While the cross-section for pair production is given by quantum chromodynamics, the single-production cross-section explicitly depends



JHEP05(2024)263

on the coupling of the VLQs to SM vector bosons. There have been numerous searches for the pair production of VLQs [49–66] that have excluded $T$-quark masses below 1.37 TeV at 95% confidence level (CL) for a variety of decay modes. For $T$-quark masses above ∼1 TeV, VLQs would mainly be produced singly if the couplings to SM particles are sufficiently large. Searches for single production of $T$ quarks have placed limits on $T$-quark production cross-sections for $T$-quark masses between 1 and 2 TeV at 95% CL for various couplings [67–77]. For these higher masses, where single VLQ production is expected to dominate [78], the cross-section depends on the VLQ mass as well as the couplings to SM particles. In this study, the coupling of $T$ quarks with top quarks is described by the generalised coupling $\kappa_T$ [10, 11]. The $T$ quarks can decay both via charged and neutral currents into $Wb$, $Zt$, or $Ht$. A singlet $T$ with a branching ratio $\mathcal{B}(T \to Zt) = 25\%$ is assumed. The $T \to Zt \to \nu\bar{\nu}q\bar{q}'b$ final state is the one considered in this search.

This paper follows a methodology similar to that used in the previous search based on the 36 fb$^{-1}$ $\sqrt{s} = 13$ TeV data sample [39]. It considers the channel in which the top quark decays hadronically, found to be the most sensitive in the previous analysis. Signal regions are defined to maximise the discovery potential, introducing an extreme gradient-boosted (XGBoost) decision tree (BDT) [79] to enhance the signal discrimination against the SM background. The output score of the XGBoost algorithm is also used as the discriminating variable in the signal regions. Improvements in the reconstruction and calibration of the final-state particles are also incorporated, in particular, related to jets and their flavour identification. Regions enriched in the main sources of background events are identified and referred to as control regions. A simultaneous fit to the data yields in the control regions and to the XGBoost output discriminant distribution in the signal regions is performed to constrain the background prediction and determine the possible signal contribution. Systematic uncertainties are considered and incorporated as nuisance parameters in the fit. A set of validation regions is defined to assess the robustness of the extrapolation on the background prediction from the control regions to the signal regions.

This paper is organised as follows. The signal models are introduced in section 2. A brief description of the ATLAS detector is given in section 3. The data and the simulated samples used in the analysis are described in section 4. The algorithms used for the reconstruction and identification of the final-state particles are summarised in section 5. The selection criteria for the events considered in the analysis and the control, validation and signal region definitions are described in section 6. An introduction to the XGBoost classifier, used to separate the background from the signal and to define the signal regions, is also given in this section. The experimental and systematic uncertainties, summarised in section 7, are accounted for in the statistical interpretation of data. The results are presented in section 8. Conclusions are given in section 9.

## 2 Signal phenomenology

This section contains the description of the models considered in this paper. Details of the model predicting DM production in association with a single top quark are given in section 2.1. The production of a singlet vector-like $T$ quark model is presented in section 2.2.



JHEP05(2024)263

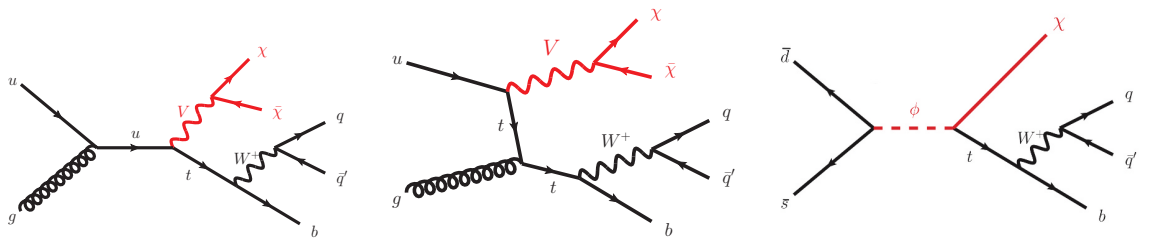


**Figure 1.** Representative Feynman diagrams for the DM production in association with a single top-quark decaying hadronically in the (a,b) vector mediator (non-resonant) and (c) scalar mediator (resonant) cases.

### 2.1 Dark Matter production in association with top quarks

The DM production in association with top quarks is considered for a scalar or a vector DM mediator particle [5, 6, 80, 81].

The vector-mediated production, also referred to in the literature as non-resonant, consists of an FCNC interaction producing a top quark and a new vector particle $V$ decaying into a pair of invisible DM particles, as shown in the diagrams in figures 1(a) and 1(b). This process is described by the following Lagrangian [5, 6, 80, 81]:

$$\mathcal{L} = aV_\mu \bar{u}\gamma^\mu P_\mathrm{R} t + g_\chi V_\mu \bar{\chi}\gamma^\mu \chi + \text{h.c.}, \tag{2.1}$$

where the massive vector boson $V$ is coupled to the DM particles $\chi$. The strength of this coupling is controlled by the parameter $g_\chi$, while the $P_\mathrm{R}$ operator is the right-handed chirality projector. The parameter $a$ stands for the coupling constant of the vector boson $V$ to the top-quark $t$ and up-type quarks $u$, and $\gamma^\mu$ are the Dirac matrices.

The scalar-mediated case, also referred to as resonant, corresponds to the production of a coloured $2/3e$-charged scalar $\phi$ that decays into a top quark and a spin-1/2 DM particle $\chi$ [80]. A representative Feynman diagram of this process is shown in figure 1(c). The Lagrangian that describes this process is the following [5, 6, 80, 81]:

$$\mathcal{L} = \lambda_q \phi \bar{d^c} P_R s + y_\chi \phi \bar{t} P_R \chi + \text{ h.c.}, \tag{2.2}$$

where $\lambda_q$ is the coupling strength of the $\phi$ scalar with $d$- and $s$-quarks, $y_\chi$ is the coupling strength of the scalar $\phi$ with the DM particle $\chi$ and the top quark, and the superscript $c$ stands for the charge conjugate.

### 2.2 Production of a single vector-like $T$ quark

The production of a single vector-like $T$ quark can occur via $WTb$ and $ZTt$ vertices. However, the contribution via $ZTt$ vertex is highly suppressed by the requirement of a top quark in the initial state. Therefore, this paper considers only $WTb$ production of the vector-like $T$ quark. The dominant process in the $WTb$ associated mode is the resonant production. The non-resonant production is also considered. Vector-like $T$ quarks decay into $Wb$, $tZ$ and $tH$ with a branching ratio that depends on the considered model [9, 10, 82]. The respective diagrams are shown in figure 2.



JHEP05(2024)263

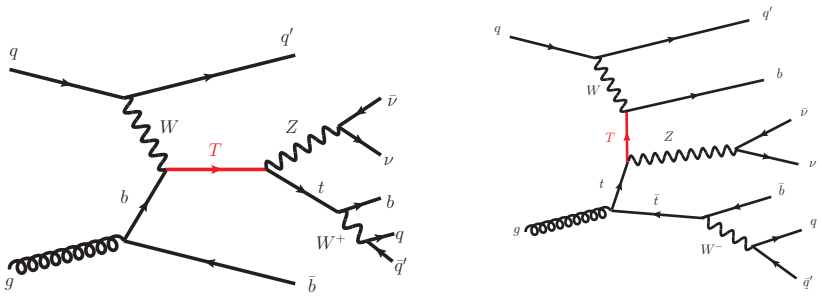


**Figure 2.** Representative Feynman diagrams for the (a) resonant and (b) non-resonant production of a single vector-like $T$ quark.

The mass of the $T$ quark, $m_T$, and the overall coupling factor, $\kappa_T$, to the SM $W$ boson, $Z$ boson, and Higgs boson are unknown parameters [10, 11]. The overall coupling factor controls both the production cross-section and the resonance width of the $T$ quark, $\Gamma_T$. For a vector-like $T$ quark with mass $m_T$, the relative width ($\Gamma_T/m_T$) of the VLQ resonance scales quadratically with both $\kappa_T$ and $m_T$ [11]. There are also three additional parameters, $\xi_W$, $\xi_Z$ and $\xi_H$, which determine the $T$-quark branching ratios to each of the SM bosons — $\mathcal{B}(T \to Wb)$, $\mathcal{B}(T \to tZ)$ and $\mathcal{B}(T \to tH)$, respectively. The relation $\xi_W + \xi_Z + \xi_H = 1$ is assumed, with $\xi_Z = \xi_H$. Consequently, any value of $\xi_W$ fully determines the value of $\xi_Z$ and the branching ratio of the $T \to tZ$ decay, targeted by the analysis. Since the $\xi_W < 0.5$ region is dominated by the suppressed $ZTt$ production vertex, only the $\xi_W > 0.5$ space is explored.

In case of a $T \to tZ$ decay, with a subsequent decay of the $Z$ boson into a pair of neutrinos, the event would have the *mono-top* signature. Differently from the production of the top quark in association with DM particles, the single vector-like $T$ quark production expects additional quarks in the final state, featuring at least one jet emitted at a small angle to the beam line.

## 3 ATLAS detector

The ATLAS detector [83] at the LHC covers nearly the entire solid angle around the collision point.[1] It consists of an inner tracking detector surrounded by a thin superconducting solenoid, electromagnetic and hadronic calorimeters, and a muon spectrometer incorporating three large superconducting air-core toroidal magnets.

The inner-detector system (ID) is immersed in a 2 T axial magnetic field and provides charged-particle tracking in the range $|\eta| < 2.5$. The high-granularity silicon pixel detector covers the vertex region and typically provides four measurements per track, the first hit generally being in the insertable B-layer (IBL) installed before Run 2 [84, 85]. It is followed

[1] ATLAS uses a right-handed coordinate system with its origin at the nominal interaction point (IP) in the centre of the detector and the $z$-axis along the beam pipe. The $x$-axis points from the IP to the centre of the LHC ring, and the $y$-axis points upwards. Cylindrical coordinates $(r, \phi)$ are used in the transverse plane, $\phi$ being the azimuthal angle around the $z$-axis. The pseudorapidity is defined in terms of the polar angle $\theta$ as $\eta = -\ln\tan(\theta/2)$. Rapidity is defined as $y = 0.5 \ln[(E + p_z)/E - p_z)]$, where $E$ denotes the energy and $p_z$ is the component of the momentum along the beam direction. Angular distance is measured in units of $\Delta R \equiv \sqrt{(\Delta\eta)^2 + (\Delta\phi)^2}$.



JHEP05(2024)263

by the SemiConductor Tracker (SCT), which usually provides eight measurements per track. These silicon detectors are complemented by the transition radiation tracker (TRT), which enables radially extended track reconstruction up to $|\eta| = 2.0$. The TRT also provides electron identification information based on the fraction of hits (typically 30 in total) above a higher energy-deposit threshold corresponding to transition radiation.

The calorimeter system covers the pseudorapidity range $|\eta| < 4.9$. Within the region $|\eta| < 3.2$, electromagnetic calorimetry is provided by barrel and endcap high-granularity lead/liquid-argon (LAr) calorimeters, with an additional thin LAr presampler covering $|\eta| < 1.8$ to correct for energy loss in material upstream of the calorimeters. Hadronic calorimetry is provided by the steel/scintillator-tile calorimeter, segmented into three barrel structures within $|\eta| < 1.7$, and two copper/LAr hadronic endcap calorimeters. The solid angle coverage is completed with forward copper/LAr and tungsten/LAr calorimeter modules optimised for electromagnetic and hadronic energy measurements respectively.

The muon spectrometer (MS) comprises separate trigger and high-precision tracking chambers measuring the deflection of muons in a magnetic field generated by the superconducting air-core toroidal magnets. The field integral of the toroids ranges between 2.0 and 6.0 T m across most of the detector. Three layers of precision chambers, each consisting of layers of monitored drift tubes, cover the region $|\eta| < 2.7$, complemented by cathode-strip chambers in the forward region, where the background is highest. The muon trigger system covers the range $|\eta| < 2.4$ with resistive-plate chambers in the barrel, and thin-gap chambers in the endcap regions.

The luminosity is measured mainly by the LUCID-2 [86] detector that records Cherenkov light produced in the quartz windows of photomultipliers located close to the beampipe.

Events are selected by the first-level trigger system implemented in custom hardware, followed by selections made by algorithms implemented in software in the high-level trigger [87]. The first-level trigger accepts events from the 40 MHz bunch crossings at a rate below 100 kHz, which the high-level trigger further reduces in order to record complete events to disk at about 1 kHz.

A software suite [88] is used in data simulation, in the reconstruction and analysis of real and simulated data, in detector operations, and in the trigger and data acquisition systems of the experiment.

## 4 Data and simulated samples

This analysis uses data from $pp$ collisions at a centre-of-mass energy of $\sqrt{s} = 13$ TeV collected by the ATLAS detector during the LHC Run 2 from 2015 to 2018. In this data taking period, the LHC operated with 25 ns proton bunch spacing with an average number of collisions per bunch crossing $\langle\mu\rangle$ of 34. Only data-taking periods in which all the necessary components for the analysis were functional are included, corresponding to an integrated luminosity of $139\,\text{fb}^{-1}$.

Events are required to pass at least one of the triggers that select events with high missing transverse momentum, with thresholds between 90 and 120 GeV depending on the data taking year [89]. All the triggers are fully efficient for events with offline $E_{\text{T}}^{\text{miss}} > 250$ GeV, as selected for analysis.



JHEP05(2024)263

Samples of simulated signal and background processes are produced using different Monte Carlo (MC) event generators including parton shower and hadronisation models.

Signal events for both the scalar and vector mediator DM scenarios are generated with the simplified model described in section 2, using MadGraph5_aMC@NLO v2.8.1 and v2.9.5 [90] with FeynRules 2.0 [91]. The generation is done at leading-order (LO) accuracy in QCD using the NNPDF3.0LO parton distribution function (PDF) set [92]. The generator is interfaced with Pythia8.245 [93] using the A14 set of tuned parameters (*tune*) [94] and the NNPDF2.3LO PDF set [95].

A total number of 40 (19) samples are simulated to cover the four dimensions in the parameter space — two couplings plus two masses — of the scalar (vector) mediator DM production. The larger number of simulations of the scalar mediator DM production is due to the non-negligible dependence of the event kinematics on $m_\phi$ and $\lambda_q$ that required the production of more samples to properly control and validate the signal predictions. The scalar DM samples were simulated in a grid of the parameter space encompassed by the following ranges: $m_\phi \in [2500, 6000]$ GeV, $m_\chi \in [500, 5500]$ GeV, $\lambda_q \in [0.2, 1]$ and $y_\chi \in [0.2, 0.6]$. For the vector-mediated signals, samples were simulated with the following parameter range: $m_V \in [1250, 3500]$ GeV, $m_\chi \in [400, 1200]$ GeV, $a \in [0.1, 0.5]$ and $g_\chi \in [0.2, 1]$. The parameters of the DM mediators and the VLQ signals are chosen to scan masses higher than the previous excluded limits [39].

The signal predictions in points of the parameter space that are not simulated are obtained through a reweighting procedure that exploits the mild dependence of the event kinematics on the other parameters. The reweighting procedure consists of assigning weights to the available simulated samples (called *reference*) to reproduce the expected kinematics and yields in a different (but close) point of the model parameter space, the *target*. This method makes use of an extensive set of samples simulated at particle-level that cover the four model parameteres for both the scalar and vector mediator DM production with a higher granularity than the set of reconstruction-level samples. The mentioned weights $\boldsymbol{w}_{\text{rw}}$, evaluated entirely with particle-level simulations, reproduce the *target* kinematics from the *reference* sample. They take into account the differences in acceptance, cross-sections at LO and kinematic shapes between the *reference* and *target* samples, as summarised in the equation:

$$w^i_{\text{rw}} = \overbrace{\frac{\epsilon_{\text{target}}}{\epsilon_{\text{reference}}}}^{\text{Acceptance}} \times \overbrace{\frac{\sigma_{\text{target}}}{\sigma_{\text{reference}}}}^{\text{Cross-section}} \times \overbrace{\frac{y^i_{\text{target}}}{y^i_{\text{reference}}}}^{\text{Shapes}} . \tag{4.1}$$

The acceptance term is determined by applying the event preselection, defined in section 6, on particle-level simulation.[2] It is measured as the ratio of the preselection efficiencies for the *target* sample ($\epsilon_{\text{target}}$) and the *reference* sample ($\epsilon_{\text{reference}}$). The change in the cross-section between the *target* ($\sigma_{\text{target}}$) and the *reference* ($\sigma_{\text{reference}}$) is accounted for by the ratio of the two values. The change in event kinematics is estimated with the ratio of the yields of the normalised binned $E_{\text{T}}^{\text{miss}}$ distribution for the *reference* ($y^i_{\text{reference}}$) and *target* ($y^i_{\text{target}}$) samples,

[2]Particle-level objects in Monte Carlo simulation are reconstructed from stable particles (with proper lifetimes $c\tau \geq 10$ mm). Particle-level jets are clustered from visible stable final-state particles, excluding prompt leptons, using the anti-$k_t$ clustering. Particle-level top jets are reconstructed using the anti-$k_t$ algorithm with radius parameter $R = 1.0$ and are required to be close to a top-quark ($\Delta R < 1$).



JHEP05(2024)263

where $i$ is the bin corresponding to the truth $E_{\mathrm{T}}^{\mathrm{miss}}$ (see section 5) of the *reference* and *target* events. The reweighting based on the $E_{\mathrm{T}}^{\mathrm{miss}}$ observable has shown to be enough to accurately reproduce the distributions of the other kinematic variables relevant to the analysis.

The single production of a singlet vector-like $T$ quark is simulated at LO in QCD using the corresponding model [11] implemented in FeynRules 2.0 with MadGraph5_aMC@NLO v.2.8.1 using the NNPDF3.0LO PDF set. The simulation comprises all the tree-level processes, including the non-resonant production. The generator is interfaced with Pythia 8.244 using the NNPDF2.3LO PDF set with the A14 tune. The samples are generated for masses of the vector-like $T$ quark ranging from 1.1 to 2.7 TeV in steps of 0.2 TeV, assuming $\kappa_T = 0.5$. Internal weights provided by MadGraph5_aMC@NLO are used to obtain predictions at masses 100 GeV smaller than the generated ones and at different values of the coupling, ranging from 0.1 to 1.6 in steps of 0.05 for $\kappa_T < 0.5$ and 0.1 for larger $\kappa_T$. The mass of the vector-like quark, $m_T$, strongly affects the boost of the top quark, while small, but non-negligible, changes of the event kinematics are observed for different values of the $\kappa_T$ coupling. Signal samples are normalised to next-to-leading-order (NLO) cross-sections in QCD that assume the narrow-width approximation for the $T$-quark decay [96]. Finite-width effects on the cross-sections are accounted for by applying a correction factor [97], ranging from a few per cent up to approximately 30% at large values of the width.

The production of a top-antitop-quark pair ($t\bar{t}$) is simulated at NLO using Powheg Box v2 [98–100], with the NNPDF3.0NNLO PDF set, interfaced with Pythia 8.210 using NNPDF2.3LO PDF set and the A14 set of tuned parameters. The events are normalised to the next-to-next-to-leading-order (NNLO) QCD cross-section, including resummation of soft gluon emissions at next-to-next-to-leading logarithmic (NNLL) accuracy calculated using the Top++2.0 [101] software.

The production of a vector boson ($V = W, Z$) in association with jets ($V$+jets) is simulated with the Sherpa v2.2.1 [102] generator in which the matrix element is accurate at NLO up to two emitted partons while at LO up to four additional partons. These calculations are performed with the Comix [103] and OpenLoops [104] libraries. The matching of the parton-shower and hadronisation algorithm with the matrix-element generator [105] is employed for different jet multiplicities, which are then merged into an inclusive sample using an improved CKKW matching procedure [106, 107] that is extended to NLO accuracy using the MEPS@NLO prescription [108] via a set of parameters provided by the authors. The NNPDF3.0NNLO PDF set is used [92]. Both processes are normalised to the NNLO cross-section [109].

Single-top $tW$ production is simulated using the Powheg Box v2 generator at NLO in QCD using the five-flavour scheme and the NNPDF3.0NNLO PDF set. The diagram removal scheme [110] is used to remove the overlap with $t\bar{t}$ production. Single-top $t$-channel production is modelled with Powheg Box v2 generator at NLO in QCD using the four-flavour scheme. The NNPDF3.0NLOnf4 PDF set is used. Single-top $s$-channel production is simulated using the Powheg Box v2 generator at NLO in QCD using the five-flavour scheme. The NNPDF3.0NNLO PDF set is used. In all the single-top-quark processes, the generator is interfaced with Pythia 8.230 using the A14 tune and the NNPDF2.3LO PDF set. Simulated samples are normalised to the NLO cross-section in QCD including the resummation of soft-gluon emission corrections [111–116].



JHEP05(2024)263

The production of $t\bar{t}$ in association with a $W$ or $Z$ boson is simulated with MadGraph5_aMC@NLO v2.3.3 [117] at NLO QCD accuracy using the NNPDF3.0NNLO PDF set. The generator is interfaced with Pythia 8.230 using the A14 tune and the NNPDF2.3LO PDF set. The samples are normalised to NLO QCD and electroweak (EW) cross-sections. The $t\bar{t}Z$ cross-section is additionally corrected by $Z$ boson off-shell contributions.

Events from $t\bar{t}H$ production are simulated at NLO QCD accuracy with Powheg Box v2 generator with the NNPDF3.0NNLO PDF set. The generator is interfaced with Pythia 8.230 using the A14 tune and the NNPDF2.3LO PDF set. The cross-section is calculated at NLO QCD and NLO EW accuracy.

Diboson events are simulated with the Sherpa v2.2.1 generator, using the same prescription as in the production of single bosons in association with jets.

The production of $tZq$ is simulated with MadGraph5_aMC@NLO v2.3.3 at NLO QCD accuracy using the NNPDF3.0NNLO PDF set. The production of $tWZ$ with $Z \to \nu\bar{\nu}$ is simulated at NLO QCD accuracy with MadGraph5_aMC@NLO v2.6.7 using the NNPDF2.3LO PDF.

The simulation of bottom and charm hadron decays is done using EvtGen [118] in all signal samples and all background samples with the exception $V$+jets and dibosons (generated with Sherpa v2.2.1). The generation also includes the effect of multiple $pp$ interactions per bunch crossing (pile-up), and the effect on the detector response due to interactions from bunch crossings before or after the one containing the hard interaction [119]. All the simulated samples are processed with a detailed simulation of the ATLAS detector [120] using Geant4 [121].

## 5 Event reconstruction and object selection

All events are required to contain a primary vertex with at least two associated tracks with transverse momentum $p_{\mathrm{T}} > 0.5$ GeV. The vertex with the highest $\sum p_{\mathrm{T}}^2$ of the associated tracks is taken as the hard-scatter primary vertex.

Electron candidates are identified from high-quality inner-detector tracks matched to calorimeter energy deposits consistent with an electromagnetic shower. The energy deposits have to form a cluster with transverse energy $E_{\mathrm{T}} > 25$ GeV and $|\eta| < 2.47$, and be outside the transition region $1.37 \leq |\eta| \leq 1.52$ between the barrel and endcap calorimeters. A tight likelihood-based requirement is used to reject fake-electron candidates [122]. Electrons are not required to be isolated to maximise the rejection of background events when applying the lepton veto preselection described in the next section.

Muon candidates are reconstructed using high-quality inner-detector tracks combined with tracks reconstructed in the muon spectrometer. Only muon candidates satisfying 'medium' identification criteria [123], with $p_{\mathrm{T}} > 25$ GeV and $|\eta| < 2.5$, are considered. No isolation criteria are applied to improve the background rejection with the lepton veto (see section 6).

Jet candidates are reconstructed using the anti-$k_t$ [124] jet algorithm with radius parameter $R = 0.4$ (1.0) for small-$R$ (large-$R$) jets, as implemented in the FastJet [125] package. The large-$R$ jets are formed from topological clusters in the calorimeter calibrated using the local calibration method described in ref. [126], while the small-$R$ jets are reconstructed



JHEP05(2024)263

from particle-flow objects [127]. Both are calibrated by applying a jet energy scale derived from 13 TeV data and simulation [128, 129].

After calibration, small-$R$ jets are considered if they fulfil $p_T > 25$ GeV and $|\eta| < 4.5$. Jets in the region $2.5 < |\eta| < 4.5$ are considered forward jets. To suppress jets originating from pile-up collisions, a requirement on the jet-vertex tagger (JVT) [130] discriminant is applied for jets with $p_{\mathrm{T}}$ below 60 GeV and $|\eta| < 2.4$. Jets that are close to an electron with a distance $\Delta R_{y,\phi} \equiv \sqrt{(\Delta y)^2 + (\Delta\phi)^2} < 0.2$ are removed to avoid double counting the energy of the electron. Jets with less than three tracks are removed if their distance to a muon is $\Delta R_{y,\phi} < 0.2$ or one of their tracks is part of the muon. Electrons or muons with a distance $\Delta R_{y,\phi} < 0.4$ from any of the remaining jets are removed.

Small-$R$ jets that contain $b$-hadrons ($b$-jets) are identified by the use of the DL1r multivariate algorithm [131]. These jets are hereafter referred to as $b$-tagged jets. The selected working point results in an efficiency of 77% per $b$-jet and rejection factors of 6 and 200 for $c$- and light-flavour jets, respectively, as measured in simulated $t\bar{t}$ events.

A trimming algorithm [132] with parameters $R_{\mathrm{sub}} = 0.2$ and $f_{\mathrm{cut}} = 0.05$ is applied to the large-$R$ jets to mitigate the impact of gluon radiation and pileup effects. Trimmed large-$R$ jets are considered if they fulfil $p_T > 250$ GeV and $|\eta| < 2.0$. To identify a large-$R$ jet originated from hadronically decaying top quarks produced with a large Lorentz boost ($t$op-tagged), the *contained* (similar to *medium*) top-quark tagging algorithm is used [133, 134]. The top-quark tagging relies on a deep neural network (DNN) that uses jet kinematics and substructure variables (e.g., energy flow) as inputs [133, 134]. The $p_{\mathrm{T}}$-dependent requirements on the DNN score provide 50% top-quark-tagging efficiency, as measured in inclusive $t\bar{t}$ events where the top-quark decay products are considered to be contained within the large-$R$ jet, and a corresponding background rejection up to 70 (95) for multijet ($\gamma$+jets) events depending on the jet $p_{\mathrm{T}}$ [133, 134].

The missing transverse momentum vector $p_{\mathrm{T}}^{\mathrm{miss}}$ is reconstructed from the negative vector sum of momenta of calibrated leptons, small-$R$ jets and a soft term built from all tracks that are associated with the primary vertex but not with these objects [135]. Its magnitude is denoted by $E_{\mathrm{T}}^{\mathrm{miss}}$. The truth $E_{\mathrm{T}}^{\mathrm{miss}}$ used in the reweighting procedure described in section 4 is calculated from the truth $p_{\mathrm{T}}$ of invisible particles.

## 6 Event selection and background estimate

The experimental signature expected in the considered DM and vector-like $T$-quark models is the presence of a top quark and significant missing transverse momentum. As the top quark is expected to be produced with a large Lorentz boost, its hadronic decay products can be collimated and reconstructed into a large-$R$ jet. Preselected events are required to contain zero leptons and at least one large-$R$ jet. The leading large-$R$ jet ($J$) is then required to be top-tagged and have a $p_{\mathrm{T}}$ between 350 GeV and 2500 GeV, and a mass between 40 GeV and 600 GeV, corresponding to the region where the top-tagging algorithm is calibrated. To reduce the number of multijet background events to a negligible level, the $E_{\mathrm{T}}^{\mathrm{miss}}$ is required to be larger than 250 GeV. Quality criteria are imposed to reject events that contain any jets arising from non-collision sources or detector noise [136]. To remove the contribution



JHEP05(2024)263

| | $N_{b\text{-tagged jets}}$ | $\Delta\phi_{\min}(j, E_{\mathrm{T}}^{\mathrm{miss}})$ | XGBoost score | $N_{\text{forward jets}}$ |
|---|---|---|---|---|
| TCR | $\geq 2$ | $\in [0.2, 1]$ | — | — |
| TVR1bLPhi | 1 | $\in [0.2, 1]$ | — | — |
| TVR1bHPhi (1f) | 1 | $\geq 1$ | $< 0.5$ | — ($\geq 1$) |
| TVR2bHPhi | $\geq 2$ | $\geq 1$ | — | — |
| VCR | 0 | $\in [0.2, 1]$ | — | — |
| VVR (1f) | 0 | $\geq 1$ | $< 0.5$ | — ($\geq 1$) |
| SR0b (1f) | 0 | $\geq 1$ | $\geq 0.5$ | — ($\geq 1$) |
| SR1b (1f) | 1 | $\geq 1$ | $\geq 0.5$ | — ($\geq 1$) |

**Table 1.** Summary of the event selections used to define the signal, control and validation regions. The signal regions are denoted by SR0b and SR1b, the $t\bar{t}$ ($V$+jets) dominated control regions are denoted by TCR (VCR) and the validation regions enhanced in $t\bar{t}$ ($V$+jets) are labelled as TVR1bLPhi, TVR1bHPhi and TVR2bHPhi (VVR). The "(1f)" notation in the signal and validation region rows indicates the additional requirement of at least one forward jet in the event, which is applied for the search of a single vector-like $T$ quark. All regions are required in addition to contain zero leptons in the final state, $E_{\mathrm{T}}^{\mathrm{miss}} \geq 250$ GeV and at least one top-tagged large-$R$ jets with $p_{\mathrm{T}} \in [350, 2500]$ GeV and a mass $\in [40, 600]$ GeV. The number of $b$-tagged (forward) jets required is indicated by $N_{b\text{-tagged jets}}$ ($N_{\text{forward-jets}}$). The symbol - indicates that no requirement on the variable is applied.

from mis-reconstructed $E_{\mathrm{T}}^{\mathrm{miss}}$ aligned to badly reconstructed jets, the minimum distance in the transverse plane between any reconstructed small-$R$ jet ($j$) and the missing transverse momentum, $\Delta\phi_{\min}(j, E_{\mathrm{T}}^{\mathrm{miss}})$, is required to be larger than 0.2.

Additional requirements are used to define several orthogonal regions: signal regions (SRs) optimised to maximise the sensitivity to the target signal models; control regions (CRs) designed to measure the normalisation of the main contributing background processes; and validation regions (VRs) to check the background modelling in regions kinematically closer to the signal regions. The control and validation regions are defined to have a negligible signal contribution. The requirements that define the analysis regions are listed in table 1, sketched in figure 3 and described as follows.

### 6.1 Signal region definition

Different SRs are defined for the three signal scenarios considered to maximise the analysis sensitivity to each model. Each signal region is defined by the output score of an XGBoost classifier [79] specifically trained to improve the sensitivity to each signal.

The XGBoost algorithm [79] combines several input observables into an extreme gradient BDT. Gradient boosting improves over a single decision tree classifier by combining a number of classifiers iteratively enhanced. Three XGBoost classifiers are trained separately with preselected simulated background and signal events for each considered model — scalar and vector DM, and VLQ. In the training of the classifier targeting the separation of events from scalar (vector) mediator DM production, the simulated sample with a mediator mass of $m_\phi = 4$ TeV ($m_V = 1.75$ TeV) is used, corresponding to an intermediate value of the



JHEP05(2024)263

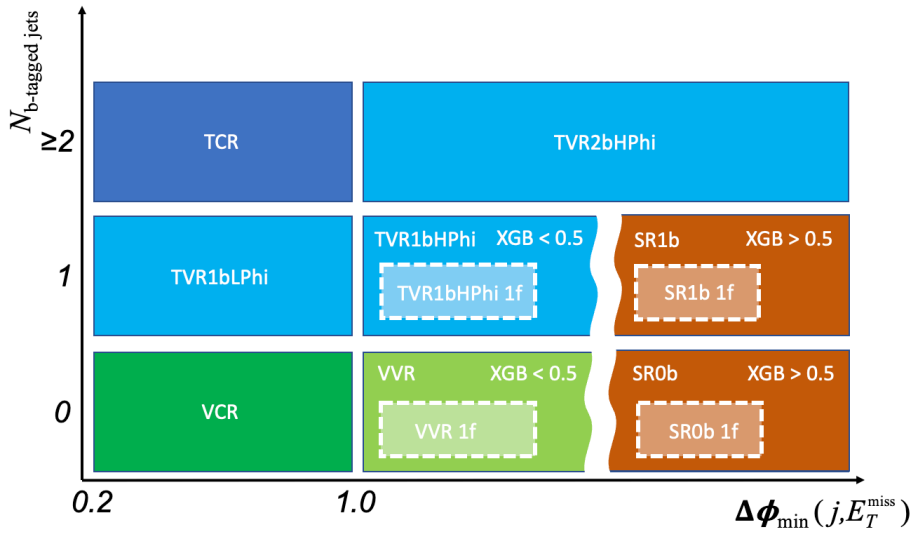


**Figure 3.** Schematic representation of the control, validation and signal regions. Regions are defined in terms of $b$-tagged jet multiplicity $N_{b\text{-tagged jets}}$ and the minimum distance in the azimuthal angle between a jet and $E_{\text{T}}^{\text{miss}}$ $\Delta\phi_{\text{min}}(j, E_{\text{T}}^{\text{miss}})$. The notation "XGB<0.5" and "XGB>0.5" indicates the requirement on the XGBoost score of the validation and signal regions, respectively. These regions are schematically separated by the curly vertical line. The "1f" label stands for requiring at least one forward jet in the event. The selections used to define the regions are described in the text and in table 1.

explored masses. The classifier targeting the identification of single vector-like $T$ production is trained using a set of samples with $m_T$ ranging from 1.5 to 1.9 TeV. This choice provides stable performances for larger masses while for lower masses, which are mostly excluded already, some degradation is observed.

The hyperparameters of each XGBoost model are optimised to maximise the integral under the receiver operating characteristic curve. Similarly, the set of variables used in the training of the classifier, listed in table 2, are selected based on their discrimination power, and good data and simulation agreement. The training of the XGBoost classifier targeting the DM scalar production required fewer input variables, as signal events are mostly characterised by large $E_{\text{T}}^{\text{miss}}$ values, of the order of the mediator mass. For the remaining signal models, the kinematic properties of signal events are more similar to those from background processes, and therefore more input features are required for the event classification. The $E_{\text{T}}^{\text{miss}}$ is the most discriminating variable for all considered models, as it is expected to be significantly larger than for background events. The reconstructed transverse mass of the system composed of the $E_{\text{T}}^{\text{miss}}$ and the closest $b$-tagged jet plays an important role in the discrimination against $t\bar{t}$ events with a top quark decaying leptonically, for which the distribution is expected to peak at around the top-quark mass. Variables based on angular distances of the reconstructed objects and energy balance between $E_{\text{T}}^{\text{miss}}$ and the jets (e.g., $\Omega$) also help in the event classification.

For signal events, the top quark is expected to recoil against the missing transverse momentum, thus the requirement of $\Delta\phi_{\text{min}}(j, E_{\text{T}}^{\text{miss}})> 1$ is applied. This requirement rejects



JHEP05(2024)263

| Variable | Description | Scalar DM mediator | Vector DM mediator | VLQ |
|---|---|---|---|---|
| $E_{\mathrm{T}}^{\mathrm{miss}}$ | Missing transverse momentum | ✓ | ✓ | ✓ |
| $\Omega$ | $E_{\mathrm{T}}^{\mathrm{miss}}$ and large-$R$ jet $p_{\mathrm{T}}$ balance: $\frac{E_{\mathrm{T}}^{\mathrm{miss}}-p_{\mathrm{T}}(J)}{E_{\mathrm{T}}^{\mathrm{miss}}+p_{\mathrm{T}}(J)}$ | ✓ | ✓ | ✓ |
| $\mathrm{N}_{\mathrm{jets}}$ | Small-$R$ jet multiplicity | ✓ | ✓ | ✓ |
| $\Delta R_{\mathrm{max}}$ | Maximum $\Delta R$ between two small-$R$ jets | ✓ | ✓ | ✓ |
| $m_{\mathrm{T,min}}(E_{\mathrm{T}}^{\mathrm{miss}}, b\text{-tagged jet})$ | Transverse mass of $E_{\mathrm{T}}^{\mathrm{miss}}$ and the closest $b$-tagged jet | ✓ | ✓ | ✓ |
| $m_{\text{top-tagged jet}}$ | Mass of the large-$R$ top-tagged jet | ✓ | | ✓ |
| $\Delta p_{\mathrm{T}}$ ($J$, jets) | Scalar difference of large-$R$ jet $p_{\mathrm{T}}$ and the sum of $p_{\mathrm{T}}$ of all small-$R$ jets. | ✓ | ✓ | |
| $H_{\mathrm{T}}$ | Sum of all small-$R$ jet $p_{\mathrm{T}}$ | | ✓ | ✓ |
| $H_{\mathrm{T}}/E_{\mathrm{T}}^{\mathrm{miss}}$ | Ratio of $H_{\mathrm{T}}$ and $E_{\mathrm{T}}^{\mathrm{miss}}$ | | ✓ | ✓ |
| $\Delta E(E_{\mathrm{T}}^{\mathrm{miss}}, J)$ | Energy difference between $E_{\mathrm{T}}^{\mathrm{miss}}$ and the large-$R$ jet | | ✓ | ✓ |
| $\Delta\phi(E_{\mathrm{T}}^{\mathrm{miss}}, J)$ | Angular distance in the transverse plane between $E_{\mathrm{T}}^{\mathrm{miss}}$ and large-$R$ jet | | ✓ | ✓ |
| $p_{\mathrm{T}}(\mathrm{J})$ | Large-$R$ jet $p_{\mathrm{T}}$ | | | ✓ |
| $m_{\mathrm{T}}(E_{\mathrm{T}}^{\mathrm{miss}}, J)$ | Transverse mass of the $E_{\mathrm{T}}^{\mathrm{miss}}$ and large-$R$ jet | | | ✓ |
| $\Delta\phi(b\text{-tagged jet}, J)$ | Angular distance in the transverse plane between the large-$R$ jet and the leading $b$-tagged jet | | | ✓ |

**Table 2.** List of variables used in the training of the XGBoost classifier for the scalar and vector DM mediator, and VLQ models. The symbol ✓ indicates that the corresponding variable is included in the training.

$t\bar{t}$ events with a boosted top quark decaying hadronically and recoiling against a $b$-jet from the leptonic decay of the other top quark. The signal regions for a given model are defined by requiring the corresponding XGBoost score to be larger than 0.5. The resulting events are separated into two orthogonal signal regions (SR0b,SR1b) by applying criteria based on $b$-tagged jet multiplicity (see figure 3). The SR1b (SR0b) signal region must contain exactly one (zero) $b$-tagged jet. Signal events are expected to have one $b$-jet from the top-quark decay in the final state, but the SR0b is expected to account for $b$-tagging inefficiencies. The signal efficiencies of the SRs targeting each DM model depend on the specific signal parameters and are within 14%–27% and 3%–9% for the scalar and vector DM, respectively.

The signal regions targeting the search for the vector-like $T$ quark production require additionally at least one forward jet since final states with jets at a small angle relative to the beam pipe are expected. The VLQ signal selection efficiency in these SRs is 1%–2% depending on the model parameters.

In summary, the analysis employs six distinct regions to target the three signal models with two SRs each: SR0b and SR1b region for the DM scalar search, SR0b and SR1b region for the DM vector, and SR0b 1f and SR1b 1f targeting single vector-like $T$-quarks.



JHEP05(2024)263

### 6.2 Background estimate

Dedicated control regions enriched in the dominant background processes are defined to constrain their normalisation to data in a profile-likelihood fit described in section 8, while the shape distributions are taken from simulation. The rest of the background processes are estimated completely from the simulation.

The main contributing background sources to the signal region are $t\bar{t}$ and $V$+jets production. The former represents approximately 65% of the background events in SR1b, consistent across all the defined signal regions with one $b$-tagged jet requirement. The other main sources of background in this region are $V$+jets (20%) and single top (10%), consisting mostly of $tW$ production. The SR0b is dominated by $V$+jets production (up to 85%) across all the inspected models, with minor contributions from diboson production (10%) and $t\bar{t}$ ($< 8\%$).

Control regions enhanced in the dominant $t\bar{t}$ and $V$+jets backgrounds are then defined by requiring $0.2 < \Delta\phi_{\min}(j, E_{\mathrm{T}}^{\mathrm{miss}}) < 1$ to reduce the signal contribution below 5% for all the considered models. The $t\bar{t}$ control region (referred to as TCR) is defined by requiring, in addition, at least two $b$-tagged jets. This region is enriched in $t\bar{t}$ production with at least one top quark decaying into leptons that are not reconstructed. This provides a significant source of $E_{\mathrm{T}}^{\mathrm{miss}}$ recoiling against the top quark, similar to what is found in the SR1b region, where this source of background is dominant. The control region enriched in $V$+jets (referred to as VCR) requires zero $b$-tagged jets in the final state. In this region, the fractions of $W$+jets processes in which the $W$ boson decays into $\tau$-leptons, and of $Z$+jets processes with the $Z$ boson decaying into neutrinos, both leading to a hadronic final state with significant $E_{\mathrm{T}}^{\mathrm{miss}}$, are similar to those expected in the SR0b signal region.

Validation regions are defined to check the modelling of the main background processes in regions kinematically closer to the signal regions, maintaining low signal contamination ($< 10\%$). The $t\bar{t}$ modelling is checked in three validation regions, approaching the SR1b from two different paths in the plane shown in figure 3. The TVR2bHPhi region extends the TCR (with at least two $b$-tagged jets) to higher values of $\Delta\phi_{\min}(j, E_{\mathrm{T}}^{\mathrm{miss}})$, by requiring $\Delta\phi_{\min}(j, E_{\mathrm{T}}^{\mathrm{miss}}) > 1$. The TVR1bLPhi region is defined with events fulfilling $0.2 < \Delta\phi_{\min}(j, E_{\mathrm{T}}^{\mathrm{miss}}) < 1$ but with a single $b$-tagged jet in the final state to validate the $t\bar{t}$ modelling with a reduced fraction of additional jets originated from heavy flavour quarks, as in SR1b. Events in these two regions are not required to fulfil any requirement in the XGBoost score. Finally, the TVR1bHPhi region extends the TVR1bLPhi to $\Delta\phi_{\min}(j, E_{\mathrm{T}}^{\mathrm{miss}}) > 1$, but XGBoost score $< 0.5$ is required to not overlap with SR1b. The $V$+jets modelling is tested in the VVR region, which requires no $b$-tagged jets in the final state, $\Delta\phi_{\min}(j, E_{\mathrm{T}}^{\mathrm{miss}}) > 1$ and XGBoost score $< 0.5$ to ensure orthogonality with the SR0b. Two specific validation regions for the search targeting the vector-like $T$ quark production are defined by adding the requirement of at least one forward jet in the final state to the selections that define the VVR and TVR1bHPhi, called VVR1f and TVR1bHPhi1f, respectively.

## 7 Systematic uncertainties

Systematic uncertainties of theoretical and instrumental sources affect the predictions of background and signal in the analysis regions. The effect of these uncertainties is included in



JHEP05(2024)263

the likelihood fit as additional nuisance parameters (NP) that are measured simultaneously with the normalisations of the main background processes and the signal strength.

Several sources of instrumental uncertainties are considered. These include systematic uncertainties in the online event selection efficiency using the high-$E_{\mathrm{T}}^{\mathrm{miss}}$ trigger, and also in the reconstruction and calibration of the objects analysed. Moreover, the normalisation of the simulated samples to the integrated luminosity collected in Run 2 has an uncertainty of 1.7% [137], obtained using the LUCID-2 detector [86] for the primary luminosity measurements. Among all the detector-related uncertainties, the most significant arise from the measurements of jet properties and tagging efficiencies.

Uncertainties associated with jets are due to the jet energy scale (JES) and jet energy resolution (JER) [128, 129]. For large-$R$ jets, uncertainties arising from the jet mass scale (JMS), and jet mass resolution (JMR) are also considered. They are derived from observations of the $W$ boson and top-quark masses in semileptonic $t\bar{t}$ events and by a double-ratio method that compares the calorimeter-to-tracker response ratio between data and simulation [128]. For small-$R$ jets, additional uncertainties related to the JVT requirement are also evaluated, arising from the correction factors used to match the efficiencies in the MC samples to data [130].

The $b$-quark tagging efficiencies in simulation, and the charm and light jet mistag rates, are corrected to match the efficiencies in data [138–140]. The efficiency for tagging $b$-jets is measured in data using $t\bar{t}$ events [138]. Uncertainties arising in the evaluation of the efficiencies are propagated to the correction factors.

The efficiency and rejection power of the DNN top-quark tagger is measured in data and correction factors are applied to MC events to match the measured efficiencies [134]. These corrections take into account the correlations between the tagging efficiencies and other jet observables such as the jet energy and mass. The uncertainties in these corrections are treated as systematic uncertainties.

A set of uncertainties that parametrise the lack of knowledge on the background prediction of theoretical nature are considered. These uncertainties are evaluated either from variations of parameter settings in the event generation or from a direct comparison to alternative simulated samples.

Uncertainties in the modelling of the $t\bar{t}$ background come from the choice of NLO-matching method, the parton shower and hadronisation modelling, the amount of additional gluon radiation, missing higher orders in the generation and the choice of PDF. The NLO-matching uncertainty is estimated by a direct comparison of the $t\bar{t}$ simulation with an alternative sample using MadGraph5_aMC@NLO. Similarly, the uncertainty in the parton shower and hadronisation model is estimated from an alternative sample using Herwig7.1 [141]. The uncertainty associated with the effects of missing QCD higher orders is estimated by independently varying the renormalisation and factorisation scales by factors of 2.0 and 0.5. The impact of initial-state radiation (ISR) is estimated by varying $\alpha_s$ in the A14 tune. Similarly, the uncertainty related to final-state radiation (FSR) is assessed by varying the renormalisation scale for the final-state radiation by a factor of 2.0 and 0.5 in the parton shower algorithm.

The uncertainties in the modelling of additional gluon radiation and missing higher orders are also estimated for all single-top processes using the same procedure as in the $t\bar{t}$ background. The corresponding NPs are treated as uncorrelated among single-top and $t\bar{t}$



JHEP05(2024)263

processes. The choice of the scheme to account for the interference between $tW$ and $t\bar{t}$ is another source of uncertainty in the background prediction and is estimated by comparing predictions using diagram removal and diagram subtraction schemes [110].

Uncertainties in the modelling of weak boson production in association with jets, $W$+jets and $Z$+jets, arise from missing higher orders in perturbation theory, resummation of the gluon radiation, matching of the parton shower, modelling of heavy-flavour quark production and the choice of PDF. The effect of the modelling uncertainties in $W$+jets and $Z$+jets are treated as uncorrelated NPs in the profile likelihood fit. The uncertainty due to missing QCD higher orders is estimated by independently varying the renormalisation and factorisation scales by a factor of two and taking the largest observed deviation from the nominal prediction. A similar procedure is used to assess the uncertainties associated to the resummation of gluon radiation and matching with the parton shower, as they are estimated by varying by a factor of two the corresponding scales. Two normalisation uncertainties of 30% are assigned to $V$+jets events with $b$-jets and $c$-jets, respectively, to cover possible discrepancies from simulations in case of heavy-flavour production [142]. The presence of $b$-jet ($c$-jets) in the final state is determined by the presence of $B$-hadrons ($D$-hadrons) in the truth record of the simulated events, which are associated with reconstructed jets. The same procedure is used to estimate the modelling uncertainties in the generation of diboson production (except for the resummation and parton shower matching uncertainties).

Uncertainties due to the PDF choice in the simulations on $t\bar{t}$, $V$+jets, single-top and diboson production simulations are estimated by following the PDF4LHC [143] recommendation.

Uncertainties in the cross-sections of the background processes whose normalisations are not measured in the control regions are also included. These background processes are single-top [144–146], diboson [147] and $t\bar{t}$+$X$ [148, 149]. The respective uncertainties are 5%, 6% and 15%.

Uncertainties in the signal prediction from the scalar and vector DM mediator productions are also considered. Missing higher-order QCD corrections are estimated by varying the renormalisation and factorisation scale by a factor of 0.5 and 2 relative to the value used in the baseline simulation. When the signal prediction is obtained with the reweighting procedure, two additional sources of uncertainty are considered. The first is a shape uncertainty, estimated by comparing the normalised XGBoost distributions at particle and reweighted level for the target point in the model parameter space. The second is a 10% normalisation uncertainty estimated as the largest difference between the event yields at particle and reconstruction levels for all the reference points.

Representative values for the impact of the considered sources of uncertainties in the background processes in the signal regions are shown in table 3. Generally, the dominant uncertainties in the background prediction consist of modelling uncertainties. The most important instrumental uncertainties are related to large-$R$ jet momentum and mass calibration, which significantly impacts the $V$+jets background expectation, and to top-tagging calibration, mostly affecting the $t\bar{t}$ prediction.



JHEP05(2024)263

| | $t\bar{t}$ | | $Z$+jets | | $W$+jets | | $tW$ | | Diboson | | $t\bar{t}V$ | |
|---|---|---|---|---|---|---|---|---|---|---|---|---|
| | SR0b | SR1b | SR0b | SR1b | SR0b | SR1b | SR0b | SR1b | SR0b | SR1b | SR0b | SR1b |
| $b$-tagging efficiency | 5 | $< 1$ | $< 1$ | 2 | $< 1$ | 2 | 5 | $< 1$ | $< 1$ | 3 | 6 | 1 |
| Jet calibration | 50 | 7 | 15 | 30 | 18 | 13 | 50 | 13 | 13 | 20 | 40 | 12 |
| $E_{\mathrm{T}}^{\mathrm{miss}}$ calibration | 3 | $< 1$ | 2 | 6 | 1 | $< 1$ | 2 | 1 | $< 1$ | 2 | 4 | 1 |
| Top-tagging efficiency | 13 | 14 | 5 | 6 | 5 | 6 | 13 | 14 | 11 | 11 | 13 | 13 |
| Other instrumental | 3 | 2 | 2 | 2 | 3 | 3 | 5 | 3 | 3 | 4 | 5 | 3 |
| Modelling | 30 | 23 | 23 | 33 | 20 | 30 | 65 | 45 | 10 | 35 | 15 | 15 |

**Table 3.** Values of the relative post-fit uncertainty (in %) on the background prediction in the signal regions SR0b and SR1b for the different sources of systematic uncertainties. The category "jet calibration" includes all the sources of uncertainty related to the reconstruction and calibration of small- and large-$R$ jets. The quoted values are obtained by averaging the post-fit uncertainties of the three fits performed assuming the background-only hypothesis, corresponding to signal regions and BDTs targeting the scalar and vector mediator DM signals and the vector-like $T$ signal. The sum in quadrature of the individual uncertainties is not expected to be equal to the total background post-fit uncertainty computed taking into account the correlations among the sources of uncertainties.

## 8 Results

For each signal model, the presence of the signal in data is tested via a profile-likelihood fit to the observed event yields in the control regions and to the corresponding XGBoost score distribution in the signal regions. The binning is chosen as a compromise between the maximum separation of the signal from the background and statistics of simulated background events. The likelihood function used to construct the test statistic consists of a product of Poisson probabilities of the yields in each bin of the fitted distributions and constraint functions for NPs describing the systematic uncertainties. The impact of statistical uncertaities from the data and MC simulation are parametrised by a Poisson distribution while the remaining uncertainties are parametrised by Gaussian distributions. Additionally, the normalisation factors of $V$+jets ($\mathrm{NF}_{V+\mathrm{jets}}$) and $t\bar{t}$ ($\mathrm{NF}_{t\bar{t}}$) background processes are included as unconstrained NPs.

Only systematic uncertainties impacting the shape or the normalisation of the expected background distribution for more than 1% are accounted for in the systematic model. In case a systematic variation leads to significant bin-to-bin statistical fluctuations in the XGBoost score distribution in the signal regions, the shape of the systematic effect is smoothed. Systematic uncertainties that are estimated via a direct comparison of a single variation with the nominal prediction are symmetrised. Some systematic uncertainties that are evaluated via the comparison of two opposite variations with respect to the nominal prediction, may show both variations above or below the nominal expectation with at least one variation compatible with the nominal prediction within the associated statistical uncertainty. In this case, the maximum distance from the nominal prediction is considered and symmetrised. A test statistic based on a profile-likelihood ratio implemented in RooStats [150] is used for the evaluation of confidence intervals and hypothesis testing. Exclusion limits are derived with the $\mathrm{CL_s}$ frequentist method [151, 152] using the asymptotic approximation [153].

The result of the fit under the background-only hypothesis leads to the determination of the normalisation factors for the main sources of background. The values obtained by the dif-



JHEP05(2024)263

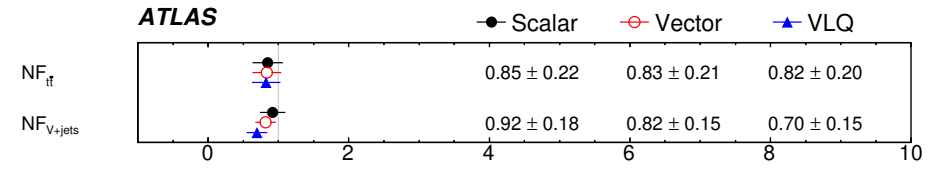


**Figure 4.** Comparison of the fitted normalisation factors of the $t\bar{t}$ and $V$+jets background processes in the fits of data in control and signal regions under the background-only hypothesis. An independent fit is performed for each signal model, using the respective signal regions.

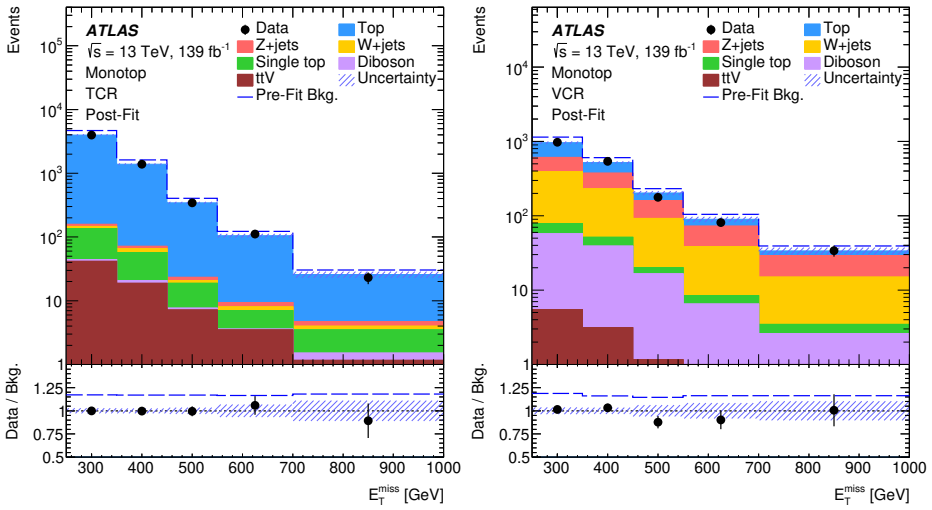


(a) (b)

**Figure 5.** Comparison of data and SM prediction for the $E_{\mathrm{T}}^{\mathrm{miss}}$ distribution in control regions targeting (a) $t\bar{t}$ and (b) $V$+jets processes. The background predictions with the corresponding uncertainties result from the simultaneous fit to data in control and signal regions under the background-only hypothesis (Post-Fit). The signal regions included in the fit correspond to those targeting the scalar DM mediator production. The dashed line indicates the pre-fit total background prediction. The last bin of the distribution contains the overflow.

ferent fits are shown in figure 4. They are consistent with unity within two standard deviations. The discrepancy observed in $\mathrm{NF}_{V+\mathrm{jets}}$ between the fits targeting DM and vector-like $T$ signals is explained by the different phase spaces of the corresponding signal regions (in particular due to the requirement of at least one forward jet in the VLQ signal regions). The deviation from the unity of the normalisation factors is mainly related to the highly boosted regime explored in this analysis with respect to the phase space in which the top-quark tagging calibration was performed. The good description of data in the control regions of the post-fit background model is shown in figure 5 for the $E_{\mathrm{T}}^{\mathrm{miss}}$ distribution. Despite that only the event yield information is used as fit input for the CRs, a very good modelling of the $E_{\mathrm{T}}^{\mathrm{miss}}$ distribution is observed.

The extrapolation of the background model from the control region to the signal region is tested in the validation regions. These regions are not included in the likelihood fit but are used to validate the background expectation, obtained from the results of the fit



JHEP05(2024)263

in the control and signal regions, in regions kinematically close to the signal phase space. Kinematical properties of $t\bar{t}$ events are validated in adjacent regions to the $t\bar{t}$ control region and common to all considered models, namely TVR1bLPhi and TVR2bHPhi, shown in figures 6(a) and 6(b) for the $E_{\mathrm{T}}^{\mathrm{miss}}$ distribution. The validation regions that are closest to the signal regions are VVR and TVR1bHPhi, which only differ by the XGBoost score requirement with the SR0b and SR1b regions, respectively. A comparison of the observed and expected distribution for the XGBoost score variable is shown in figures 6(c) and 6(d), respectively. No significant mismodelling of data is observed in these regions, meaning that the lower tail of the XGBoost score distribution in $N_{b\text{-tagged jets}}$-$\Delta\phi_{\mathrm{min}}(j, E_{\mathrm{T}}^{\mathrm{miss}})$ phase space is well modelled. The agreement of the event yields in data with the background model in all the validation regions considered in the analysis is shown in figure 7 for each signal model targeted. Since no significant discrepancy between data and the background expectation was observed in any of the validation regions, no additional non-closure uncertainties are included in the systematic model of the profile-likelihood fit.

The distribution of the XGBoost score in the signal regions for data and the fitted SM expectation under the background-only hypothesis are shown in figure 8. No significant excess above the SM expectation is found in any of the signal regions. The results are therefore interpreted in terms of expected and observed upper limits on the signal cross-section as a function of the model parameters.

The upper limit on the signal cross-sections at 95% confidence level is shown in figure 9, together with the theoretical signal cross-section prediction for the considered benchmarks. The limit on the cross-section of the scalar-mediated DM production as a function of the mediator mass $m_\phi$ is shown in figure 9(a). A degradation of the cross-section limit at high $m_\phi$ masses is observed, justified by a general decrease in the event selection efficiency. Assuming the couplings $\lambda_q = 0.6$ and $y_\chi = 0.4$, and the mass of the DM candidate $m_\chi = 1$ GeV, the model is excluded for masses of the mediator scalar particle $m_\phi < 4.3$ TeV, improving the limits with respect to the previous search with *mono-top* events by 800 GeV [39]. The limit on the cross-section of the vector-mediated DM production as a function of the mass of the vector particle $m_V$ is shown in figure 9(b). The predictions of the signal distribution for a mass of the vector mediator $m_V$ different from 1.75 TeV are obtained using the weighting procedure described in section 4. Assuming the couplings $a = 0.5$ and $g_X = 1$, and the mass of the DM candidate $m_\chi = 1$ GeV, the model is excluded for masses of the vector particle $m_V < 2.3$ TeV, which corresponds to an 300 GeV improvement from the previous result of the *mono-top* channel [39].

The limit on the cross-section of the vector-like $T$ quark production as a function of its mass $m_T$ is shown in figure 9(c). Assuming the coupling $\kappa_T = 0.5$ and the branching ratio $\mathcal{B}(T \to Zt) = 25\%$, the singlet model is excluded for $m_T < 1.8$ TeV. This constitutes an improvement of 400 GeV in the excluded mass when comparing to the previous similar analysis [39]. The cross-section limit is decreased by a factor 10, mainly due to improved object reconstruction algorithms, calibrations and event selection, the use of XGBoost for enhanced signal sensitivity and increased data statistics. This result is competitive with the 1–2 TeV exclusion limits obtained analysing different final state events in searches for single vector-like $T$-quarks [67–77], as discussed in section 1.



JHEP05(2024)263

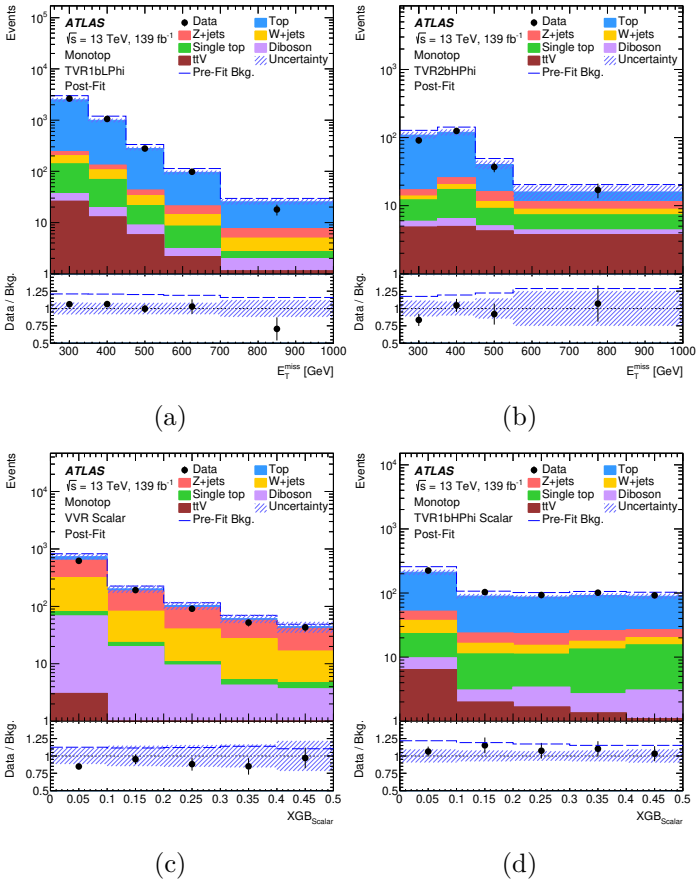


**Figure 6.** Comparison of data and SM prediction in the validation regions. The $E_{\mathrm{T}}^{\mathrm{miss}}$ distribution is shown in the $t\bar{t}$ validation regions (a) TVR1bLPhi and (b) TVR2bHPhi. The XGBoost score is shown in the validation regions (c) VVR and (d) TVR1bHPhi, which are inclusive in forward jet multiplicity. The background predictions with the corresponding uncertainties result from the simultaneous fit to data in control and signal regions under the background-only hypothesis (Post-Fit). The signal regions included in the fit correspond to those targeting the scalar DM mediator production. The dashed line indicate the pre-fit total background prediction. The last bin of the distributions in (a) and (b) contains the overflow.

Contours of the observed and expected upper limits in four dimensions of the parameter space of the scalar and vector mediator DM models are produced using the set of simulations and reweighting procedure developed for this analysis. These are shown in figures 10 and 11, respectively. The limit in the scalar mediator mass $m_\phi$ of the DM production appears to be almost constant for different values of $\lambda_q$ and $y_\chi$, except for very low values associated with tiny cross-sections, and all values of $\lambda_q$ ($y_\chi$) are excluded for $m_\phi$ up to 3.4 (2.5) TeV, improving the results of the previous analysis. The $m_\phi$ limits are also constant in the $(m_\phi, m_\chi)$ plane, for the lower region of the DM candidate mass, and the $m_\chi$ reach is 2.2 TeV. This analysis is not sensitive to the region of the parameter space where $(m_\phi - m_\chi) < 500$ GeV as it does not result in a boosted top-quark topology. For the vector DM mediator production model, the exclusion limits obtained are improved with respect to the previous analysis, all values of $g_\chi$ ($a$) are excluded for $m_V$ up to 1.1 (1.5) TeV, and the reach in $m_\chi$ is improved



JHEP05(2024)263

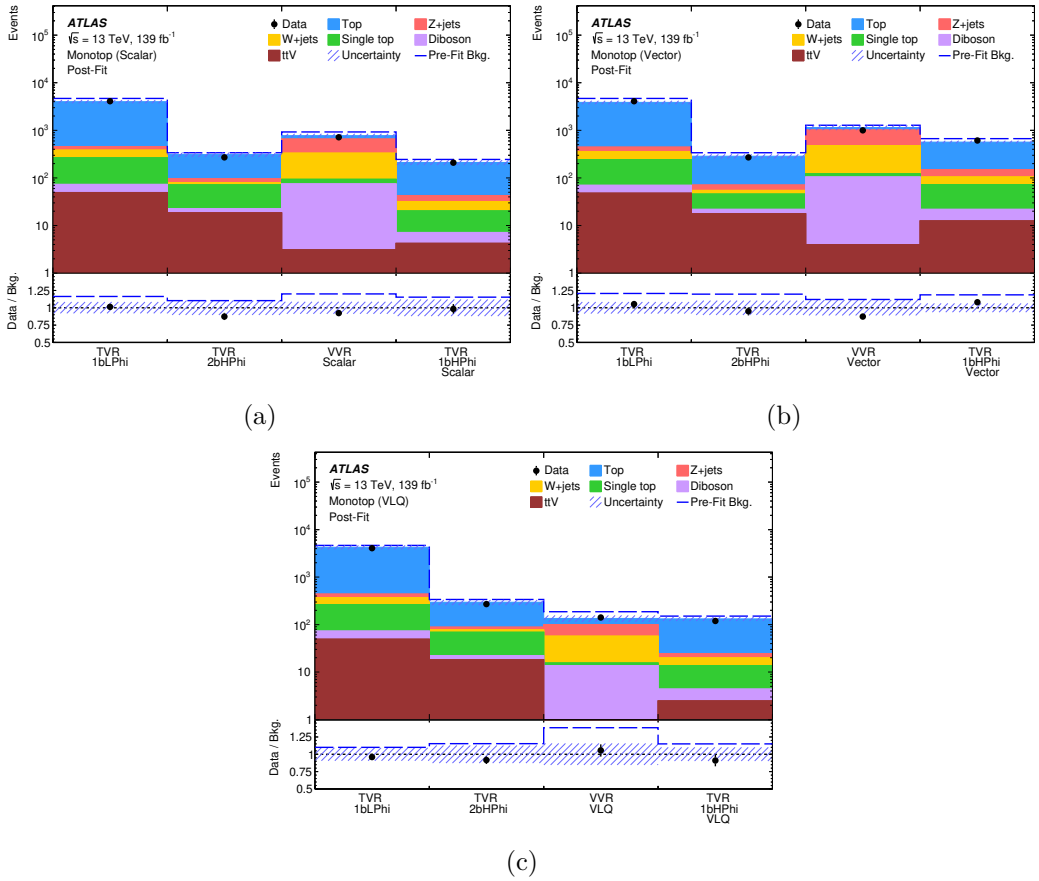


**Figure 7.** Comparison of data and SM predictions for the event yields in each validation region defined for the (a) DM scalar mediator, (b) DM vector mediator and (c) vector-like $T$ search. The background predictions with the corresponding uncertainties result from the simultaneous fit to data in control and signal regions under the background-only hypothesis (Post-Fit). The signal regions included in each fit correspond to those targeting the respective signal model. The dashed line indicate the pre-fit total background prediction.

by approximately 100 GeV. These results are complementary to the ones obtained in a search for same-charge top-quark pair production [34], providing sensitivity to lower values of the $a$ coupling parameter.

The two-dimensional exclusion contours in the plane $(m_T, \kappa_T)$ of the single vector-like $T$ quark production, shown in figure 12, were similarly obtained using the internal weights of the generated signal samples. Figure 12(a) provides exclusion limits on $\kappa_T$ and the $T$ quark mass, while figure 12(b) shows the exclusion limits on the signal cross-section normalised to the theoretical value, derived also as a function of the mass and coupling. Masses of the vector-like $T$ quark below 1.6 TeV are excluded for a value of the coupling $\kappa_T > 0.4$. For $\kappa_T > 0.5$, the model is mostly excluded for masses $m_T < 1.8$ TeV.

The exclusion limits on the $T$ quark mass can be given in a more generalised representation of the parameter space. Figure 13 displays the largest excluded mass as a function of the relative resonance width $\Gamma_T/m_T$ and the relative coupling parameter $\xi_W$, which, as discussed



JHEP05(2024)263

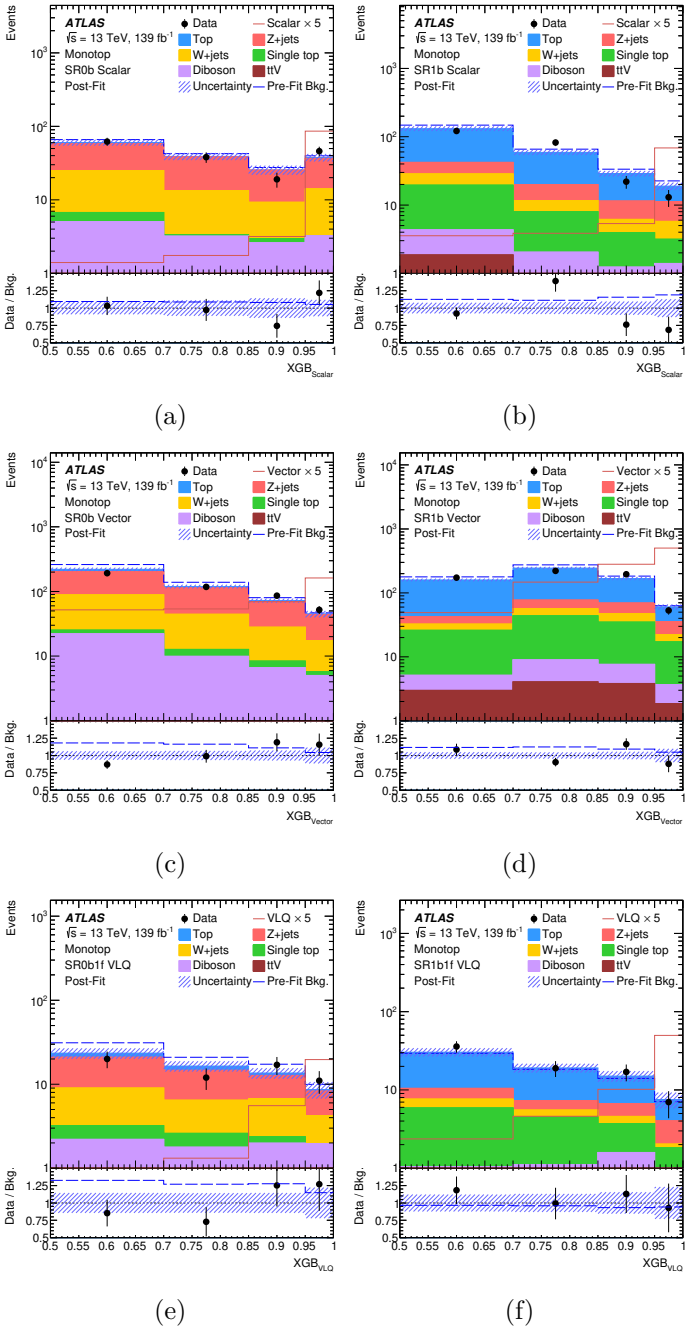


**Figure 8.** Comparison of data and fitted expectation for the XGBoost score distribution in the signal regions targeting the three considered signal models: (a) SR0b and (b) SR1b for the scalar DM mediator production, (c) SR0b and (d) SR1b for the vector DM mediator production and (d) SR0b (e) SR1b for the single vector-like $T$ quark production. The background predictions with the corresponding uncertainties result from the simultaneous fit to data in control and signal regions under the background-only hypothesis (Post-Fit). The signal regions included in each fit correspond to those targeting the respective signal model. The dashed line indicates the pre-fit total background prediction. The overlayed signal distributions correspond to scalar DM mediator production with $m_\phi = 4$ TeV (Scalar), vector DM mediator production with $m_V = 1.75$ TeV (Vector) and single vector-like $T$ production with $m_T = 1.7$ TeV (VLQ) scaled by a factor 5.

JHEP05(2024)263

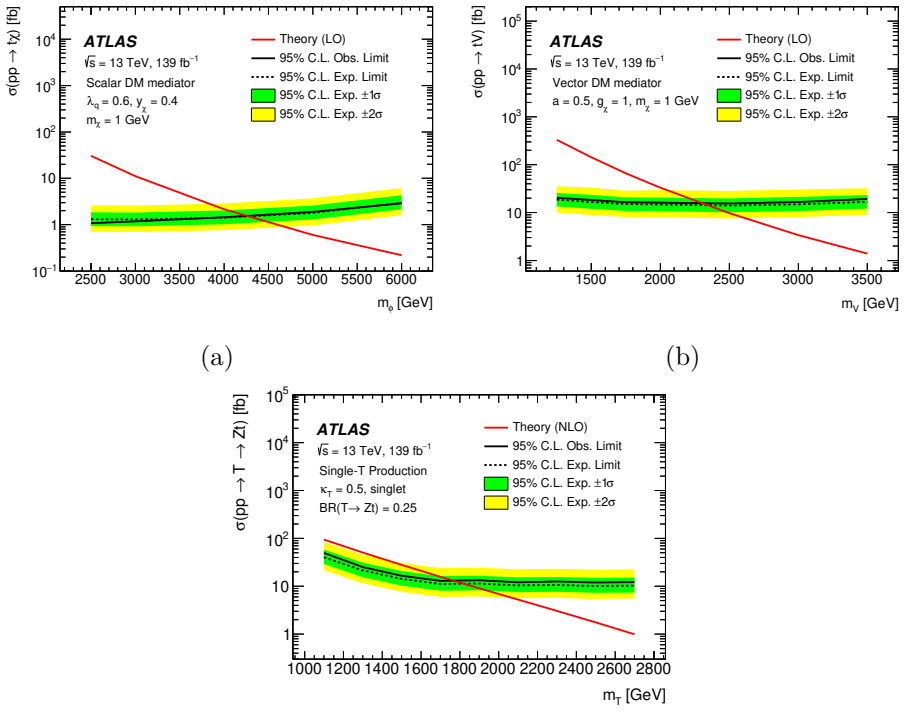


**Figure 9.** 95% CL upper limits on the cross-section of the considered signal models as a function of: (a) the DM scalar mediator $\phi$ mass (for fixed model parameters of $\lambda_q = 0.6$, $y_\chi = 0.4$ and $m_\chi = 1$ GeV), (b) the DM vector mediator $V$ mass (for $a = 0.5$, $g_\chi = 1$ and $m_\chi = 1$ GeV) and (c) the vector-like $T$ quark mass (for $\kappa_T = 0.5$).

in section 2, controls the branching ratio $\mathcal{B}(T \to Wb)$ and fully contrains $\mathcal{B}(T \to tZ)$. As expected, the exclusion limits on the $T$ quark mass are degraded for larger values of $\xi_W$, corresponding to lower values of the branching ratio associated with the decay explored in this analysis, $\mathcal{B}(T \to Zt)$.

JHEP05(2024)263

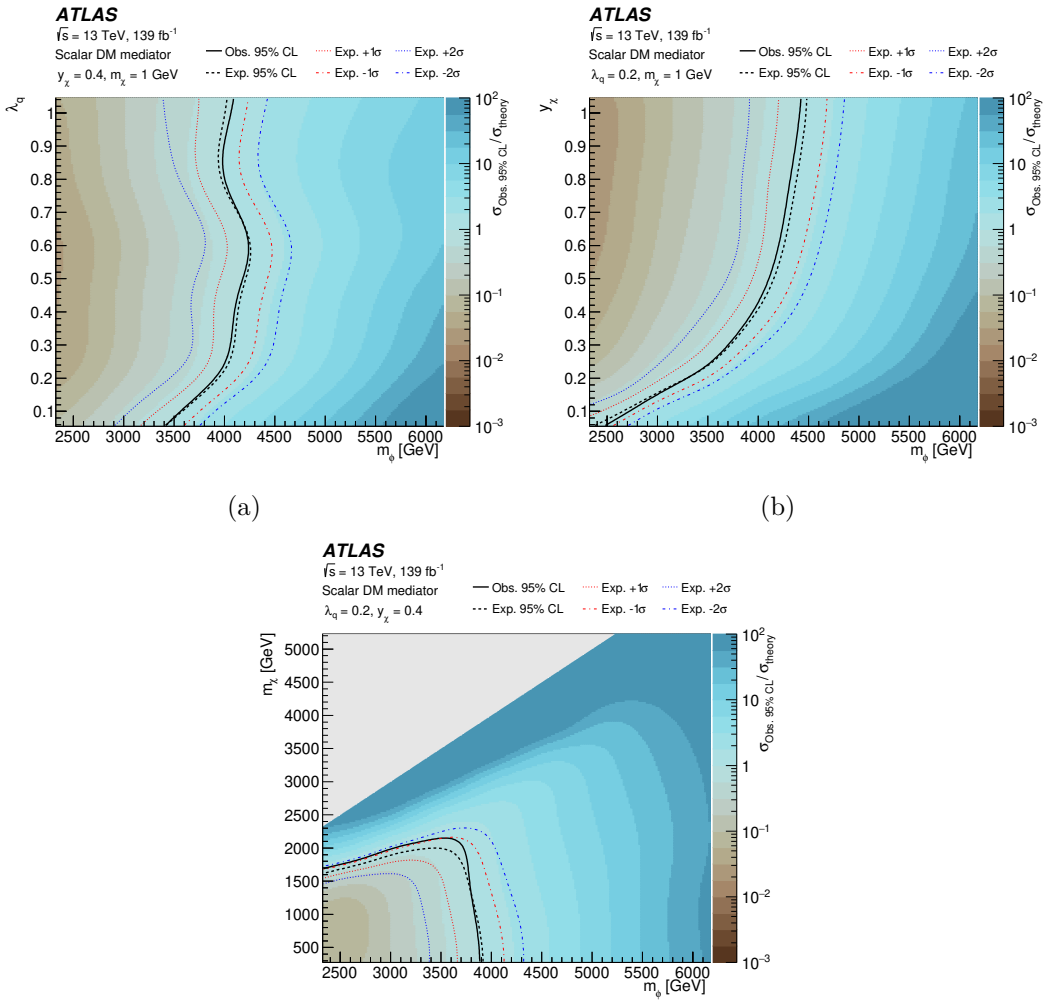


**Figure 10.** Observed 95% CL upper limits on the scalar-mediated DM signal cross-section divided by the theoretical value in three planes of the model parameters space: (a) $(m_\phi, \lambda_q)$, (b) $(m_\phi, y_\chi)$ and (c) $(m_\phi, m_\chi)$. The observed (expected) 95% CL exclusion limits on the parameters are drawn as solid (dashed) lines. The $\pm 1$ and $\pm 2$ standard deviations around the expected limit are also shown.

JHEP05(2024)263

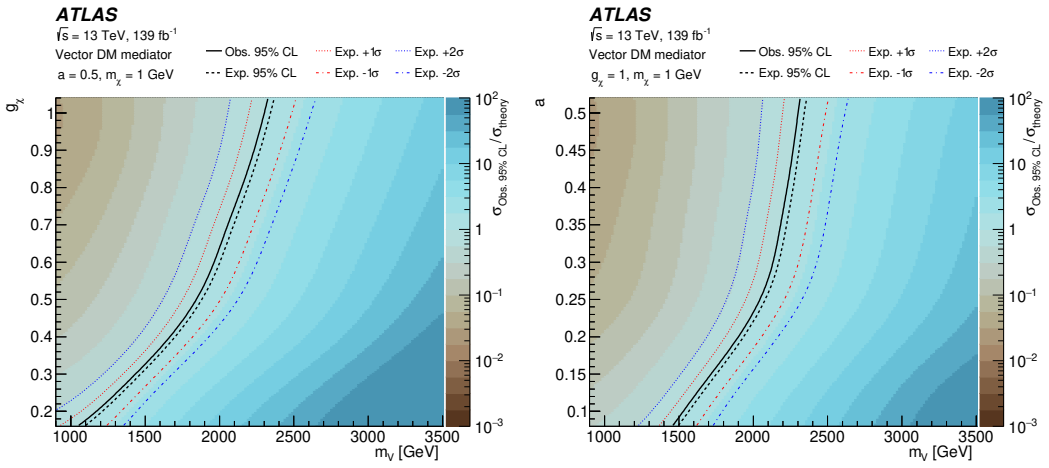


(a) (b)

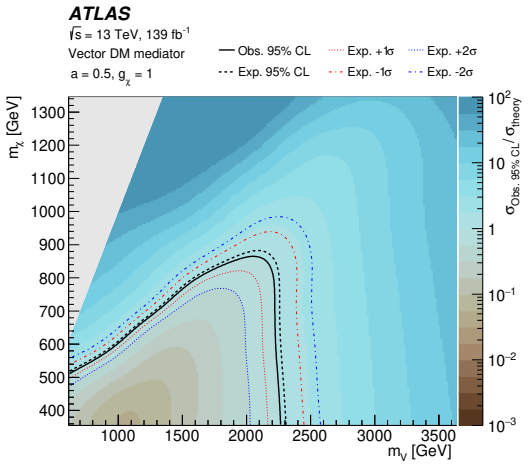


(c)

**Figure 11.** Observed 95% CL upper limits on the vector-mediated DM signal cross-section divided by the theoretical value in three planes of the model parameters space: (a) $(m_V, g_\chi)$, (b) $(m_V, a)$ and (c) $(m_V, m_\chi)$. The observed (expected) 95% CL exclusion limits on the parameters are drawn as solid (dashed) lines. The $\pm 1$ and $\pm 2$ standard deviations around the expected limit are also shown.

JHEP05(2024)263

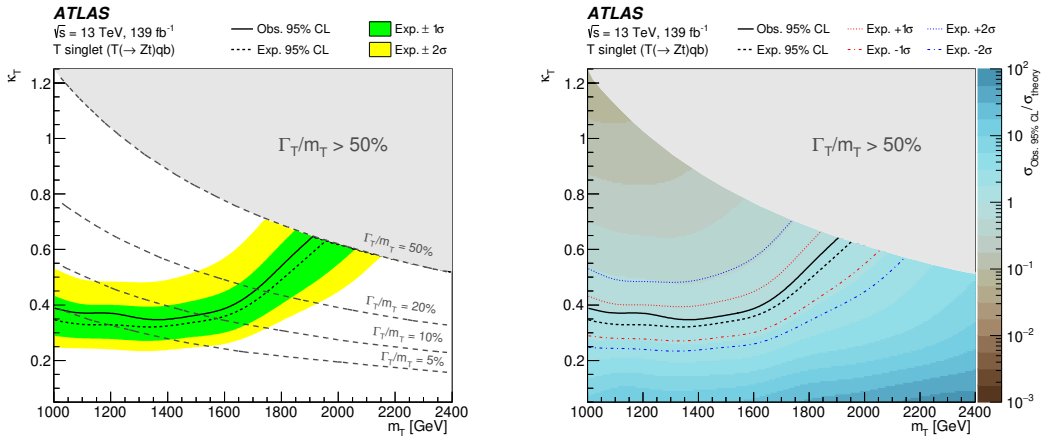


(a) (b)

**Figure 12.** Exclusion limits in terms of the universal coupling constant $\kappa_T$ as a function of the $T$ quark mass in the singlet SU(2) scenario, in the regime where $\Gamma_T/m_T \leq 50\%$, for which the theory calculations are known to be valid. (a) Expected (dashed line) and observed (solid line) 95% CL exclusion limits on $\kappa_T$ as a function of the $T$ quark mass. Different $\Gamma_T/m_T$ hypotheses are shown as dashed lines. The shaded bands correspond to $\pm 1$ and $\pm 2$ standard deviations around the expected limit. (b) Observed 95% CL upper limits on the $T$ quark signal cross-section divided by the theoretical value as a function of $\kappa_T$ and the $T$ quark mass. The observed (expected) 95% CL exclusion limits on the parameters are drawn as solid (dashed) lines, with all values of $\kappa_T$ above the contour line being excluded at each mass point. The $\pm 1$ and $\pm 2$ standard deviations around the expected limit are also shown.

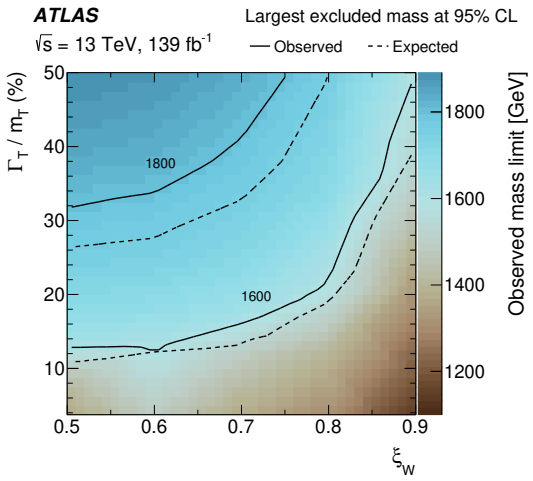


**Figure 13.** Observed 95% CL exclusion limits on the $T$ quark mass in the singlet SU(2) scenario as a function of the relative resonance width $\Gamma_T/m_T$ and the relative coupling parameter $\xi_W$. The solid (dashed) contour lines indicate observed (expected) exclusion limits of equal mass in units of GeV.

JHEP05(2024)263

## 9 Conclusions

This paper reports the search for anomalous production of events with a single top quark and large missing transverse momentum using the 139 $\text{fb}^{-1}$ dataset of $pp$ collisions at $\sqrt{s} = 13$ TeV collected by ATLAS at the LHC during the Run 2 data-taking.

No deviations from the SM predictions are observed and the results are interpreted in terms of upper limits on the cross-sections of BSM models expected to populate the considered phase space. The models are the production of DM in association with a single top quark via a scalar or vector mediator, and the production of a single vector-like $T$ quark in the singlet scenario decaying into $tZ(\to \nu\bar{\nu})$. The observed limits on cross-sections are used to exclude ranges of values of model parameters: the scalar (vector) mediated production of DM in association with a single top quark is excluded for masses of the scalar (vector) particle up to 4.3 (2.3) TeV for $m_\chi = 1$ GeV and couplings $\lambda_q = 0.6$ and $y_\chi = 0.4$ ($a = 0.5$ and $g_\chi = 1$). This result improves the limits on the mediator mass of the scalar (vector) model by approximately 800 (300) GeV when compared to the previous analysis of *mono-top* final states. The production of a single vector-like $T$ quark decaying into $tZ(\to \nu\bar{\nu})$ is excluded for masses of the singlet $T$ quark up to 1.8 TeV, assuming $\kappa_T = 0.5$. This limit outperforms previous results using the *mono-top* topology by approximately 400 GeV. This significant improvement partially comes from the refined object reconstruction and calibration, as well as the analysis strategy, optimising the event preselection and applying a XGBoost algorithm to improve the background discrimination. The increased dataset statistics also play a significant role in the improved sensitivity.


## Acknowledgments

We thank CERN for the very successful operation of the LHC and its injectors, as well as the support staff at CERN and at our institutions worldwide without whom ATLAS could not be operated efficiently.

The crucial computing support from all WLCG partners is acknowledged gratefully, in particular from CERN, the ATLAS Tier-1 facilities at TRIUMF/SFU (Canada), NDGF (Denmark, Norway, Sweden), CC-IN2P3 (France), KIT/GridKA (Germany), INFN-CNAF (Italy), NL-T1 (Netherlands), PIC (Spain), RAL (U.K.) and BNL (U.S.A.), the Tier-2 facilities worldwide and large non-WLCG resource providers. Major contributors of computing resources are listed in ref. [154].

We gratefully acknowledge the support of ANPCyT, Argentina; YerPhI, Armenia; ARC, Australia; BMWFW and FWF, Austria; ANAS, Azerbaijan; CNPq and FAPESP, Brazil; NSERC, NRC and CFI, Canada; CERN; ANID, Chile; CAS, MOST and NSFC, China; Minciencias, Colombia; MEYS CR, Czech Republic; DNRF and DNSRC, Denmark; IN2P3-CNRS and CEA-DRF/IRFU, France; SRNSFG, Georgia; BMBF, HGF and MPG, Germany; GSRI, Greece; RGC and Hong Kong SAR, China; ISF and Benoziyo Center, Israel; INFN, Italy; MEXT and JSPS, Japan; CNRST, Morocco; NWO, Netherlands; RCN, Norway; MEiN, Poland; FCT, Portugal; MNE/IFA, Romania; MESTD, Serbia; MSSR, Slovakia; ARRS and MIZŠ, Slovenia; DSI/NRF, South Africa; MICINN, Spain; SRC and Wallenberg Foundation, Sweden; SERI, SNSF and Cantons of Bern and Geneva, Switzerland; MOST, Taipei; TENMAK, Türkiye; STFC, United Kingdom; DOE and NSF, United States of America.




JHEP05(2024)263

Individual groups and members have received support from BCKDF, CANARIE, CRC and DRAC, Canada; CERN-CZ, PRIMUS 21/SCI/017 and UNCE SCI/013, Czech Republic; COST, ERC, ERDF, Horizon 2020, ICSC-NextGenerationEU and Marie Skłodowska-Curie Actions, European Union; Investissements d'Avenir Labex, Investissements d'Avenir Idex and ANR, France; DFG and AvH Foundation, Germany; Herakleitos, Thales and Aristeia programmes co-financed by EU-ESF and the Greek NSRF, Greece; BSF-NSF and MINERVA, Israel; Norwegian Financial Mechanism 2014-2021, Norway; NCN and NAWA, Poland; La Caixa Banking Foundation, CERCA Programme Generalitat de Catalunya and PROMETEO and GenT Programmes Generalitat Valenciana, Spain; Göran Gustafssons Stiftelse, Sweden; The Royal Society and Leverhulme Trust, United Kingdom.

In addition, individual members wish to acknowledge support from Chile: Agencia Nacional de Investigación y Desarrollo (FONDECYT 1190886, FONDECYT 1210400, FONDECYT 1230987); China: National Natural Science Foundation of China (NSFC — 12175119, NSFC 12275265, NSFC-12075060); European Union: European Research Council (ERC — 948254), Horizon 2020 Framework Programme (MUCCA — CHIST-ERA-19-XAI-00), Italian Center for High Performance Computing, Big Data and Quantum Computing (ICSC, NextGenerationEU), Marie Sklodowska-Curie Actions (EU H2020 MSC IF GRANT NO 101033496); France: Agence Nationale de la Recherche (ANR-20-CE31-0013, ANR-21-CE31-0013, ANR-21-CE31-0022), Investissements d'Avenir Idex (ANR-11-LABX-0012), Investissements d'Avenir Labex (ANR-11-LABX-0012); Germany: Baden-Württemberg Stiftung (BW Stiftung-Postdoc Eliteprogramme), Deutsche Forschungsgemeinschaft (DFG — 469666862, DFG — CR 312/5-1); Italy: Istituto Nazionale di Fisica Nucleare (FELLINI G.A. n. 754496, ICSC, NextGenerationEU); Japan: Japan Society for the Promotion of Science (JSPS KAKENHI 22H01227, JSPS KAKENHI 22KK0227, JSPS KAKENHI JP21H05085, JSPS KAKENHI JP22H04944); Netherlands: Netherlands Organisation for Scientific Research (NWO Veni 2020 — VI.Veni.202.179); Norway: Research Council of Norway (RCN-314472); Poland: Polish National Agency for Academic Exchange (PPN/PPO/2020/1/00002/U/00001), Polish National Science Centre (NCN 2021/42/E/ST2/00350, NCN OPUS nr 2022/47/B/ST2/03059, NCN UMO-2019/34/E/ST2/00393, UMO-2020/37/B/ST2/01043, UMO-2021/40/C/ST2/00187); Slovenia: Slovenian Research Agency (ARIS grant J1-3010); Spain: BBVA Foundation (LEO22-1-603), Generalitat Valenciana (Artemisa, FEDER, IDIFEDER/2018/048), La Caixa Banking Foundation (LCF/BQ/PI20/11760025), Ministry of Science and Innovation (RYC2019-028510-I, RYC2020-030254-I), PROMETEO and GenT Programmes Generalitat Valenciana (CIDEGENT/2019/023, CIDEGENT/2019/027); Sweden: Swedish Research Council (VR 2018-00482, VR 2022-03845, VR 2022-04683), Knut and Alice Wallenberg Foundation (KAW 2017.0100, KAW 2018.0157, KAW 2018.0458, KAW 2019.0447); Switzerland: Swiss National Science Foundation (SNSF — PCEFP2_194658); United Kingdom: Leverhulme Trust (Leverhulme Trust RPG-2020-004); United States of America: Neubauer Family Foundation.

**Open Access.** This article is distributed under the terms of the Creative Commons Attribution License (CC-BY4.0), which permits any use, distribution and reproduction in any medium, provided the original author(s) and source are credited.



JHEP05(2024)263

## References


[1] V. Trimble, *Existence and nature of dark matter in the universe*, *Ann. Rev. Astron. Astrophys.* **25** (1987) 425 [INSPIRE].

[2] J.L. Feng, *Dark matter candidates from particle physics and methods of detection*, *Ann. Rev. Astron. Astrophys.* **48** (2010) 495 [arXiv:1003.0904] [INSPIRE].

[3] G. Bertone, D. Hooper and J. Silk, *Particle dark matter: evidence, candidates and constraints*, *Phys. Rept.* **405** (2005) 279 [hep-ph/0404175] [INSPIRE].

[4] L. Susskind, *Dynamics of spontaneous symmetry breaking in the Weinberg-Salam theory*, *Phys. Rev. D* **20** (1979) 2619 [INSPIRE].

[5] D. Abercrombie et al., *Dark matter benchmark models for early LHC run-2 searches: report of the ATLAS/CMS dark matter forum*, *Phys. Dark Univ.* **27** (2020) 100371 [arXiv:1507.00966] [INSPIRE].

[6] J. Andrea, B. Fuks and F. Maltoni, *Monotops at the LHC*, *Phys. Rev. D* **84** (2011) 074025 [arXiv:1106.6199] [INSPIRE].

[7] D. Pinna, A. Zucchetta, M.R. Buckley and F. Canelli, *Single top quarks and dark matter*, *Phys. Rev. D* **96** (2017) 035031 [arXiv:1701.05195] [INSPIRE].

[8] P. Pani and G. Polesello, *Dark matter production in association with a single top-quark at the LHC in a two-Higgs-doublet model with a pseudoscalar mediator*, *Phys. Dark Univ.* **21** (2018) 8 [arXiv:1712.03874] [INSPIRE].

[9] J.A. Aguilar-Saavedra, *Identifying top partners at LHC*, *JHEP* **11** (2009) 030 [arXiv:0907.3155] [INSPIRE].

[10] O. Matsedonskyi, G. Panico and A. Wulzer, *On the interpretation of top partners searches*, *JHEP* **12** (2014) 097 [arXiv:1409.0100] [INSPIRE].

[11] M. Buchkremer, G. Cacciapaglia, A. Deandrea and L. Panizzi, *Model independent framework for searches of top partners*, *Nucl. Phys. B* **876** (2013) 376 [arXiv:1305.4172] [INSPIRE].

[12] WMAP collaboration, *Nine-year Wilkinson Microwave Anisotropy Probe (WMAP) observations: cosmological parameter results*, *Astrophys. J. Suppl.* **208** (2013) 19 [arXiv:1212.5226] [INSPIRE].

[13] Planck collaboration, *Planck* 2018 *results. I. Overview and the cosmological legacy of Planck*, *Astron. Astrophys.* **641** (2020) A1 [arXiv:1807.06205] [INSPIRE].

[14] G. Steigman and M.S. Turner, *Cosmological constraints on the properties of weakly interacting massive particles*, *Nucl. Phys. B* **253** (1985) 375 [INSPIRE].

[15] ATLAS collaboration, *Search for new phenomena in events with an energetic jet and missing transverse momentum in pp collisions at* $\sqrt{s} = 13$ *TeV with the ATLAS detector*, *Phys. Rev. D* **103** (2021) 112006 [arXiv:2102.10874] [INSPIRE].

[16] CMS collaboration, *Search for new particles in events with energetic jets and large missing transverse momentum in proton-proton collisions at* $\sqrt{s} = 13$ *TeV*, *JHEP* **11** (2021) 153 [arXiv:2107.13021] [INSPIRE].

[17] ATLAS collaboration, *Search for dark matter in association with an energetic photon in pp collisions at* $\sqrt{s} = 13$ *TeV with the ATLAS detector*, *JHEP* **02** (2021) 226 [arXiv:2011.05259] [INSPIRE].




JHEP05(2024)263

[18] CMS collaboration, *Search for new physics in final states with a single photon and missing transverse momentum in proton-proton collisions at* $\sqrt{s} = 13$ *TeV*, *JHEP* **02** (2019) 074 [arXiv:1810.00196] [INSPIRE].

[19] ATLAS collaboration, *Search for associated production of a Z boson with an invisibly decaying Higgs boson or dark matter candidates at* $\sqrt{s} = 13$ *TeV with the ATLAS detector*, *Phys. Lett. B* **829** (2022) 137066 [arXiv:2111.08372] [INSPIRE].

[20] CMS collaboration, *Search for dark matter produced in association with a leptonically decaying Z boson in proton-proton collisions at* $\sqrt{s} = 13$ *TeV*, *Eur. Phys. J. C* **81** (2021) 13 [*Erratum ibid.* **81** (2021) 333] [arXiv:2008.04735] [INSPIRE].

[21] ATLAS collaboration, *Search for dark matter in events with a hadronically decaying vector boson and missing transverse momentum in pp collisions at* $\sqrt{s} = 13$ *TeV with the ATLAS detector*, *JHEP* **10** (2018) 180 [arXiv:1807.11471] [INSPIRE].

[22] CMS collaboration, *Search for new physics in final states with an energetic jet or a hadronically decaying W or Z boson and transverse momentum imbalance at* $\sqrt{s} = 13$ *TeV*, *Phys. Rev. D* **97** (2018) 092005 [arXiv:1712.02345] [INSPIRE].

[23] ATLAS collaboration, *Search for dark matter produced in association with a Standard Model Higgs boson decaying into b-quarks using the full run* 2 *dataset from the ATLAS detector*, *JHEP* **11** (2021) 209 [arXiv:2108.13391] [INSPIRE].

[24] ATLAS collaboration, *Search for dark matter in events with missing transverse momentum and a Higgs boson decaying into two photons in pp collisions at* $\sqrt{s} = 13$ *TeV with the ATLAS detector*, *JHEP* **10** (2021) 013 [arXiv:2104.13240] [INSPIRE].

[25] CMS collaboration, *Search for dark matter particles produced in association with a Higgs boson in proton-proton collisions at* $\sqrt{s} = 13$ *TeV*, *JHEP* **03** (2020) 025 [arXiv:1908.01713] [INSPIRE].

[26] ATLAS collaboration, *Search for new phenomena in final states with b-jets and missing transverse momentum in* $\sqrt{s} = 13$ *TeV pp collisions with the ATLAS detector*, *JHEP* **05** (2021) 093 [arXiv:2101.12527] [INSPIRE].

[27] CMS collaboration, *Search for supersymmetry in proton-proton collisions at* 13 *TeV in final states with jets and missing transverse momentum*, *JHEP* **10** (2019) 244 [arXiv:1908.04722] [INSPIRE].

[28] ATLAS collaboration, *Search for new phenomena in events with two opposite-charge leptons, jets and missing transverse momentum in pp collisions at* $\sqrt{s} = 13$ *TeV with the ATLAS detector*, *JHEP* **04** (2021) 165 [arXiv:2102.01444] [INSPIRE].

[29] CMS collaboration, *Search for dark matter particles produced in association with a top quark pair at* $\sqrt{s} = 13$ *TeV*, *Phys. Rev. Lett.* **122** (2019) 011803 [arXiv:1807.06522] [INSPIRE].

[30] CMS collaboration, *Search for dark matter produced in association with a single top quark or a top quark pair in proton-proton collisions at* $\sqrt{s} = 13$ *TeV*, *JHEP* **03** (2019) 141 [arXiv:1901.01553] [INSPIRE].

[31] ATLAS collaboration, *Constraints on spin-*0 *dark matter mediators and invisible Higgs decays using ATLAS* 13 *TeV pp collision data with two top quarks and missing transverse momentum in the final state*, *Eur. Phys. J. C* **83** (2023) 503 [arXiv:2211.05426] [INSPIRE].

[32] ATLAS collaboration, *Search for dark matter produced in association with a single top quark in* $\sqrt{s} = 13$ *TeV pp collisions with the ATLAS detector*, *Eur. Phys. J. C* **81** (2021) 860 [arXiv:2011.09308] [INSPIRE].



JHEP05(2024)263

[33] ATLAS collaboration, *Search for dark matter produced in association with a single top quark and an energetic $W$ boson in $\sqrt{s} = 13$ TeV pp collisions with the ATLAS detector*, *Eur. Phys. J. C* **83** (2023) 603 [arXiv:2211.13138] [INSPIRE].

[34] ATLAS collaboration, *Search for new phenomena in events with same-charge leptons and b-jets in pp collisions at $\sqrt{s} = 13$ TeV with the ATLAS detector*, *JHEP* **12** (2018) 039 [arXiv:1807.11883] [INSPIRE].

[35] T. Aaltonen et al., *Search for a dark matter candidate produced in association with a single top quark in $p\bar{p}$ collisions at $\sqrt{s} = 1.96$ TeV*, *Phys. Rev. Lett.* **108** (2012) 201802 [arXiv:1202.5653].

[36] CMS collaboration, *Search for monotop signatures in proton-proton collisions at $\sqrt{s} = 8$ TeV*, *Phys. Rev. Lett.* **114** (2015) 101801 [arXiv:1410.1149] [INSPIRE].

[37] ATLAS collaboration, *Search for invisible particles produced in association with single-top-quarks in proton-proton collisions at $\sqrt{s} = 8$ TeV with the ATLAS detector*, *Eur. Phys. J. C* **75** (2015) 79 [arXiv:1410.5404] [INSPIRE].

[38] CMS collaboration, *Search for dark matter in events with energetic, hadronically decaying top quarks and missing transverse momentum at $\sqrt{s} = 13$ TeV*, *JHEP* **06** (2018) 027 [arXiv:1801.08427] [INSPIRE].

[39] ATLAS collaboration, *Search for large missing transverse momentum in association with one top-quark in proton-proton collisions at $\sqrt{s} = 13$ TeV with the ATLAS detector*, *JHEP* **05** (2019) 041 [arXiv:1812.09743] [INSPIRE].

[40] N. Arkani-Hamed, A.G. Cohen, E. Katz and A.E. Nelson, *The littlest Higgs*, *JHEP* **07** (2002) 034 [hep-ph/0206021] [INSPIRE].

[41] M. Schmaltz and D. Tucker-Smith, *Little Higgs review*, *Ann. Rev. Nucl. Part. Sci.* **55** (2005) 229 [hep-ph/0502182] [INSPIRE].

[42] D.B. Kaplan, H. Georgi and S. Dimopoulos, *Composite Higgs scalars*, *Phys. Lett. B* **136** (1984) 187 [INSPIRE].

[43] K. Agashe, R. Contino and A. Pomarol, *The minimal composite Higgs model*, *Nucl. Phys. B* **719** (2005) 165 [hep-ph/0412089] [INSPIRE].

[44] F. del Aguila and M.J. Bowick, *The possibility of new fermions with $\Delta I = 0$ mass*, *Nucl. Phys. B* **224** (1983) 107 [INSPIRE].

[45] F. del Aguila, M. Perez-Victoria and J. Santiago, *Effective description of quark mixing*, *Phys. Lett. B* **492** (2000) 98 [hep-ph/0007160] [INSPIRE].

[46] F. del Aguila, M. Pérez-Victoria and J. Santiago, *Observable contributions of new exotic quarks to quark mixing*, *JHEP* **09** (2000) 011 [hep-ph/0007316] [INSPIRE].

[47] A. Atre, M. Carena, T. Han and J. Santiago, *Heavy quarks above the top at the Tevatron*, *Phys. Rev. D* **79** (2009) 054018 [arXiv:0806.3966] [INSPIRE].

[48] A. Atre et al., *Model-independent searches for new quarks at the LHC*, *JHEP* **08** (2011) 080 [arXiv:1102.1987] [INSPIRE].

[49] CMS collaboration, *Search for a vector-like quark with charge 2/3 in $t + Z$ events from pp collisions at $\sqrt{s} = 7$ TeV*, *Phys. Rev. Lett.* **107** (2011) 271802 [arXiv:1109.4985] [INSPIRE].

[50] CMS collaboration, *Search for pair produced fourth-generation up-type quarks in pp collisions at $\sqrt{s} = 7$ TeV with a lepton in the final state*, *Phys. Lett. B* **718** (2012) 307 [arXiv:1209.0471] [INSPIRE].



JHEP05(2024)263

[51] ATLAS collaboration, *Search for pair production of a new quark that decays to a Z boson and a bottom quark with the ATLAS detector*, *Phys. Rev. Lett.* **109** (2012) 071801 [arXiv:1204.1265] [INSPIRE].

[52] CMS collaboration, *Search for vector-like charge 2/3 T quarks in proton-proton collisions at* $\sqrt{s} = 8$ *TeV*, *Phys. Rev. D* **93** (2016) 012003 [arXiv:1509.04177] [INSPIRE].

[53] CMS collaboration, *Search for pair-produced vectorlike B quarks in proton-proton collisions at* $\sqrt{s} = 8$ *TeV*, *Phys. Rev. D* **93** (2016) 112009 [arXiv:1507.07129] [INSPIRE].

[54] ATLAS collaboration, *Search for pair production of a new heavy quark that decays into a W boson and a light quark in pp collisions at* $\sqrt{s} = 8$ *TeV with the ATLAS detector*, *Phys. Rev. D* **92** (2015) 112007 [arXiv:1509.04261] [INSPIRE].

[55] ATLAS collaboration, *Search for production of vector-like quark pairs and of four top quarks in the lepton-plus-jets final state in pp collisions at* $\sqrt{s} = 8$ *TeV with the ATLAS detector*, *JHEP* **08** (2015) 105 [arXiv:1505.04306] [INSPIRE].

[56] ATLAS collaboration, *Search for pair production of vector-like top quarks in events with one lepton, jets, and missing transverse momentum in* $\sqrt{s} = 13$ *TeV pp collisions with the ATLAS detector*, *JHEP* **08** (2017) 052 [arXiv:1705.10751] [INSPIRE].

[57] CMS collaboration, *Search for pair production of vector-like T and B quarks in single-lepton final states using boosted jet substructure in proton-proton collisions at* $\sqrt{s} = 13$ *TeV*, *JHEP* **11** (2017) 085 [arXiv:1706.03408] [INSPIRE].

[58] CMS collaboration, *Search for pair production of vector-like quarks in the* $bW\bar{b}W$ *channel from proton-proton collisions at* $\sqrt{s} = 13$ *TeV*, *Phys. Lett. B* **779** (2018) 82 [arXiv:1710.01539] [INSPIRE].

[59] CMS collaboration, *Search for vector-like T and B quark pairs in final states with leptons at* $\sqrt{s} = 13$ *TeV*, *JHEP* **08** (2018) 177 [arXiv:1805.04758] [INSPIRE].

[60] CMS collaboration, *Search for vector-like quarks in events with two oppositely charged leptons and jets in proton-proton collisions at* $\sqrt{s} = 13$ *TeV*, *Eur. Phys. J. C* **79** (2019) 364 [arXiv:1812.09768] [INSPIRE].

[61] ATLAS collaboration, *Search for pair production of heavy vector-like quarks decaying to high-*$p_T$ *W bosons and b quarks in the lepton-plus-jets final state in pp collisions at* $\sqrt{s} = 13$ *TeV with the ATLAS detector*, *JHEP* **10** (2017) 141 [arXiv:1707.03347] [INSPIRE].

[62] ATLAS collaboration, *Search for pair production of up-type vector-like quarks and for four-top-quark events in final states with multiple b-jets with the ATLAS detector*, *JHEP* **07** (2018) 089 [arXiv:1803.09678] [INSPIRE].

[63] ATLAS collaboration, *Search for pair production of heavy vector-like quarks decaying into high-*$p_T$ *W bosons and top quarks in the lepton-plus-jets final state in pp collisions at* $\sqrt{s} = 13$ *TeV with the ATLAS detector*, *JHEP* **08** (2018) 048 [arXiv:1806.01762] [INSPIRE].

[64] ATLAS collaboration, *Combination of the searches for pair-produced vector-like partners of the third-generation quarks at* $\sqrt{s} = 13$ *TeV with the ATLAS detector*, *Phys. Rev. Lett.* **121** (2018) 211801 [arXiv:1808.02343] [INSPIRE].

[65] ATLAS collaboration, *Search for pair-production of vector-like quarks in pp collision events at* $\sqrt{s} = 13$ *TeV with at least one leptonically decaying Z boson and a third-generation quark with the ATLAS detector*, *Phys. Lett. B* **843** (2023) 138019 [arXiv:2210.15413] [INSPIRE].

[66] CMS collaboration, *Search for pair production of vectorlike quarks in the fully hadronic final state*, *Phys. Rev. D* **100** (2019) 072001 [arXiv:1906.11903] [INSPIRE].

JHEP05(2024)263

[67] ATLAS collaboration, *Search for single production of vector-like quarks decaying into $Wb$ in pp collisions at $\sqrt{s} = 8$ TeV with the ATLAS detector*, *Eur. Phys. J. C* **76** (2016) 442 [arXiv:1602.05606] [INSPIRE].

[68] ATLAS collaboration, *Search for the production of single vector-like and excited quarks in the $Wt$ final state in pp collisions at $\sqrt{s} = 8$ TeV with the ATLAS detector*, *JHEP* **02** (2016) 110 [arXiv:1510.02664] [INSPIRE].

[69] ATLAS collaboration, *Search for single production of vector-like $T$ quarks decaying into $Ht$ or $Zt$ in pp collisions at $\sqrt{s} = 13$ TeV with the ATLAS detector*, *JHEP* **08** (2023) 153 [arXiv:2305.03401] [INSPIRE].

[70] ATLAS collaboration, *Search for singly produced vector-like top partners in multilepton final states with 139 $fb^{-1}$ of pp collision data at $\sqrt{s} = 13$ TeV with the ATLAS detector*, arXiv:2307.07584 [INSPIRE].

[71] CMS collaboration, *Search for single production of a heavy vector-like $T$ quark decaying to a Higgs boson and a top quark with a lepton and jets in the final state*, *Phys. Lett. B* **771** (2017) 80 [arXiv:1612.00999] [INSPIRE].

[72] CMS collaboration, *Search for single production of vector-like quarks decaying to a $Z$ boson and a top or a bottom quark in proton-proton collisions at $\sqrt{s} = 13$ TeV*, *JHEP* **05** (2017) 029 [arXiv:1701.07409] [INSPIRE].

[73] CMS collaboration, *Search for electroweak production of a vector-like quark decaying to a top quark and a Higgs boson using boosted topologies in fully hadronic final states*, *JHEP* **04** (2017) 136 [arXiv:1612.05336] [INSPIRE].

[74] CMS collaboration, *Search for a heavy resonance decaying to a top quark and a vector-like top quark at $\sqrt{s} = 13$ TeV*, *JHEP* **09** (2017) 053 [arXiv:1703.06352] [INSPIRE].

[75] CMS collaboration, *Search for single production of a vector-like $T$ quark decaying to a $Z$ boson and a top quark in proton-proton collisions at $\sqrt{s} = 13$ TeV*, *Phys. Lett. B* **781** (2018) 574 [arXiv:1708.01062] [INSPIRE].

[76] CMS collaboration, *Search for single production of vector-like quarks decaying to a top quark and a $W$ boson in proton-proton collisions at $\sqrt{s} = 13$ TeV*, *Eur. Phys. J. C* **79** (2019) 90 [arXiv:1809.08597] [INSPIRE].

[77] CMS collaboration, *Search for electroweak production of a vector-like $T$ quark using fully hadronic final states*, *JHEP* **01** (2020) 036 [arXiv:1909.04721] [INSPIRE].

[78] J.A. Aguilar-Saavedra, R. Benbrik, S. Heinemeyer and M. Pérez-Victoria, *Handbook of vectorlike quarks: mixing and single production*, *Phys. Rev. D* **88** (2013) 094010 [arXiv:1306.0572] [INSPIRE].

[79] T. Chen and C. Guestrin, *XGBoost: a scalable tree boosting system*, arXiv:1603.02754 [DOI:10.1145/2939672.2939785] [INSPIRE].

[80] J. Wang, C.S. Li, D.Y. Shao and H. Zhang, *Search for the signal of monotop production at the early LHC*, *Phys. Rev. D* **86** (2012) 034008 [arXiv:1109.5963] [INSPIRE].

[81] *Feynrules model database*, https://feynrules.irmp.ucl.ac.be/wiki/Monotops.

[82] *Feynrules model database*, https://feynrules.irmp.ucl.ac.be/wiki/VLQ.

[83] ATLAS collaboration, *The ATLAS experiment at the CERN Large Hadron Collider*, 2008 *JINST* **3** S08003 [INSPIRE].

JHEP05(2024)263

[84] ATLAS collaboration, *ATLAS Insertable B-Layer technical design report*, CERN-LHCC-2010-013, CERN, Geneva, Switzerland (2010).

[85] ATLAS IBL collaboration, *Production and integration of the ATLAS Insertable B-Layer*, 2018 *JINST* **13** T05008 [arXiv:1803.00844] [INSPIRE].

[86] G. Avoni et al., *The new LUCID-2 detector for luminosity measurement and monitoring in ATLAS*, 2018 *JINST* **13** P07017 [INSPIRE].

[87] ATLAS collaboration, *Performance of the ATLAS trigger system in* 2015, *Eur. Phys. J. C* **77** (2017) 317 [arXiv:1611.09661] [INSPIRE].

[88] ATLAS collaboration, *The ATLAS collaboration software and firmware*, ATL-SOFT-PUB-2021-001, CERN, Geneva, Switzerland (2021).

[89] ATLAS collaboration, *Performance of the missing transverse momentum triggers for the ATLAS detector during run-2 data taking*, *JHEP* **08** (2020) 080 [arXiv:2005.09554] [INSPIRE].

[90] J. Alwall et al., *MadGraph 5: going beyond*, *JHEP* **06** (2011) 128 [arXiv:1106.0522] [INSPIRE].

[91] A. Alloul et al., *FeynRules 2.0 — a complete toolbox for tree-level phenomenology*, *Comput. Phys. Commun.* **185** (2014) 2250 [arXiv:1310.1921] [INSPIRE].

[92] NNPDF collaboration, *Parton distributions for the LHC run II*, *JHEP* **04** (2015) 040 [arXiv:1410.8849] [INSPIRE].

[93] T. Sjöstrand et al., *An introduction to PYTHIA 8.2*, *Comput. Phys. Commun.* **191** (2015) 159 [arXiv:1410.3012] [INSPIRE].

[94] ATLAS collaboration, *ATLAS PYTHIA 8 tunes to 7 TeV data*, ATL-PHYS-PUB-2014-021, CERN, Geneva, Switzerland (2014).

[95] R.D. Ball et al., *Parton distributions with LHC data*, *Nucl. Phys. B* **867** (2013) 244 [arXiv:1207.1303] [INSPIRE].

[96] G. Cacciapaglia et al., *Next-to-leading-order predictions for single vector-like quark production at the LHC*, *Phys. Lett. B* **793** (2019) 206 [arXiv:1811.05055] [INSPIRE].

[97] A. Roy, N. Nikiforou, N. Castro and T. Andeen, *Novel interpretation strategy for searches of singly produced vectorlike quarks at the LHC*, *Phys. Rev. D* **101** (2020) 115027 [arXiv:2003.00640] [INSPIRE].

[98] P. Nason, *A new method for combining NLO QCD with shower Monte Carlo algorithms*, *JHEP* **11** (2004) 040 [hep-ph/0409146] [INSPIRE].

[99] S. Frixione, P. Nason and C. Oleari, *Matching NLO QCD computations with parton shower simulations: the POWHEG method*, *JHEP* **11** (2007) 070 [arXiv:0709.2092] [INSPIRE].

[100] S. Alioli, P. Nason, C. Oleari and E. Re, *A general framework for implementing NLO calculations in shower Monte Carlo programs: the POWHEG BOX*, *JHEP* **06** (2010) 043 [arXiv:1002.2581] [INSPIRE].

[101] M. Czakon and A. Mitov, *Top++: a program for the calculation of the top-pair cross-section at hadron colliders*, *Comput. Phys. Commun.* **185** (2014) 2930 [arXiv:1112.5675] [INSPIRE].

[102] T. Gleisberg et al., *Event generation with SHERPA 1.1*, *JHEP* **02** (2009) 007 [arXiv:0811.4622] [INSPIRE].

[103] T. Gleisberg and S. Höche, *Comix, a new matrix element generator*, *JHEP* **12** (2008) 039 [arXiv:0808.3674] [INSPIRE].



JHEP05(2024)263

[104] F. Cascioli, P. Maierhöfer and S. Pozzorini, *Scattering amplitudes with OpenLoops*, *Phys. Rev. Lett.* **108** (2012) 111601 [arXiv:1111.5206] [INSPIRE].

[105] S. Höche, F. Krauss, M. Schönherr and F. Siegert, *A critical appraisal of NLO+PS matching methods*, *JHEP* **09** (2012) 049 [arXiv:1111.1220] [INSPIRE].

[106] S. Catani, F. Krauss, R. Kuhn and B.R. Webber, *QCD matrix elements + parton showers*, *JHEP* **11** (2001) 063 [hep-ph/0109231] [INSPIRE].

[107] S. Höche, F. Krauss, S. Schumann and F. Siegert, *QCD matrix elements and truncated showers*, *JHEP* **05** (2009) 053 [arXiv:0903.1219] [INSPIRE].

[108] S. Höche, F. Krauss, M. Schönherr and F. Siegert, *QCD matrix elements + parton showers: the NLO case*, *JHEP* **04** (2013) 027 [arXiv:1207.5030] [INSPIRE].

[109] C. Anastasiou, L.J. Dixon, K. Melnikov and F. Petriello, *High precision QCD at hadron colliders: electroweak gauge boson rapidity distributions at NNLO*, *Phys. Rev. D* **69** (2004) 094008 [hep-ph/0312266] [INSPIRE].

[110] S. Frixione et al., *Single-top hadroproduction in association with a W boson*, *JHEP* **07** (2008) 029 [arXiv:0805.3067] [INSPIRE].

[111] G. Bordes and B. van Eijk, *Calculating QCD corrections to single top production in hadronic interactions*, *Nucl. Phys. B* **435** (1995) 23 [INSPIRE].

[112] T. Stelzer, Z. Sullivan and S. Willenbrock, *Single top quark production at hadron colliders*, *Phys. Rev. D* **58** (1998) 094021 [hep-ph/9807340] [INSPIRE].

[113] T. Stelzer, Z. Sullivan and S. Willenbrock, *Single top quark production via W-gluon fusion at next-to-leading order*, *Phys. Rev. D* **56** (1997) 5919 [hep-ph/9705398] [INSPIRE].

[114] N. Kidonakis, *Next-to-next-to-leading-order collinear and soft gluon corrections for t-channel single top quark production*, *Phys. Rev. D* **83** (2011) 091503 [arXiv:1103.2792] [INSPIRE].

[115] N. Kidonakis, *NNLL resummation for s-channel single top quark production*, *Phys. Rev. D* **81** (2010) 054028 [arXiv:1001.5034] [INSPIRE].

[116] N. Kidonakis, *Two-loop soft anomalous dimensions for single top quark associated production with a $W^-$ or $H^-$*, *Phys. Rev. D* **82** (2010) 054018 [arXiv:1005.4451] [INSPIRE].

[117] J. Alwall et al., *The automated computation of tree-level and next-to-leading order differential cross sections, and their matching to parton shower simulations*, *JHEP* **07** (2014) 079 [arXiv:1405.0301] [INSPIRE].

[118] D.J. Lange, *The EvtGen particle decay simulation package*, *Nucl. Instrum. Meth. A* **462** (2001) 152 [INSPIRE].

[119] ATLAS collaboration, *The PYTHIA 8 A3 tune description of ATLAS minimum bias and inelastic measurements incorporating the Donnachie-Landshoff diffractive model*, ATL-PHYS-PUB-2016-017, CERN, Geneva, Switzerland (2016).

[120] ATLAS collaboration, *The ATLAS simulation infrastructure*, *Eur. Phys. J. C* **70** (2010) 823 [arXiv:1005.4568] [INSPIRE].

[121] GEANT4 collaboration, *GEANT4 — a simulation toolkit*, *Nucl. Instrum. Meth. A* **506** (2003) 250 [INSPIRE].

[122] ATLAS collaboration, *Electron and photon performance measurements with the ATLAS detector using the* 2015–2017 *LHC proton-proton collision data*, 2019 *JINST* **14** P12006 [arXiv:1908.00005] [INSPIRE].

JHEP05(2024)263

[123] ATLAS collaboration, *Muon reconstruction and identification efficiency in ATLAS using the full run 2 pp collision data set at* $\sqrt{s} = 13$ *TeV*, *Eur. Phys. J. C* **81** (2021) 578 [arXiv:2012.00578] [INSPIRE].

[124] M. Cacciari, G.P. Salam and G. Soyez, *The anti-*$k_t$ *jet clustering algorithm*, *JHEP* **04** (2008) 063 [arXiv:0802.1189] [INSPIRE].

[125] M. Cacciari, G.P. Salam and G. Soyez, *FastJet user manual*, *Eur. Phys. J. C* **72** (2012) 1896 [arXiv:1111.6097] [INSPIRE].

[126] ATLAS collaboration, *Topological cell clustering in the ATLAS calorimeters and its performance in LHC run* 1, *Eur. Phys. J. C* **77** (2017) 490 [arXiv:1603.02934] [INSPIRE].

[127] ATLAS collaboration, *Jet reconstruction and performance using particle flow with the ATLAS detector*, *Eur. Phys. J. C* **77** (2017) 466 [arXiv:1703.10485] [INSPIRE].

[128] ATLAS collaboration, *In situ calibration of large-radius jet energy and mass in* 13 *TeV proton-proton collisions with the ATLAS detector*, *Eur. Phys. J. C* **79** (2019) 135 [arXiv:1807.09477] [INSPIRE].

[129] ATLAS collaboration, *Jet energy scale and resolution measured in proton-proton collisions at* $\sqrt{s} = 13$ *TeV with the ATLAS detector*, *Eur. Phys. J. C* **81** (2021) 689 [arXiv:2007.02645] [INSPIRE].

[130] ATLAS collaboration, *Performance of pile-up mitigation techniques for jets in pp collisions at* $\sqrt{s} = 8$ *TeV using the ATLAS detector*, *Eur. Phys. J. C* **76** (2016) 581 [arXiv:1510.03823] [INSPIRE].

[131] ATLAS collaboration, *ATLAS flavour-tagging algorithms for the LHC run* 2 *pp collision dataset*, *Eur. Phys. J. C* **83** (2023) 681 [arXiv:2211.16345] [INSPIRE].

[132] D. Krohn, J. Thaler and L.-T. Wang, *Jet trimming*, *JHEP* **02** (2010) 084 [arXiv:0912.1342] [INSPIRE].

[133] ATLAS collaboration, *Performance of top-quark and* $W$*-boson tagging with ATLAS in run* 2 *of the LHC*, *Eur. Phys. J. C* **79** (2019) 375 [arXiv:1808.07858] [INSPIRE].

[134] ATLAS collaboration, *Boosted hadronic vector boson and top quark tagging with ATLAS using run* 2 *data*, ATL-PHYS-PUB-2020-017, CERN, Geneva, Switzerland (2020).

[135] ATLAS collaboration, *The performance of missing transverse momentum reconstruction and its significance with the ATLAS detector using* $140\,fb^{-1}$ *of* $\sqrt{s} = 13$ *TeV pp collisions*, arXiv:2402.05858 [INSPIRE].

[136] ATLAS collaboration, *Selection of jets produced in* 13 *TeV proton-proton collisions with the ATLAS detector*, ATLAS-CONF-2015-029, CERN, Geneva, Switzerland (2015).

[137] ATLAS collaboration, *Luminosity determination in pp collisions at* $\sqrt{s} = 13$ *TeV using the ATLAS detector at the LHC*, ATLAS-CONF-2019-021, CERN, Geneva, Switzerland (2019).

[138] ATLAS collaboration, *ATLAS b-jet identification performance and efficiency measurement with* $t\bar{t}$ *events in pp collisions at* $\sqrt{s} = 13$ *TeV*, *Eur. Phys. J. C* **79** (2019) 970 [arXiv:1907.05120] [INSPIRE].

[139] ATLAS collaboration, *Measurement of the c-jet mistagging efficiency in* $t\bar{t}$ *events using pp collision data at* $\sqrt{s} = 13$ *TeV collected with the ATLAS detector*, *Eur. Phys. J. C* **82** (2022) 95 [arXiv:2109.10627] [INSPIRE].



JHEP05(2024)263

[140] ATLAS collaboration, *Calibration of the light-flavour jet mistagging efficiency of the b-tagging algorithms with Z+jets events using* 139 $fb^{-1}$ *of ATLAS proton-proton collision data at* $\sqrt{s} = 13$ *TeV*, *Eur. Phys. J. C* **83** (2023) 728 [arXiv:2301.06319] [INSPIRE].

[141] J. Bellm et al., *Herwig* 7.1 *release note*, arXiv:1705.06919 [INSPIRE].

[142] ATLAS collaboration, *ATLAS simulation of boson plus jets processes in run* 2, ATL-PHYS-PUB-2017-006, CERN, Geneva, Switzerland (2017).

[143] J. Butterworth et al., *PDF4LHC recommendations for LHC run II*, *J. Phys. G* **43** (2016) 023001 [arXiv:1510.03865] [INSPIRE].

[144] P. Kant et al., *HatHor for single top-quark production: updated predictions and uncertainty estimates for single top-quark production in hadronic collisions*, *Comput. Phys. Commun.* **191** (2015) 74 [arXiv:1406.4403] [INSPIRE].

[145] N. Kidonakis, *Two-loop soft anomalous dimensions for single top quark associated production with a* $W^-$ *or* $H^-$, *Phys. Rev. D* **82** (2010) 054018 [arXiv:1005.4451] [INSPIRE].

[146] N. Kidonakis, *Top quark production*, in *Proceedings, Helmholtz international summer school on physics of heavy quarks and hadrons*, (2013).

[147] ATLAS collaboration, *Multi-boson simulation for* 13 *TeV ATLAS analyses*, ATL-PHYS-PUB-2016-002, CERN, Geneva, Switzerland (2016).

[148] LHC Higgs Cross Section Working Group collaboration, *Handbook of LHC Higgs cross sections:* 4. *Deciphering the nature of the Higgs sector*, arXiv:1610.07922 [DOI:10.23731/CYRM-2017-002] [INSPIRE].

[149] ATLAS collaboration, *Modelling of the* $t\bar{t}H$ *and* $t\bar{t}V$ $(V = W, Z)$ *processes for* $\sqrt{s} = 13$ *TeV ATLAS analyses*, ATL-PHYS-PUB-2016-005, CERN, Geneva, Switzerland (2016).

[150] W. Verkerke and D.P. Kirkby, *The RooFit toolkit for data modeling*, *eConf C* **0303241** (2003) MOLT007 [physics/0306116] [INSPIRE].

[151] T. Junk, *Confidence level computation for combining searches with small statistics*, *Nucl. Instrum. Meth. A* **434** (1999) 435 [hep-ex/9902006] [INSPIRE].

[152] A.L. Read, *Presentation of search results: the* $CL_s$ *technique*, *J. Phys. G* **28** (2002) 2693 [INSPIRE].

[153] G. Cowan, K. Cranmer, E. Gross and O. Vitells, *Asymptotic formulae for likelihood-based tests of new physics*, *Eur. Phys. J. C* **71** (2011) 1554 [*Erratum ibid.* **73** (2013) 2501] [arXiv:1007.1727] [INSPIRE].

[154] ATLAS collaboration, *ATLAS computing acknowledgements*, ATL-SOFT-PUB-2023-001, CERN, Geneva, Switzerland (2023).

JHEP05(2024)263

## The ATLAS collaboration

G. Aad[102], B. Abbott[120], K. Abeling[55], N.J. Abicht[49], S.H. Abidi[29], A. Aboulhorma[35e], H. Abramowicz[151], H. Abreu[150], Y. Abulaiti[117], B.S. Acharya[69a,69b,m], C. Adam Bourdarios[4], L. Adamczyk[86a], S.V. Addepalli[26], M.J. Addison[101], J. Adelman[115], A. Adiguzel[21c], T. Adye[134], A.A. Affolder[136], Y. Afik[39], M.N. Agaras[13], J. Agarwala[73a,73b], A. Aggarwal[100], C. Agheorghiesei[27c], A. Ahmad[36], F. Ahmadov[38,z], W.S. Ahmed[104], S. Ahuja[95], X. Ai[62e], G. Aielli[76a,76b], A. Aikot[163], M. Ait Tamlihat[35e], B. Aitbenchikh[35a], I. Aizenberg[169], M. Akbiyik[100], T.P.A. Åkesson[98], A.V. Akimov[37], D. Akiyama[168], N.N. Akolkar[24], S. Aktas[21a], K. Al Khoury[41], G.L. Alberghi[23b], J. Albert[165], P. Albicocco[53], G.L. Albouy[60], S. Alderweireldt[52], Z.L. Alegria[121], M. Aleksa[36], I.N. Aleksandrov[38], C. Alexa[27b], T. Alexopoulos[10], F. Alfonsi[23b], M. Algren[56], M. Alhroob[120], B. Ali[132], H.M.J. Ali[91], S. Ali[148], S.W. Alibocus[92], M. Aliev[145], G. Alimonti[71a], W. Alkakhi[55], C. Allaire[66], B.M.M. Allbrooke[146], J.F. Allen[52], C.A. Allendes Flores[137f], P.P. Allport[20], A. Aloisio[72a,72b], F. Alonso[90], C. Alpigiani[138], M. Alvarez Estevez[99], A. Alvarez Fernandez[100], M. Alves Cardoso[56], M.G. Alviggi[72a,72b], M. Aly[101], Y. Amaral Coutinho[83b], A. Ambler[104], C. Amelung[36], M. Amerl[101], C.G. Ames[109], D. Amidei[106], S.P. Amor Dos Santos[130a], K.R. Amos[163], V. Ananiev[125], C. Anastopoulos[139], T. Andeen[11], J.K. Anders[36], S.Y. Andrean[47a,47b], A. Andreazza[71a,71b], S. Angelidakis[9], A. Angerami[41,ac], A.V. Anisenkov[37], A. Annovi[74a], C. Antel[56], M.T. Anthony[139], E. Antipov[145], M. Antonelli[53], F. Anulli[75a], M. Aoki[84], T. Aoki[153], J.A. Aparisi Pozo[163], M.A. Aparo[146], L. Aperio Bella[48], C. Appelt[18], A. Apyan[26], N. Aranzabal[36], S.J. Arbiol Val[87], C. Arcangeletti[53], A.T.H. Arce[51], E. Arena[92], J-F. Arguin[108], S. Argyropoulos[54], J.-H. Arling[48], O. Arnaez[4], H. Arnold[114], G. Artoni[75a,75b], H. Asada[111], K. Asai[118], S. Asai[153], N.A. Asbah[61], K. Assamagan[29], R. Astalos[28a], S. Atashi[159], R.J. Atkin[33a], M. Atkinson[162], H. Atmani[35f], P.A. Atmasiddha[128], K. Augsten[132], S. Auricchio[72a,72b], A.D. Auriol[20], V.A. Austrup[101], G. Avolio[36], K. Axiotis[56], G. Azuelos[108,ag], D. Babal[28b], H. Bachacou[135], K. Bachas[152,q], A. Bachiu[34], F. Backman[47a,47b], A. Badea[61], T.M. Baer[106], P. Bagnaia[75a,75b], M. Bahmani[18], D. Bahner[54], A.J. Bailey[163], V.R. Bailey[162], J.T. Baines[134], L. Baines[94], O.K. Baker[172], E. Bakos[15], D. Bakshi Gupta[8], V. Balakrishnan[120], R. Balasubramanian[114], E.M. Baldin[37], P. Balek[86a], E. Ballabene[23b,23a], F. Balli[135], L.M. Baltes[63a], W.K. Balunas[32], J. Balz[100], E. Banas[87], M. Bandieramonte[129], A. Bandyopadhyay[24], S. Bansal[24], L. Barak[151], M. Barakat[48], E.L. Barberio[105], D. Barberis[57b,57a], M. Barbero[102], M.Z. Barel[114], K.N. Barends[33a], T. Barillari[110], M-S. Barisits[36], T. Barklow[143], P. Baron[122], D.A. Baron Moreno[101], A. Baroncelli[62a], G. Barone[29], A.J. Barr[126], J.D. Barr[96], L. Barranco Navarro[47a,47b], F. Barreiro[99], J. Barreiro Guimarães da Costa[14a], U. Barron[151], M.G. Barros Teixeira[130a], S. Barsov[37], F. Bartels[63a], R. Bartoldus[143], A.E. Barton[91], P. Bartos[28a], A. Basan[100], M. Baselga[49], A. Bassalat[66,b], M.J. Basso[156a], C.R. Basson[101], R.L. Bates[59], S. Batlamous[35e], J.R. Batley[32], B. Batool[141], M. Battaglia[136], D. Battulga[18], M. Bauce[75a,75b], M. Bauer[36], P. Bauer[24], L.T. Bazzano Hurrell[30], J.B. Beacham[51], T. Beau[127], J.Y. Beaucamp[90], P.H. Beauchemin[158], P. Bechtle[24], H.P. Beck[19,p], K. Becker[167], A.J. Beddall[82], V.A. Bednyakov[38], C.P. Bee[145], L.J. Beemster[15], T.A. Beermann[36],



JHEP05(2024)263

M. Begalli[83d], M. Begel[29], A. Behera[145], J.K. Behr[48], J.F. Beirer[36], F. Beisiegel[24], M. Belfkir[116b], G. Bella[151], L. Bellagamba[23b], A. Bellerive[34], P. Bellos[20], K. Beloborodov[37], D. Benchekroun[35a], F. Bendebba[35a], Y. Benhammou[151], M. Benoit[29], J.R. Bensinger[26], S. Bentvelsen[114], L. Beresford[48], M. Beretta[53], E. Bergeaas Kuutmann[161], N. Berger[4], B. Bergmann[132], J. Beringer[17a], G. Bernardi[5], C. Bernius[143], F.U. Bernlochner[24], F. Bernon[36,102], A. Berrocal Guardia[13], T. Berry[95], P. Berta[133], A. Berthold[50], I.A. Bertram[91], S. Bethke[110], A. Betti[75a,75b], A.J. Bevan[94], N.K. Bhalla[54], M. Bhamjee[33c], S. Bhatta[145], D.S. Bhattacharya[166], P. Bhattarai[143], V.S. Bhopatkar[121], R. Bi[29,aj], R.M. Bianchi[129], G. Bianco[23b,23a], O. Biebel[109], R. Bielski[123], M. Biglietti[77a], M. Bindi[55], A. Bingul[21b], C. Bini[75a,75b], A. Biondini[92], C.J. Birch-sykes[101], G.A. Bird[20,134], M. Birman[169], M. Biros[133], S. Biryukov[146], T. Bisanz[49], E. Bisceglie[43b,43a], J.P. Biswal[134], D. Biswas[141], A. Bitadze[101], K. Bjørke[125], I. Bloch[48], A. Blue[59], U. Blumenschein[94], J. Blumenthal[100], G.J. Bobbink[114], V.S. Bobrovnikov[37], M. Boehler[54], B. Boehm[166], D. Bogavac[36], A.G. Bogdanchikov[37], C. Bohm[47a], V. Boisvert[95], P. Bokan[48], T. Bold[86a], M. Bomben[5], M. Bona[94], M. Boonekamp[135], C.D. Booth[95], A.G. Borbély[59], I.S. Bordulev[37], H.M. Borecka-Bielska[108], G. Borissov[91], D. Bortoletto[126], D. Boscherini[23b], M. Bosman[13], J.D. Bossio Sola[36], K. Bouaouda[35a], N. Bouchhar[163], J. Boudreau[129], E.V. Bouhova-Thacker[91], D. Boumediene[40], R. Bouquet[165], A. Boveia[119], J. Boyd[36], D. Boye[29], I.R. Boyko[38], J. Bracinik[20], N. Brahimi[62d], G. Brandt[171], O. Brandt[32], F. Braren[48], B. Brau[103], J.E. Brau[123], R. Brener[169], L. Brenner[114], R. Brenner[161], S. Bressler[169], D. Britton[59], D. Britzger[110], I. Brock[24], G. Brooijmans[41], W.K. Brooks[137f], E. Brost[29], L.M. Brown[165], L.E. Bruce[61], T.L. Bruckler[126], P.A. Bruckman de Renstrom[87], B. Brüers[48], A. Bruni[23b], G. Bruni[23b], M. Bruschi[23b], N. Bruscino[75a,75b], T. Buanes[16], Q. Buat[138], D. Buchin[110], A.G. Buckley[59], O. Bulekov[37], B.A. Bullard[143], S. Burdin[92], C.D. Burgard[49], A.M. Burger[40], B. Burghgrave[8], O. Burlayenko[54], J.T.P. Burr[32], C.D. Burton[11], J.C. Burzynski[142], E.L. Busch[41], V. Büscher[100], P.J. Bussey[59], J.M. Butler[25], C.M. Buttar[59], J.M. Butterworth[96], W. Buttinger[134], C.J. Buxo Vazquez[107], A.R. Buzykaev[37], S. Cabrera Urbán[163], L. Cadamuro[66], D. Caforio[58], H. Cai[129], Y. Cai[14a,14e], Y. Cai[14c], V.M.M. Cairo[36], O. Cakir[3a], N. Calace[36], P. Calafiura[17a], G. Calderini[127], P. Calfayan[68], G. Callea[59], L.P. Caloba[83b], D. Calvet[40], S. Calvet[40], M. Calvetti[74a,74b], R. Camacho Toro[127], S. Camarda[36], D. Camarero Munoz[26], P. Camarri[76a,76b], M.T. Camerlingo[72a,72b], D. Cameron[36], C. Camincher[165], M. Campanelli[96], A. Camplani[42], V. Canale[72a,72b], A. Canesse[104], J. Cantero[163], Y. Cao[162], F. Capocasa[26], M. Capua[43b,43a], A. Carbone[71a,71b], R. Cardarelli[76a], J.C.J. Cardenas[8], F. Cardillo[163], G. Carducci[43b,43a], T. Carli[36], G. Carlino[72a], J.I. Carlotto[13], B.T. Carlson[129,r], E.M. Carlson[165,156a], L. Carminati[71a,71b], A. Carnelli[135], M. Carnesale[75a,75b], S. Caron[113], E. Carquin[137f], S. Carrá[71a], G. Carratta[23b,23a], F. Carrio Argos[33g], J.W.S. Carter[155], T.M. Carter[52], M.P. Casado[13,i], M. Caspar[48], F.L. Castillo[4], L. Castillo Garcia[13], V. Castillo Gimenez[163], N.F. Castro[130a,130e], A. Catinaccio[36], J.R. Catmore[125], V. Cavaliere[29], N. Cavalli[23b,23a], V. Cavasinni[74a,74b], Y.C. Cekmecelioglu[48], E. Celebi[21a], F. Celli[126], M.S. Centonze[70a,70b], V. Cepaitis[56],



JHEP05(2024)263

K. Cerny[122], A.S. Cerqueira[83a], A. Cerri[146], L. Cerrito[76a,76b], F. Cerutti[17a], B. Cervato[141], A. Cervelli[23b], G. Cesarini[53], S.A. Cetin[82], D. Chakraborty[115], J. Chan[170], W.Y. Chan[153], J.D. Chapman[32], E. Chapon[135], B. Chargeishvili[149b], D.G. Charlton[20], M. Chatterjee[19], C. Chauhan[133], S. Chekanov[6], S.V. Chekulaev[156a], G.A. Chelkov[38,a], A. Chen[106], B. Chen[151], B. Chen[165], H. Chen[14c], H. Chen[29], J. Chen[62c], J. Chen[142], M. Chen[126], S. Chen[153], S.J. Chen[14c], X. Chen[62c,135], X. Chen[14b,af], Y. Chen[62a], C.L. Cheng[170], H.C. Cheng[64a], S. Cheong[143], A. Cheplakov[38], E. Cheremushkina[48], E. Cherepanova[114], R. Cherkaoui El Moursli[35e], E. Cheu[7], K. Cheung[65], L. Chevalier[135], V. Chiarella[53], G. Chiarelli[74a], N. Chiedde[102], G. Chiodini[70a], A.S. Chisholm[20], A. Chitan[27b], M. Chitishvili[163], M.V. Chizhov[38], K. Choi[11], A.R. Chomont[75a,75b], Y. Chou[103], E.Y.S. Chow[113], T. Chowdhury[33g], K.L. Chu[169], M.C. Chu[64a], X. Chu[14a,14e], J. Chudoba[131], J.J. Chwastowski[87], D. Cieri[110], K.M. Ciesla[86a], V. Cindro[93], A. Ciocio[17a], F. Cirotto[72a,72b], Z.H. Citron[169,k], M. Citterio[71a], D.A. Ciubotaru[27b], A. Clark[56], P.J. Clark[52], C. Clarry[155], J.M. Clavijo Columbie[48], S.E. Clawson[48], C. Clement[47a,47b], J. Clercx[48], Y. Coadou[102], M. Cobal[69a,69c], A. Coccaro[57b], R.F. Coelho Barrue[130a], R. Coelho Lopes De Sa[103], S. Coelli[71a], A.E.C. Coimbra[71a,71b], B. Cole[41], J. Collot[60], P. Conde Muiño[130a,130g], M.P. Connell[33c], S.H. Connell[33c], I.A. Connelly[59], E.I. Conroy[126], F. Conventi[72a,ah], H.G. Cooke[20], A.M. Cooper-Sarkar[126], A. Cordeiro Oudot Choi[127], L.D. Corpe[40], M. Corradi[75a,75b], F. Corriveau[104,x], A. Cortes-Gonzalez[18], M.J. Costa[163], F. Costanza[4], D. Costanzo[139], B.M. Cote[119], G. Cowan[95], K. Cranmer[170], D. Cremonini[23b,23a], S. Crépé-Renaudin[60], F. Crescioli[127], M. Cristinziani[141], M. Cristoforetti[78a,78b], V. Croft[114], J.E. Crosby[121], G. Crosetti[43b,43a], A. Cueto[99], T. Cuhadar Donszelmann[159], H. Cui[14a,14e], Z. Cui[7], W.R. Cunningham[59], F. Curcio[43b,43a], P. Czodrowski[36], M.M. Czurylo[63b], M.J. Da Cunha Sargedas De Sousa[57b,57a], J.V. Da Fonseca Pinto[83b], C. Da Via[101], W. Dabrowski[86a], T. Dado[49], S. Dahbi[33g], T. Dai[106], D. Dal Santo[19], C. Dallapiccola[103], M. Dam[42], G. D'amen[29], V. D'Amico[109], J. Damp[100], J.R. Dandoy[34], M. Danninger[142], V. Dao[36], G. Darbo[57b], S. Darmora[6], S.J. Das[29,aj], S. D'Auria[71a,71b], C. David[156b], T. Davidek[133], B. Davis-Purcell[34], I. Dawson[94], H.A. Day-hall[132], K. De[8], R. De Asmundis[72a], N. De Biase[48], S. De Castro[23b,23a], N. De Groot[113], P. de Jong[114], H. De la Torre[115], A. De Maria[14c], A. De Salvo[75a], U. De Sanctis[76a,76b], F. De Santis[70a,70b], A. De Santo[146], J.B. De Vivie De Regie[60], D.V. Dedovich[38], J. Degens[114], A.M. Deiana[44], F. Del Corso[23b,23a], J. Del Peso[99], F. Del Rio[63a], L. Delagrange[127], F. Deliot[135], C.M. Delitzsch[49], M. Della Pietra[72a,72b], D. Della Volpe[56], A. Dell'Acqua[36], L. Dell'Asta[71a,71b], M. Delmastro[4], P.A. Delsart[60], S. Demers[172], M. Demichev[38], S.P. Denisov[37], L. D'Eramo[40], D. Derendarz[87], F. Derue[127], P. Dervan[92], K. Desch[24], C. Deutsch[24], F.A. Di Bello[57b,57a], A. Di Ciaccio[76a,76b], L. Di Ciaccio[4], A. Di Domenico[75a,75b], C. Di Donato[72a,72b], A. Di Girolamo[36], G. Di Gregorio[36], A. Di Luca[78a,78b], B. Di Micco[77a,77b], R. Di Nardo[77a,77b], C. Diaconu[102], M. Diamantopoulou[34], F.A. Dias[114], T. Dias Do Vale[142], M.A. Diaz[137a,137b], F.G. Diaz Capriles[24], M. Didenko[163], E.B. Diehl[106], L. Diehl[54], S. Díez Cornell[48], C. Diez Pardos[141], C. Dimitriadi[161,24], A. Dimitrievska[17a], J. Dingfelder[24], I-M. Dinu[27b], S.J. Dittmeier[63b], F. Dittus[36], F. Djama[102], T. Djobava[149b], C. Doglioni[101,98],



JHEP05(2024)263

A. Dohnalova[28a], J. Dolejsi[133], Z. Dolezal[133], K.M. Dona[39], M. Donadelli[83c], B. Dong[107], J. Donini[40], A. D'Onofrio[72a,72b], M. D'Onofrio[92], J. Dopke[134], A. Doria[72a], N. Dos Santos Fernandes[130a], P. Dougan[101], M.T. Dova[90], A.T. Doyle[59], M.A. Draguet[126], E. Dreyer[169], I. Drivas-koulouris[10], M. Drnevich[117], A.S. Drobac[158], M. Drozdova[56], D. Du[62a], T.A. du Pree[114], F. Dubinin[37], M. Dubovsky[28a], E. Duchovni[169], G. Duckeck[109], O.A. Ducu[27b], D. Duda[52], A. Dudarev[36], E.R. Duden[26], M. D'uffizi[101], L. Duflot[66], M. Dührssen[36], A.E. Dumitriu[27b], M. Dunford[63a], S. Dungs[49], K. Dunne[47a,47b], A. Duperrin[102], H. Duran Yildiz[3a], M. Düren[58], A. Durglishvili[149b], B.L. Dwyer[115], G.I. Dyckes[17a], M. Dyndal[86a], B.S. Dziedzic[87], Z.O. Earnshaw[146], G.H. Eberwein[126], B. Eckerova[28a], S. Eggebrecht[55], E. Egidio Purcino De Souza[127], L.F. Ehrke[56], G. Eigen[16], K. Einsweiler[17a], T. Ekelof[161], P.A. Ekman[98], S. El Farkh[35b], Y. El Ghazali[35b], H. El Jarrari[36], A. El Moussaouy[108], V. Ellajosyula[161], M. Ellert[161], F. Ellinghaus[171], N. Ellis[36], J. Elmsheuser[29], M. Elsing[36], D. Emeliyanov[134], Y. Enari[153], I. Ene[17a], S. Epari[13], P.A. Erland[87], M. Errenst[171], M. Escalier[66], C. Escobar[163], E. Etzion[151], G. Evans[130a], H. Evans[68], L.S. Evans[95], M.O. Evans[146], A. Ezhilov[37], S. Ezzarqtouni[35a], F. Fabbri[59], L. Fabbri[23b,23a], G. Facini[96], V. Fadeyev[136], R.M. Fakhrutdinov[37], D. Fakoudis[100], S. Falciano[75a], L.F. Falda Ulhoa Coelho[36], P.J. Falke[24], J. Faltova[133], C. Fan[162], Y. Fan[14a], Y. Fang[14a,14e], M. Fanti[71a,71b], M. Faraj[69a,69b], Z. Farazpay[97], A. Farbin[8], A. Farilla[77a], T. Farooque[107], S.M. Farrington[52], F. Fassi[35e], D. Fassouliotis[9], M. Faucci Giannelli[76a,76b], W.J. Fawcett[32], L. Fayard[66], P. Federic[133], P. Federicova[131], O.L. Fedin[37,a], G. Fedotov[37], M. Feickert[170], L. Feligioni[102], D.E. Fellers[123], C. Feng[62b], M. Feng[14b], Z. Feng[114], M.J. Fenton[159], A.B. Fenyuk[37], L. Ferencz[48], R.A.M. Ferguson[91], S.I. Fernandez Luengo[137f], P. Fernandez Martinez[13], M.J.V. Fernoux[102], J. Ferrando[91], A. Ferrari[161], P. Ferrari[114,113], R. Ferrari[73a], D. Ferrere[56], C. Ferretti[106], F. Fiedler[100], P. Fiedler[132], A. Filipčič[93], E.K. Filmer[1], F. Filthaut[113], M.C.N. Fiolhais[130a,130c,c], L. Fiorini[163], W.C. Fisher[107], T. Fitschen[101], P.M. Fitzhugh[135], I. Fleck[141], P. Fleischmann[106], T. Flick[171], M. Flores[33d,ad], L.R. Flores Castillo[64a], L. Flores Sanz De Acedo[36], F.M. Follega[78a,78b], N. Fomin[16], J.H. Foo[155], B.C. Forland[68], A. Formica[135], A.C. Forti[101], E. Fortin[36], A.W. Fortman[61], M.G. Foti[17a], L. Fountas[9,j], D. Fournier[66], H. Fox[91], P. Francavilla[74a,74b], S. Francescato[61], S. Franchellucci[56], M. Franchini[23b,23a], S. Franchino[63a], D. Francis[36], L. Franco[113], V. Franco Lima[36], L. Franconi[48], M. Franklin[61], G. Frattari[26], A.C. Freegard[94], W.S. Freund[83b], Y.Y. Frid[151], J. Friend[59], N. Fritzsche[50], A. Froch[54], D. Froidevaux[36], J.A. Frost[126], Y. Fu[62a], S. Fuenzalida Garrido[137f], M. Fujimoto[102], K.Y. Fung[64a], E. Furtado De Simas Filho[83b], M. Furukawa[153], J. Fuster[163], A. Gabrielli[23b,23a], A. Gabrielli[155], P. Gadow[36], G. Gagliardi[57b,57a], L.G. Gagnon[17a], E.J. Gallas[126], B.J. Gallop[134], K.K. Gan[119], S. Ganguly[153], Y. Gao[52], F.M. Garay Walls[137a,137b], B. Garcia[29], C. García[163], A. Garcia Alonso[114], A.G. Garcia Caffaro[172], J.E. García Navarro[163], M. Garcia-Sciveres[17a], G.L. Gardner[128], R.W. Gardner[39], N. Garelli[158], D. Garg[80], R.B. Garg[143,n], J.M. Gargan[52], C.A. Garner[155], C.M. Garvey[33a], P. Gaspar[83b], V.K. Gassmann[158], G. Gaudio[73a], V. Gautam[13], P. Gauzzi[75a,75b], I.L. Gavrilenko[37], A. Gavrilyuk[37], C. Gay[164], G. Gaycken[48], E.N. Gazis[10], A.A. Geanta[27b], C.M. Gee[136], A. Gekow[119],

JHEP05(2024)263

C. Gemme[57b], M.H. Genest[60], S. Gentile[75a,75b], A.D. Gentry[112], S. George[95], W.F. George[20], T. Geralis[46], P. Gessinger-Befurt[36], M.E. Geyik[171], M. Ghani[167], M. Ghneimat[141], K. Ghorbanian[94], A. Ghosal[141], A. Ghosh[159], A. Ghosh[7], B. Giacobbe[23b], S. Giagu[75a,75b], T. Giani[114], P. Giannetti[74a], A. Giannini[62a], S.M. Gibson[95], M. Gignac[136], D.T. Gil[86b], A.K. Gilbert[86a], B.J. Gilbert[41], D. Gillberg[34], G. Gilles[114], N.E.K. Gillwald[48], L. Ginabat[127], D.M. Gingrich[2,ag], M.P. Giordani[69a,69c], P.F. Giraud[135], G. Giugliarelli[69a,69c], D. Giugni[71a], F. Giuli[36], I. Gkialas[9,j], L.K. Gladilin[37], C. Glasman[99], G.R. Gledhill[123], G. Glemža[48], M. Glisic[123], I. Gnesi[43b,f], Y. Go[29,aj], M. Goblirsch-Kolb[36], B. Gocke[49], D. Godin[108], B. Gokturk[21a], S. Goldfarb[105], T. Golling[56], M.G.D. Gololo[33g], D. Golubkov[37], J.P. Gombas[107], A. Gomes[130a,130b], G. Gomes Da Silva[141], A.J. Gomez Delegido[163], R. Gonçalo[130a,130c], G. Gonella[123], L. Gonella[20], A. Gongadze[149c], F. Gonnella[20], J.L. Gonski[41], R.Y. González Andana[52], S. González de la Hoz[163], R. Gonzalez Lopez[92], C. Gonzalez Renteria[17a], M.V. Gonzalez Rodrigues[48], R. Gonzalez Suarez[161], S. Gonzalez-Sevilla[56], G.R. Gonzalvo Rodriguez[163], L. Goossens[36], B. Gorini[36], E. Gorini[70a,70b], A. Gorišek[93], T.C. Gosart[128], A.T. Goshaw[51], M.I. Gostkin[38], S. Goswami[121], C.A. Gottardo[36], S.A. Gotz[109], M. Gouighri[35b], V. Goumarre[48], A.G. Goussiou[138], N. Govender[33c], I. Grabowska-Bold[86a], K. Graham[34], E. Gramstad[125], S. Grancagnolo[70a,70b], M. Grandi[146], C.M. Grant[1,135], P.M. Gravila[27f], F.G. Gravili[70a,70b], H.M. Gray[17a], M. Greco[70a,70b], C. Grefe[24], I.M. Gregor[48], P. Grenier[143], S.G. Grewe[110], C. Grieco[13], A.A. Grillo[136], K. Grimm[31], S. Grinstein[13,t], J.-F. Grivaz[66], E. Gross[169], J. Grosse-Knetter[55], C. Grud[106], J.C. Grundy[126], L. Guan[106], W. Guan[29], C. Gubbels[164], J.G.R. Guerrero Rojas[163], G. Guerrieri[69a,69c], F. Guescini[110], R. Gugel[100], J.A.M. Guhit[106], A. Guida[18], E. Guilloton[167,134], S. Guindon[36], F. Guo[14a,14e], J. Guo[62c], L. Guo[48], Y. Guo[106], R. Gupta[48], R. Gupta[129], S. Gurbuz[24], S.S. Gurdasani[54], G. Gustavino[36], M. Guth[56], P. Gutierrez[120], L.F. Gutierrez Zagazeta[128], M. Gutsche[50], C. Gutschow[96], C. Gwenlan[126], C.B. Gwilliam[92], E.S. Haaland[125], A. Haas[117], M. Habedank[48], C. Haber[17a], H.K. Hadavand[8], A. Hadef[50], S. Hadzic[110], A.I. Hagan[91], J.J. Hahn[141], E.H. Haines[96], M. Haleem[166], J. Haley[121], J.J. Hall[139], G.D. Hallewell[102], L. Halser[19], K. Hamano[165], M. Hamer[24], G.N. Hamity[52], E.J. Hampshire[95], J. Han[62b], K. Han[62a], L. Han[14c], L. Han[62a], S. Han[17a], Y.F. Han[155], K. Hanagaki[84], M. Hance[136], D.A. Hangal[41,ac], H. Hanif[142], M.D. Hank[128], J.B. Hansen[42], J.D. Hansen[42], P.H. Hansen[42], K. Hara[157], D. Harada[56], T. Harenberg[171], S. Harkusha[37], M.L. Harris[103], Y.T. Harris[126], J. Harrison[13], N.M. Harrison[119], P.F. Harrison[167], N.M. Hartman[110], N.M. Hartmann[109], Y. Hasegawa[140], R. Hauser[107], C.M. Hawkes[20], R.J. Hawkings[36], Y. Hayashi[153], S. Hayashida[111], D. Hayden[107], C. Hayes[106], R.L. Hayes[114], C.P. Hays[126], J.M. Hays[94], H.S. Hayward[92], F. He[62a], M. He[14a,14e], Y. He[154], Y. He[48], N.B. Heatley[94], V. Hedberg[98], A.L. Heggelund[125], N.D. Hehir[94,*], C. Heidegger[54], K.K. Heidegger[54], W.D. Heidorn[81], J. Heilman[34], S. Heim[48], T. Heim[17a], J.G. Heinlein[128], J.J. Heinrich[123], L. Heinrich[110,ae], J. Hejbal[131], L. Helary[48], A. Held[170], S. Hellesund[16], C.M. Helling[164], S. Hellman[47a,47b], R.C.W. Henderson[91], L. Henkelmann[32], A.M. Henriques Correia[36], H. Herde[98], Y. Hernández Jiménez[145], L.M. Herrmann[24], T. Herrmann[50], G. Herten[54], R. Hertenberger[109], L. Hervas[36], M.E. Hesping[100], N.P. Hessey[156a], H. Hibi[85], E. Hill[155],



JHEP05(2024)263

S.J. Hillier[20], J.R. Hinds[107], F. Hinterkeuser[24], M. Hirose[124], S. Hirose[157], D. Hirschbuehl[171], T.G. Hitchings[101], B. Hiti[93], J. Hobbs[145], R. Hobincu[27e], N. Hod[169], M.C. Hodgkinson[139], B.H. Hodkinson[32], A. Hoecker[36], D.D. Hofer[106], J. Hofer[48], T. Holm[24], M. Holzbock[110], L.B.A.H. Hommels[32], B.P. Honan[101], J. Hong[62c], T.M. Hong[129], B.H. Hooberman[162], W.H. Hopkins[6], Y. Horii[111], S. Hou[148], A.S. Howard[93], J. Howarth[59], J. Hoya[6], M. Hrabovsky[122], A. Hrynevich[48], T. Hryn'ova[4], P.J. Hsu[65], S.-C. Hsu[138], Q. Hu[62a], Y.F. Hu[14a,14e], S. Huang[64b], X. Huang[14c], X. Huang[14a,14e], Y. Huang[139], Y. Huang[14a], Z. Huang[101], Z. Hubacek[132], M. Huebner[24], F. Huegging[24], T.B. Huffman[126], C.A. Hugli[48], M. Huhtinen[36], S.K. Huiberts[16], R. Hulsken[104], N. Huseynov[12], J. Huston[107], J. Huth[61], R. Hyneman[143], G. Iacobucci[56], G. Iakovidis[29], I. Ibragimov[141], L. Iconomidou-Fayard[66], P. Iengo[72a,72b], R. Iguchi[153], T. Iizawa[126], Y. Ikegami[84], N. Ilic[155], H. Imam[35a], M. Ince Lezki[56], T. Ingebretsen Carlson[47a,47b], G. Introzzi[73a,73b], M. Iodice[77a], V. Ippolito[75a,75b], R.K. Irwin[92], M. Ishino[153], W. Islam[170], C. Issever[18,48], S. Istin[21a,al], H. Ito[168], J.M. Iturbe Ponce[64a], R. Iuppa[78a,78b], A. Ivina[169], J.M. Izen[45], V. Izzo[72a], P. Jacka[131,132], P. Jackson[1], R.M. Jacobs[48], B.P. Jaeger[142], C.S. Jagfeld[109], G. Jain[156a], P. Jain[54], K. Jakobs[54], T. Jakoubek[169], J. Jamieson[59], K.W. Janas[86a], M. Javurkova[103], F. Jeanneau[135], L. Jeanty[123], J. Jejelava[149a,aa], P. Jenni[54,g], C.E. Jessiman[34], S. Jézéquel[4], C. Jia[62b], J. Jia[145], X. Jia[61], X. Jia[14a,14e], Z. Jia[14c], S. Jiggins[48], J. Jimenez Pena[13], S. Jin[14c], A. Jinaru[27b], O. Jinnouchi[154], P. Johansson[139], K.A. Johns[7], J.W. Johnson[136], D.M. Jones[32], E. Jones[48], P. Jones[32], R.W.L. Jones[91], T.J. Jones[92], H.L. Joos[55,36], R. Joshi[119], J. Jovicevic[15], X. Ju[17a], J.J. Junggeburth[103], T. Junkermann[63a], A. Juste Rozas[13,t], M.K. Juzek[87], S. Kabana[137e], A. Kaczmarska[87], M. Kado[110], H. Kagan[119], M. Kagan[143], A. Kahn[41], A. Kahn[128], C. Kahra[100], T. Kaji[153], E. Kajomovitz[150], N. Kakati[169], I. Kalaitzidou[54], C.W. Kalderon[29], A. Kamenshchikov[155], N.J. Kang[136], D. Kar[33g], K. Karava[126], M.J. Kareem[156b], E. Karentzos[54], I. Karkanias[152], O. Karkout[114], S.N. Karpov[38], Z.M. Karpova[38], V. Kartvelishvili[91], A.N. Karyukhin[37], E. Kasimi[152], J. Katzy[48], S. Kaur[34], K. Kawade[140], M.P. Kawale[120], C. Kawamoto[88], T. Kawamoto[62a], E.F. Kay[36], F.I. Kaya[158], S. Kazakos[107], V.F. Kazanin[37], Y. Ke[145], J.M. Keaveney[33a], R. Keeler[165], G.V. Kehris[61], J.S. Keller[34], A.S. Kelly[96], J.J. Kempster[146], K.E. Kennedy[41], P.D. Kennedy[100], O. Kepka[131], B.P. Kerridge[167], S. Kersten[171], B.P. Kerševan[93], S. Keshri[66], L. Keszeghova[28a], S. Ketabchi Haghighat[155], R.A. Khan[129], A. Khanov[121], A.G. Kharlamov[37], T. Kharlamova[37], E.E. Khoda[138], M. Kholodenko[37], T.J. Khoo[18], G. Khoriauli[166], J. Khubua[149b], Y.A.R. Khwaira[66], A. Kilgallon[123], D.W. Kim[47a,47b], Y.K. Kim[39], N. Kimura[96], M.K. Kingston[55], A. Kirchhoff[55], C. Kirfel[24], F. Kirfel[24], J. Kirk[134], A.E. Kiryunin[110], C. Kitsaki[10], O. Kivernyk[24], M. Klassen[63a], C. Klein[34], L. Klein[166], M.H. Klein[44], M. Klein[92], S.B. Klein[56], U. Klein[92], P. Klimek[36], A. Klimentov[29], T. Klioutchnikova[36], P. Kluit[114], S. Kluth[110], E. Kneringer[79], T.M. Knight[155], A. Knue[49], R. Kobayashi[88], D. Kobylianskii[169], S.F. Koch[126], M. Kocian[143], P. Kodyš[133], D.M. Koeck[123], P.T. Koenig[24], T. Koffas[34], O. Kolay[50], I. Koletsou[4], T. Komarek[122], K. Köneke[54], A.X.Y. Kong[1], T. Kono[118], N. Konstantinidis[96], P. Kontaxakis[56], B. Konya[98], R. Kopeliansky[68], S. Koperny[86a],

JHEP05(2024)263

K. Korcyl[87], K. Kordas[152,e], A. Korn[96], S. Korn[55], I. Korolkov[13], N. Korotkova[37], B. Kortman[114], O. Kortner[110], S. Kortner[110], W.H. Kostecka[115], V.V. Kostyukhin[141], A. Kotsokechagia[135], A. Kotwal[51], A. Koulouris[36], A. Kourkoumeli-Charalampidi[73a,73b], C. Kourkoumelis[9], E. Kourlitis[110,ae], O. Kovanda[146], R. Kowalewski[165], W. Kozanecki[135], A.S. Kozhin[37], V.A. Kramarenko[37], G. Kramberger[93], P. Kramer[100], M.W. Krasny[127], A. Krasznahorkay[36], J.W. Kraus[171], J.A. Kremer[48], T. Kresse[50], J. Kretzschmar[92], K. Kreul[18], P. Krieger[155], S. Krishnamurthy[103], M. Krivos[133], K. Krizka[20], K. Kroeninger[49], H. Kroha[110], J. Kroll[131], J. Kroll[128], K.S. Krowpman[107], U. Kruchonak[38], H. Krüger[24], N. Krumnack[81], M.C. Kruse[51], O. Kuchinskaia[37], S. Kuday[3a], S. Kuehn[36], R. Kuesters[54], T. Kuhl[48], V. Kukhtin[38], Y. Kulchitsky[37,a], S. Kuleshov[137d,137b], M. Kumar[33g], N. Kumari[48], P. Kumari[156b], A. Kupco[131], T. Kupfer[49], A. Kupich[37], O. Kuprash[54], H. Kurashige[85], L.L. Kurchaninov[156a], O. Kurdysh[66], Y.A. Kurochkin[37], A. Kurova[37], M. Kuze[154], A.K. Kvam[103], J. Kvita[122], T. Kwan[104], N.G. Kyriacou[106], L.A.O. Laatu[102], C. Lacasta[163], F. Lacava[75a,75b], H. Lacker[18], D. Lacour[127], N.N. Lad[96], E. Ladygin[38], B. Laforge[127], T. Lagouri[137e], F.Z. Lahbabi[35a], S. Lai[55], I.K. Lakomiec[86a], N. Lalloue[60], J.E. Lambert[165], S. Lammers[68], W. Lampl[7], C. Lampoudis[152,e], A.N. Lancaster[115], E. Lançon[29], U. Landgraf[54], M.P.J. Landon[94], V.S. Lang[54], R.J. Langenberg[103], O.K.B. Langrekken[125], A.J. Lankford[159], F. Lanni[36], K. Lantzsch[24], A. Lanza[73a], A. Lapertosa[57b,57a], J.F. Laporte[135], T. Lari[71a], F. Lasagni Manghi[23b], M. Lassnig[36], V. Latonova[131], A. Laudrain[100], A. Laurier[150], S.D. Lawlor[139], Z. Lawrence[101], R. Lazaridou[167], M. Lazzaroni[71a,71b], B. Le[101], E.M. Le Boulicaut[51], B. Leban[93], A. Lebedev[81], M. LeBlanc[101], F. Ledroit-Guillon[60], A.C.A. Lee[96], S.C. Lee[148], S. Lee[47a,47b], T.F. Lee[92], L.L. Leeuw[33c], H.P. Lefebvre[95], M. Lefebvre[165], C. Leggett[17a], G. Lehmann Miotto[36], M. Leigh[56], W.A. Leight[103], W. Leinonen[113], A. Leisos[152,s], M.A.L. Leite[83c], C.E. Leitgeb[48], R. Leitner[133], K.J.C. Leney[44], T. Lenz[24], S. Leone[74a], C. Leonidopoulos[52], A. Leopold[144], C. Leroy[108], R. Les[107], C.G. Lester[32], M. Levchenko[37], J. Levêque[4], D. Levin[106], L.J. Levinson[169], M.P. Lewicki[87], D.J. Lewis[4], A. Li[5], B. Li[62b], C. Li[62a], C-Q. Li[110], H. Li[62a], H. Li[62b], H. Li[14c], H. Li[14b], H. Li[62b], J. Li[62c], K. Li[138], L. Li[62c], M. Li[14a,14e], Q.Y. Li[62a], S. Li[14a,14e], S. Li[62d,62c,d], T. Li[5], X. Li[104], Z. Li[126], Z. Li[104], Z. Li[14a,14e], S. Liang[14a,14e], Z. Liang[14a], M. Liberatore[135], B. Liberti[76a], K. Lie[64c], J. Lieber Marin[83b], H. Lien[68], K. Lin[107], R.E. Lindley[7], J.H. Lindon[2], E. Lipeles[128], A. Lipniacka[16], A. Lister[164], J.D. Little[4], B. Liu[14a], B.X. Liu[142], D. Liu[62d,62c], J.B. Liu[62a], J.K.K. Liu[32], K. Liu[62d,62c], M. Liu[62a], M.Y. Liu[62a], P. Liu[14a], Q. Liu[62d,138,62c], X. Liu[62a], X. Liu[62b], Y. Liu[14d,14e], Y.L. Liu[62b], Y.W. Liu[62a], J. Llorente Merino[142], S.L. Lloyd[94], E.M. Lobodzinska[48], P. Loch[7], T. Lohse[18], K. Lohwasser[139], E. Loiacono[48], M. Lokajicek[131,*], J.D. Lomas[20], J.D. Long[162], I. Longarini[159], L. Longo[70a,70b], R. Longo[162], I. Lopez Paz[67], A. Lopez Solis[48], N. Lorenzo Martinez[4], A.M. Lory[109], G. Löschcke Centeno[146], O. Loseva[37], X. Lou[47a,47b], X. Lou[14a,14e], A. Lounis[66], J. Love[6], P.A. Love[91], G. Lu[14a,14e], M. Lu[80], S. Lu[128], Y.J. Lu[65], H.J. Lubatti[138], C. Luci[75a,75b], F.L. Lucio Alves[14c], A. Lucotte[60], F. Luehring[68], I. Luise[145], O. Lukianchuk[66], O. Lundberg[144], B. Lund-Jensen[144], N.A. Luongo[6], M.S. Lutz[151], A.B. Lux[25], D. Lynn[29], H. Lyons[92], R. Lysak[131], E. Lytken[98],

JHEP05(2024)263

V. Lyubushkin[38], T. Lyubushkina[38], M.M. Lyukova[145], H. Ma[29], K. Ma[62a], L.L. Ma[62b], W. Ma[62a], Y. Ma[121], D.M. Mac Donell[165], G. Maccarrone[53], J.C. MacDonald[100], P.C. Machado De Abreu Farias[83b], R. Madar[40], W.F. Mader[50], T. Madula[96], J. Maeda[85], T. Maeno[29], H. Maguire[139], V. Maiboroda[135], A. Maio[130a,130b,130d], K. Maj[86a], O. Majersky[48], S. Majewski[123], N. Makovec[66], V. Maksimovic[15], B. Malaescu[127], Pa. Malecki[87], V.P. Maleev[37], F. Malek[60,o], M. Mali[93], D. Malito[95], U. Mallik[80], S. Maltezos[10], S. Malyukov[38], J. Mamuzic[13], G. Mancini[53], G. Manco[73a,73b], J.P. Mandalia[94], I. Mandić[93], L. Manhaes de Andrade Filho[83a], I.M. Maniatis[169], J. Manjarres Ramos[102,ab], D.C. Mankad[169], A. Mann[109], B. Mansoulie[135], S. Manzoni[36], L. Mao[62c], X. Mapekula[33c], A. Marantis[152,s], G. Marchiori[5], M. Marcisovsky[131], C. Marcon[71a], M. Marinescu[20], S. Marium[48], M. Marjanovic[120], E.J. Marshall[91], Z. Marshall[17a], S. Marti-Garcia[163], T.A. Martin[167], V.J. Martin[52], B. Martin dit Latour[16], L. Martinelli[75a,75b], M. Martinez[13,t], P. Martinez Agullo[163], V.I. Martinez Outschoorn[103], P. Martinez Suarez[13], S. Martin-Haugh[134], V.S. Martoiu[27b], A.C. Martyniuk[96], A. Marzin[36], D. Mascione[78a,78b], L. Masetti[100], T. Mashimo[153], J. Masik[101], A.L. Maslennikov[37], P. Massarotti[72a,72b], P. Mastrandrea[74a,74b], A. Mastroberardino[43b,43a], T. Masubuchi[153], T. Mathisen[161], J. Matousek[133], N. Matsuzawa[153], J. Maurer[27b], B. Maček[93], D.A. Maximov[37], R. Mazini[148], I. Maznas[152], M. Mazza[107], S.M. Mazza[136], E. Mazzeo[71a,71b], C. Mc Ginn[29], J.P. Mc Gowan[104], S.P. Mc Kee[106], C.C. McCracken[164], E.F. McDonald[105], A.E. McDougall[114], J.A. Mcfayden[146], R.P. McGovern[128], G. Mchedlidze[149b], R.P. Mckenzie[33g], T.C. Mclachlan[48], D.J. Mclaughlin[96], S.J. McMahon[134], C.M. Mcpartland[92], R.A. McPherson[165,x], S. Mehlhase[109], A. Mehta[92], D. Melini[163], B.R. Mellado Garcia[33g], A.H. Melo[55], F. Meloni[48], A.M. Mendes Jacques Da Costa[101], H.Y. Meng[155], L. Meng[91], S. Menke[110], M. Mentink[36], E. Meoni[43b,43a], G. Mercado[115], C. Merlassino[69a,69c], L. Merola[72a,72b], C. Meroni[71a,71b], J. Metcalfe[6], A.S. Mete[6], C. Meyer[68], J-P. Meyer[135], R.P. Middleton[134], L. Mijović[52], G. Mikenberg[169], M. Mikestikova[131], M. Mikuž[93], H. Mildner[100], A. Milic[36], C.D. Milke[44], D.W. Miller[39], E.H. Miller[143], L.S. Miller[34], A. Milov[169], D.A. Milstead[47a,47b], T. Min[14c], A.A. Minaenko[37], I.A. Minashvili[149b], L. Mince[59], A.I. Mincer[117], B. Mindur[86a], M. Mineev[38], Y. Mino[88], L.M. Mir[13], M. Miralles Lopez[163], M. Mironova[17a], A. Mishima[153], M.C. Missio[113], A. Mitra[167], V.A. Mitsou[163], Y. Mitsumori[111], O. Miu[155], P.S. Miyagawa[94], T. Mkrtchyan[63a], M. Mlinarevic[96], T. Mlinarevic[96], M. Mlynarikova[36], S. Mobius[19], P. Moder[48], P. Mogg[109], M.H. Mohamed Farook[112], A.F. Mohammed[14a,14e], S. Mohapatra[41], G. Mokgatitswane[33g], L. Moleri[169], B. Mondal[141], S. Mondal[132], K. Mönig[48], E. Monnier[102], L. Monsonis Romero[163], J. Montejo Berlingen[13], M. Montella[119], F. Montereali[77a,77b], F. Monticelli[90], S. Monzani[69a,69c], N. Morange[66], A.L. Moreira De Carvalho[130a], M. Moreno Llácer[163], C. Moreno Martinez[56], P. Morettini[57b], S. Morgenstern[36], M. Morii[61], M. Morinaga[153], A.K. Morley[36], F. Morodei[75a,75b], L. Morvaj[36], P. Moschovakos[36], B. Moser[36], M. Mosidze[149b], T. Moskalets[54], P. Moskvitina[113], J. Moss[31,l], E.J.W. Moyse[103], O. Mtintsilana[33g], S. Muanza[102], J. Mueller[129], D. Muenstermann[91], R. Müller[19], G.A. Mullier[161], A.J. Mullin[32], J.J. Mullin[128], D.P. Mungo[155], D. Munoz Perez[163], F.J. Munoz Sanchez[101], M. Murin[101],

JHEP05(2024)263

W.J. Murray[167,134], A. Murrone[71a,71b], M. Muškinja[17a], C. Mwewa[29], A.G. Myagkov[37,a], A.J. Myers[8], G. Myers[68], M. Myska[132], B.P. Nachman[17a], O. Nackenhorst[49], A. Nag[50], K. Nagai[126], K. Nagano[84], J.L. Nagle[29,aj], E. Nagy[102], A.M. Nairz[36], Y. Nakahama[84], K. Nakamura[84], K. Nakkalil[5], H. Nanjo[124], R. Narayan[44], E.A. Narayanan[112], I. Naryshkin[37], M. Naseri[34], S. Nasri[116b], C. Nass[24], G. Navarro[22a], J. Navarro-Gonzalez[163], R. Nayak[151], A. Nayaz[18], P.Y. Nechaeva[37], F. Nechansky[48], L. Nedic[126], T.J. Neep[20], A. Negri[73a,73b], M. Negrini[23b], C. Nellist[114], C. Nelson[104], K. Nelson[106], S. Nemecek[131], M. Nessi[36,h], M.S. Neubauer[162], F. Neuhaus[100], J. Neundorf[48], R. Newhouse[164], P.R. Newman[20], C.W. Ng[129], Y.W.Y. Ng[48], B. Ngair[116a], H.D.N. Nguyen[108], R.B. Nickerson[126], R. Nicolaidou[135], J. Nielsen[136], M. Niemeyer[55], J. Niermann[55,36], N. Nikiforou[36], V. Nikolaenko[37,a], I. Nikolic-Audit[127], K. Nikolopoulos[20], P. Nilsson[29], I. Ninca[48], H.R. Nindhito[56], G. Ninio[151], A. Nisati[75a], N. Nishu[2], R. Nisius[110], J-E. Nitschke[50], E.K. Nkadimeng[33g], T. Nobe[153], D.L. Noel[32], T. Nommensen[147], M.B. Norfolk[139], R.R.B. Norisam[96], B.J. Norman[34], M. Noury[35a], J. Novak[93], T. Novak[48], L. Novotny[132], R. Novotny[112], L. Nozka[122], K. Ntekas[159], N.M.J. Nunes De Moura Junior[83b], E. Nurse[96], J. Ocariz[127], A. Ochi[85], I. Ochoa[130a], S. Oerdek[48,u], J.T. Offermann[39], A. Ogrodnik[133], A. Oh[101], C.C. Ohm[144], H. Oide[84], R. Oishi[153], M.L. Ojeda[48], Y. Okumura[153], L.F. Oleiro Seabra[130a], S.A. Olivares Pino[137d], D. Oliveira Damazio[29], D. Oliveira Goncalves[83a], J.L. Oliver[159], Ö.O. Öncel[54], A.P. O'Neill[19], A. Onofre[130a,130e], P.U.E. Onyisi[11], M.J. Oreglia[39], G.E. Orellana[90], D. Orestano[77a,77b], N. Orlando[13], R.S. Orr[155], V. O'Shea[59], L.M. Osojnak[128], R. Ospanov[62a], G. Otero y Garzon[30], H. Otono[89], P.S. Ott[63a], G.J. Ottino[17a], M. Ouchrif[35d], J. Ouellette[29], F. Ould-Saada[125], M. Owen[59], R.E. Owen[134], K.Y. Oyulmaz[21a], V.E. Ozcan[21a], F. Ozturk[87], N. Ozturk[8], S. Ozturk[82], H.A. Pacey[126], A. Pacheco Pages[13], C. Padilla Aranda[13], G. Padovano[75a,75b], S. Pagan Griso[17a], G. Palacino[68], A. Palazzo[70a,70b], J. Pan[172], T. Pan[64a], D.K. Panchal[11], C.E. Pandini[114], J.G. Panduro Vazquez[95], H.D. Pandya[1], H. Pang[14b], P. Pani[48], G. Panizzo[69a,69c], L. Paolozzi[56], C. Papadatos[108], S. Parajuli[162], A. Paramonov[6], C. Paraskevopoulos[10], D. Paredes Hernandez[64b], K.R. Park[41], T.H. Park[155], M.A. Parker[32], F. Parodi[57b,57a], E.W. Parrish[115], V.A. Parrish[52], J.A. Parsons[41], U. Parzefall[54], B. Pascual Dias[108], L. Pascual Dominguez[151], E. Pasqualucci[75a], S. Passaggio[57b], F. Pastore[95], P. Pasuwan[47a,47b], P. Patel[87], U.M. Patel[51], J.R. Pater[101], T. Pauly[36], J. Pearkes[143], M. Pedersen[125], R. Pedro[130a], S.V. Peleganchuk[37], O. Penc[36], E.A. Pender[52], K.E. Penski[109], M. Penzin[37], B.S. Peralva[83d], A.P. Pereira Peixoto[60], L. Pereira Sanchez[47a,47b], D.V. Perepelitsa[29,aj], E. Perez Codina[156a], M. Perganti[10], L. Perini[71a,71b,*], H. Pernegger[36], O. Perrin[40], K. Peters[48], R.F.Y. Peters[101], B.A. Petersen[36], T.C. Petersen[42], E. Petit[102], V. Petousis[132], C. Petridou[152,e], A. Petrukhin[141], M. Pettee[17a], N.E. Pettersson[36], A. Petukhov[37], K. Petukhova[133], R. Pezoa[137f], L. Pezzotti[36], G. Pezzullo[172], T.M. Pham[170], T. Pham[105], P.W. Phillips[134], G. Piacquadio[145], E. Pianori[17a], F. Piazza[123], R. Piegaia[30], D. Pietreanu[27b], A.D. Pilkington[101], M. Pinamonti[69a,69c], J.L. Pinfold[2], B.C. Pinheiro Pereira[130a], A.E. Pinto Pinoargote[100,135], L. Pintucci[69a,69c], K.M. Piper[146], A. Pirttikoski[56], D.A. Pizzi[34], L. Pizzimento[64b], A. Pizzini[114], M.-A. Pleier[29],

JHEP05(2024)263

V. Plesanovs[54], V. Pleskot[133], E. Plotnikova[38], G. Poddar[4], R. Poettgen[98], L. Poggioli[127], I. Pokharel[55], S. Polacek[133], G. Polesello[73a], A. Poley[142,156a], R. Polifka[132], A. Polini[23b], C.S. Pollard[167], Z.B. Pollock[119], V. Polychronakos[29], E. Pompa Pacchi[75a,75b], D. Ponomarenko[113], L. Pontecorvo[36], S. Popa[27a], G.A. Popeneciu[27d], A. Poreba[36], D.M. Portillo Quintero[156a], S. Pospisil[132], M.A. Postill[139], P. Postolache[27c], K. Potamianos[167], P.A. Potepa[86a], I.N. Potrap[38], C.J. Potter[32], H. Potti[1], T. Poulsen[48], J. Poveda[163], M.E. Pozo Astigarraga[36], A. Prades Ibanez[163], J. Pretel[54], D. Price[101], M. Primavera[70a], M.A. Principe Martin[99], R. Privara[122], T. Procter[59], M.L. Proffitt[138], N. Proklova[128], K. Prokofiev[64c], G. Proto[110], S. Protopopescu[29], J. Proudfoot[6], M. Przybycien[86a], W.W. Przygoda[86b], A. Psallidas[46], J.E. Puddefoot[139], D. Pudzha[37], D. Pyatiizbyantseva[37], J. Qian[106], D. Qichen[101], Y. Qin[101], T. Qiu[52], A. Quadt[55], M. Queitsch-Maitland[101], G. Quetant[56], R.P. Quinn[164], G. Rabanal Bolanos[61], D. Rafanoharana[54], F. Ragusa[71a,71b], J.L. Rainbolt[39], J.A. Raine[56], S. Rajagopalan[29], E. Ramakoti[37], I.A. Ramirez-Berend[34], K. Ran[48,14e], N.P. Rapheeha[33g], H. Rasheed[27b], V. Raskina[127], D.F. Rassloff[63a], A. Rastogi[17a], S. Rave[100], B. Ravina[55], I. Ravinovich[169], M. Raymond[36], A.L. Read[125], N.P. Readioff[139], D.M. Rebuzzi[73a,73b], G. Redlinger[29], A.S. Reed[110], K. Reeves[26], J.A. Reidelsturz[171], D. Reikher[151], A. Rej[49], C. Rembser[36], A. Renardi[48], M. Renda[27b], M.B. Rendel[110], F. Renner[48], A.G. Rennie[159], A.L. Rescia[48], S. Resconi[71a], M. Ressegotti[57b,57a], S. Rettie[36], J.G. Reyes Rivera[107], E. Reynolds[17a], O.L. Rezanova[37], P. Reznicek[133], N. Ribaric[91], E. Ricci[78a,78b], R. Richter[110], S. Richter[47a,47b], E. Richter-Was[86b], M. Ridel[127], S. Ridouani[35d], P. Rieck[117], P. Riedler[36], E.M. Riefel[47a,47b], J.O. Rieger[114], M. Rijssenbeek[145], A. Rimoldi[73a,73b], M. Rimoldi[36], L. Rinaldi[23b,23a], T.T. Rinn[29], M.P. Rinnagel[109], G. Ripellino[161], I. Riu[13], P. Rivadeneira[48], J.C. Rivera Vergara[165], F. Rizatdinova[121], E. Rizvi[94], B.A. Roberts[167], B.R. Roberts[17a], S.H. Robertson[104,x], D. Robinson[32], C.M. Robles Gajardo[137f], M. Robles Manzano[100], A. Robson[59], A. Rocchi[76a,76b], C. Roda[74a,74b], S. Rodriguez Bosca[63a], Y. Rodriguez Garcia[22a], A. Rodriguez Rodriguez[54], A.M. Rodríguez Vera[156b], S. Roe[36], J.T. Roemer[159], A.R. Roepe-Gier[136], J. Roggel[171], O. Røhne[125], R.A. Rojas[103], C.P.A. Roland[127], J. Roloff[29], A. Romaniouk[37], E. Romano[73a,73b], M. Romano[23b], A.C. Romero Hernandez[162], N. Rompotis[92], L. Roos[127], S. Rosati[75a], B.J. Rosser[39], E. Rossi[126], E. Rossi[72a,72b], L.P. Rossi[57b], L. Rossini[54], R. Rosten[119], M. Rotaru[27b], B. Rottler[54], C. Rougier[102,ab], D. Rousseau[66], D. Rousso[32], A. Roy[162], S. Roy-Garand[155], A. Rozanov[102], Z.M.A. Rozario[59], Y. Rozen[150], X. Ruan[33g], A. Rubio Jimenez[163], A.J. Ruby[92], V.H. Ruelas Rivera[18], T.A. Ruggeri[1], A. Ruggiero[126], A. Ruiz-Martinez[163], A. Rummler[36], Z. Rurikova[54], N.A. Rusakovich[38], H.L. Russell[165], G. Russo[75a,75b], J.P. Rutherfoord[7], S. Rutherford Colmenares[32], K. Rybacki[91], M. Rybar[133], E.B. Rye[125], A. Ryzhov[44], J.A. Sabater Iglesias[56], P. Sabatini[163], H.F-W. Sadrozinski[136], F. Safai Tehrani[75a], B. Safarzadeh Samani[134], M. Safdari[143], S. Saha[165], M. Sahinsoy[110], A. Saibel[163], M. Saimpert[135], M. Saito[153], T. Saito[153], D. Salamani[36], A. Salnikov[143], J. Salt[163], A. Salvador Salas[151], D. Salvatore[43b,43a], F. Salvatore[146], A. Salzburger[36], D. Sammel[54], D. Sampsonidis[152,e], D. Sampsonidou[123], J. Sánchez[163], A. Sanchez Pineda[4], V. Sanchez Sebastian[163], H. Sandaker[125], C.O. Sander[48], J.A. Sandesara[103], M. Sandhoff[171], C. Sandoval[22b],

JHEP05(2024)263

D.P.C. Sankey[134], T. Sano[88], A. Sansoni[53], L. Santi[75a,75b], C. Santoni[40], H. Santos[130a,130b], A. Santra[169], K.A. Saoucha[160], J.G. Saraiva[130a,130d], J. Sardain[7], O. Sasaki[84], K. Sato[157], C. Sauer[63b], F. Sauerburger[54], E. Sauvan[4], P. Savard[155,ag], R. Sawada[153], C. Sawyer[134], L. Sawyer[97], I. Sayago Galvan[163], C. Sbarra[23b], A. Sbrizzi[23b,23a], T. Scanlon[96], J. Schaarschmidt[138], U. Schäfer[100], A.C. Schaffer[66,44], D. Schaile[109], R.D. Schamberger[145], C. Scharf[18], M.M. Schefer[19], V.A. Schegelsky[37], D. Scheirich[133], F. Schenck[18], M. Schernau[159], C. Scheulen[55], C. Schiavi[57b,57a], E.J. Schioppa[70a,70b], M. Schioppa[43b,43a], B. Schlag[143,n], K.E. Schleicher[54], S. Schlenker[36], J. Schmeing[171], M.A. Schmidt[171], K. Schmieden[100], C. Schmitt[100], N. Schmitt[100], S. Schmitt[48], L. Schoeffel[135], A. Schoening[63b], P.G. Scholer[54], E. Schopf[126], M. Schott[100], J. Schovancova[36], S. Schramm[56], F. Schroeder[171], T. Schroer[56], H-C. Schultz-Coulon[63a], M. Schumacher[54], B.A. Schumm[136], Ph. Schune[135], A.J. Schuy[138], H.R. Schwartz[136], A. Schwartzman[143], T.A. Schwarz[106], Ph. Schwemling[135], R. Schwienhorst[107], A. Sciandra[136], G. Sciolla[26], F. Scuri[74a], C.D. Sebastiani[92], K. Sedlaczek[115], P. Seema[18], S.C. Seidel[112], A. Seiden[136], B.D. Seidlitz[41], C. Seitz[48], J.M. Seixas[83b], G. Sekhniaidze[72a], L. Selem[60], N. Semprini-Cesari[23b,23a], D. Sengupta[56], V. Senthilkumar[163], L. Serin[66], L. Serkin[69a,69b], M. Sessa[76a,76b], H. Severini[120], F. Sforza[57b,57a], A. Sfyrla[56], E. Shabalina[55], R. Shaheen[144], J.D. Shahinian[128], D. Shaked Renous[169], L.Y. Shan[14a], M. Shapiro[17a], A. Sharma[36], A.S. Sharma[164], P. Sharma[80], S. Sharma[48], P.B. Shatalov[37], K. Shaw[146], S.M. Shaw[101], A. Shcherbakova[37], Q. Shen[62c,5], D.J. Sheppard[142], P. Sherwood[96], L. Shi[96], X. Shi[14a], C.O. Shimmin[172], J.D. Shinner[95], I.P.J. Shipsey[126], S. Shirabe[56,h], M. Shiyakova[38,v], J. Shlomi[169], M.J. Shochet[39], J. Shojaii[105], D.R. Shope[125], B. Shrestha[120], S. Shrestha[119,ak], E.M. Shrif[33g], M.J. Shroff[165], P. Sicho[131], A.M. Sickles[162], E. Sideras Haddad[33g], A. Sidoti[23b], F. Siegert[50], Dj. Sijacki[15], F. Sili[90], J.M. Silva[20], M.V. Silva Oliveira[29], S.B. Silverstein[47a], S. Simion[66], R. Simoniello[36], E.L. Simpson[59], H. Simpson[146], L.R. Simpson[106], N.D. Simpson[98], S. Simsek[82], S. Sindhu[55], P. Sinervo[155], S. Singh[155], S. Sinha[48], S. Sinha[101], M. Sioli[23b,23a], I. Siral[36], E. Sitnikova[48], S.Yu. Sivoklokov[37,*], J. Sjölin[47a,47b], A. Skaf[55], E. Skorda[20], P. Skubic[120], M. Slawinska[87], V. Smakhtin[169], B.H. Smart[134], S.Yu. Smirnov[37], Y. Smirnov[37], L.N. Smirnova[37,a], O. Smirnova[98], A.C. Smith[41], E.A. Smith[39], H.A. Smith[126], J.L. Smith[92], R. Smith[143], M. Smizanska[91], K. Smolek[132], A.A. Snesarev[37], S.R. Snider[155], H.L. Snoek[114], S. Snyder[29], R. Sobie[165,x], A. Soffer[151], C.A. Solans Sanchez[36], E.Yu. Soldatov[37], U. Soldevila[163], A.A. Solodkov[37], S. Solomon[26], A. Soloshenko[38], K. Solovieva[54], O.V. Solovyanov[40], V. Solovyev[37], P. Sommer[36], A. Sonay[13], W.Y. Song[156b], J.M. Sonneveld[114], A. Sopczak[132], A.L. Sopio[96], F. Sopkova[28b], J.D. Sorenson[112], I.R. Sotarriva Alvarez[154], V. Sothilingam[63a], O.J. Soto Sandoval[137c,137b], S. Sottocornola[68], R. Soualah[160], Z. Soumaimi[35e], D. South[48], N. Soybelman[169], S. Spagnolo[70a,70b], M. Spalla[110], D. Sperlich[54], G. Spigo[36], S. Spinali[91], D.P. Spiteri[59], M. Spousta[133], E.J. Staats[34], A. Stabile[71a,71b], R. Stamen[63a], A. Stampekis[20], M. Standke[24], E. Stanecka[87], M.V. Stange[50], B. Stanislaus[17a], M.M. Stanitzki[48], B. Stapf[48], E.A. Starchenko[37], G.H. Stark[136], J. Stark[102,ab], P. Staroba[131], P. Starovoitov[63a], S. Stärz[104], R. Staszewski[87], G. Stavropoulos[46], J. Steentoft[161],



JHEP05(2024)263

P. Steinberg[29], B. Stelzer[142,156a], H.J. Stelzer[129], O. Stelzer-Chilton[156a], H. Stenzel[58], T.J. Stevenson[146], G.A. Stewart[36], J.R. Stewart[121], M.C. Stockton[36], G. Stoicea[27b], M. Stolarski[130a], S. Stonjek[110], A. Straessner[50], J. Strandberg[144], S. Strandberg[47a,47b], M. Stratmann[171], M. Strauss[120], T. Strebler[102], P. Strizenec[28b], R. Ströhmer[166], D.M. Strom[123], R. Stroynowski[44], A. Strubig[47a,47b], S.A. Stucci[29], B. Stugu[16], J. Stupak[120], N.A. Styles[48], D. Su[143], S. Su[62a], W. Su[62d], X. Su[62a,66], K. Sugizaki[153], V.V. Sulin[37], M.J. Sullivan[92], D.M.S. Sultan[78a,78b], L. Sultanaliyeva[37], S. Sultansoy[3b], T. Sumida[88], S. Sun[106], S. Sun[170], O. Sunneborn Gudnadottir[161], N. Sur[102], M.R. Sutton[146], H. Suzuki[157], M. Svatos[131], M. Swiatlowski[156a], T. Swirski[166], I. Sykora[28a], M. Sykora[133], T. Sykora[133], D. Ta[100], K. Tackmann[48,u], A. Taffard[159], R. Tafirout[156a], J.S. Tafoya Vargas[66], E.P. Takeva[52], Y. Takubo[84], M. Talby[102], A.A. Talyshev[37], K.C. Tam[64b], N.M. Tamir[151], A. Tanaka[153], J. Tanaka[153], R. Tanaka[66], M. Tanasini[57b,57a], Z. Tao[164], S. Tapia Araya[137f], S. Tapprogge[100], A. Tarek Abouelfadl Mohamed[107], S. Tarem[150], K. Tariq[14a], G. Tarna[102,27b], G.F. Tartarelli[71a], P. Tas[133], M. Tasevsky[131], E. Tassi[43b,43a], A.C. Tate[162], G. Tateno[153], Y. Tayalati[35e,w], G.N. Taylor[105], W. Taylor[156b], A.S. Tee[170], R. Teixeira De Lima[143], P. Teixeira-Dias[95], J.J. Teoh[155], K. Terashi[153], J. Terron[99], S. Terzo[13], M. Testa[53], R.J. Teuscher[155,x], A. Thaler[79], O. Theiner[56], N. Themistokleous[52], T. Theveneaux-Pelzer[102], O. Thielmann[171], D.W. Thomas[95], J.P. Thomas[20], E.A. Thompson[17a], P.D. Thompson[20], E. Thomson[128], Y. Tian[55], V. Tikhomirov[37,a], Yu.A. Tikhonov[37], S. Timoshenko[37], D. Timoshyn[133], E.X.L. Ting[1], P. Tipton[172], S.H. Tlou[33g], A. Tnourji[40], K. Todome[154], S. Todorova-Nova[133], S. Todt[50], M. Togawa[84], J. Tojo[89], S. Tokár[28a], K. Tokushuku[84], O. Toldaiev[68], R. Tombs[32], M. Tomoto[84,111], L. Tompkins[143,n], K.W. Topolnicki[86b], E. Torrence[123], H. Torres[102,ab], E. Torró Pastor[163], M. Toscani[30], C. Tosciri[39], M. Tost[11], D.R. Tovey[139], A. Traeet[16], I.S. Trandafir[27b], T. Trefzger[166], A. Tricoli[29], I.M. Trigger[156a], S. Trincaz-Duvoid[127], D.A. Trischuk[26], B. Trocmé[60], C. Troncon[71a], L. Truong[33c], M. Trzebinski[87], A. Trzupek[87], F. Tsai[145], M. Tsai[106], A. Tsiamis[152,e], P.V. Tsiareshka[37], S. Tsigaridas[156a], A. Tsirigotis[152,s], V. Tsiskaridze[155], E.G. Tskhadadze[149a], M. Tsopoulou[152,e], Y. Tsujikawa[88], I.I. Tsukerman[37], V. Tsulaia[17a], S. Tsuno[84], K. Tsuri[118], D. Tsybychev[145], Y. Tu[64b], A. Tudorache[27b], V. Tudorache[27b], A.N. Tuna[61], S. Turchikhin[57b,57a], I. Turk Cakir[3a], R. Turra[71a], T. Turtuvshin[38,y], P.M. Tuts[41], S. Tzamarias[152,e], P. Tzanis[10], E. Tzovara[100], F. Ukegawa[157], P.A. Ulloa Poblete[137c,137b], E.N. Umaka[29], G. Unal[36], M. Unal[11], A. Undrus[29], G. Unel[159], J. Urban[28b], P. Urquijo[105], P. Urrejola[137a], G. Usai[8], R. Ushioda[154], M. Usman[108], Z. Uysal[82], V. Vacek[132], B. Vachon[104], K.O.H. Vadla[125], T. Vafeiadis[36], A. Vaitkus[96], C. Valderanis[109], E. Valdes Santurio[47a,47b], M. Valente[156a], S. Valentinetti[23b,23a], A. Valero[163], E. Valiente Moreno[163], A. Vallier[102,ab], J.A. Valls Ferrer[163], D.R. Van Arneman[114], T.R. Van Daalen[138], A. Van Der Graaf[49], P. Van Gemmeren[6], M. Van Rijnbach[125,36], S. Van Stroud[96], I. Van Vulpen[114], M. Vanadia[76a,76b], W. Vandelli[36], M. Vandenbroucke[135], E.R. Vandewall[121], D. Vannicola[151], L. Vannoli[57b,57a], R. Vari[75a], E.W. Varnes[7], C. Varni[17b], T. Varol[148], D. Varouchas[66], L. Varriale[163], K.E. Varvell[147], M.E. Vasile[27b], L. Vaslin[84], G.A. Vasquez[165], A. Vasyukov[38], F. Vazeille[40], T. Vazquez Schroeder[36], J. Veatch[31],



JHEP05(2024)263

V. Vecchio[101], M.J. Veen[103], I. Veliscek[126], L.M. Veloce[155], F. Veloso[130a,130c], S. Veneziano[75a], A. Ventura[70a,70b], S. Ventura Gonzalez[135], A. Verbytskyi[110], M. Verducci[74a,74b], C. Vergis[24], M. Verissimo De Araujo[83b], W. Verkerke[114], J.C. Vermeulen[114], C. Vernieri[143], M. Vessella[103], M.C. Vetterli[142,ag], A. Vgenopoulos[152,e], N. Viaux Maira[137f], T. Vickey[139], O.E. Vickey Boeriu[139], G.H.A. Viehhauser[126], L. Vigani[63b], M. Villa[23b,23a], M. Villaplana Perez[163], E.M. Villhauer[52], E. Vilucchi[53], M.G. Vincter[34], G.S. Virdee[20], A. Vishwakarma[52], A. Visibile[114], C. Vittori[36], I. Vivarelli[146], E. Voevodina[110], F. Vogel[109], J.C. Voigt[50], P. Vokac[132], Yu. Volkotrub[86a], J. Von Ahnen[48], E. Von Toerne[24], B. Vormwald[36], V. Vorobel[133], K. Vorobev[37], M. Vos[163], K. Voss[141], J.H. Vossebeld[92], M. Vozak[114], L. Vozdecky[94], N. Vranjes[15], M. Vranjes Milosavljevic[15], M. Vreeswijk[114], N.K. Vu[62d,62c], R. Vuillermet[36], O. Vujinovic[100], I. Vukotic[39], S. Wada[157], C. Wagner[103], J.M. Wagner[17a], W. Wagner[171], S. Wahdan[171], H. Wahlberg[90], M. Wakida[111], J. Walder[134], R. Walker[109], W. Walkowiak[141], A. Wall[128], T. Wamorkar[6], A.Z. Wang[136], C. Wang[100], C. Wang[62c], H. Wang[17a], J. Wang[64a], R.-J. Wang[100], R. Wang[61], R. Wang[6], S.M. Wang[148], S. Wang[62b], T. Wang[62a], W.T. Wang[80], W. Wang[14a], X. Wang[14c], X. Wang[162], X. Wang[62c], Y. Wang[62d], Y. Wang[14c], Z. Wang[106], Z. Wang[62d,51,62c], Z. Wang[106], A. Warburton[104], R.J. Ward[20], N. Warrack[59], A.T. Watson[20], H. Watson[59], M.F. Watson[20], E. Watton[59,134], G. Watts[138], B.M. Waugh[96], C. Weber[29], H.A. Weber[18], M.S. Weber[19], S.M. Weber[63a], C. Wei[62a], Y. Wei[126], A.R. Weidberg[126], E.J. Weik[117], J. Weingarten[49], M. Weirich[100], C. Weiser[54], C.J. Wells[48], T. Wenaus[29], B. Wendland[49], T. Wengler[36], N.S. Wenke[110], N. Wermes[24], M. Wessels[63a], A.M. Wharton[91], A.S. White[61], A. White[8], M.J. White[1], D. Whiteson[159], L. Wickremasinghe[124], W. Wiedenmann[170], M. Wielers[134], C. Wiglesworth[42], D.J. Wilbern[120], H.G. Wilkens[36], D.M. Williams[41], H.H. Williams[128], S. Williams[32], S. Willocq[103], B.J. Wilson[101], P.J. Windischhofer[39], F.I. Winkel[30], F. Winklmeier[123], B.T. Winter[54], J.K. Winter[101], M. Wittgen[143], M. Wobisch[97], Z. Wolffs[114], J. Wollrath[159], M.W. Wolter[87], H. Wolters[130a,130c], A.F. Wongel[48], E.L. Woodward[41], S.D. Worm[48], B.K. Wosiek[87], K.W. Woźniak[87], S. Wozniewski[55], K. Wraight[59], C. Wu[20], J. Wu[14a,14e], M. Wu[64a], M. Wu[113], S.L. Wu[170], X. Wu[56], Y. Wu[62a], Z. Wu[135], J. Wuerzinger[110,ae], T.R. Wyatt[101], B.M. Wynne[52], S. Xella[42], L. Xia[14c], M. Xia[14b], J. Xiang[64c], M. Xie[62a], X. Xie[62a], S. Xin[14a,14e], A. Xiong[123], J. Xiong[17a], D. Xu[14a], H. Xu[62a], L. Xu[62a], R. Xu[128], T. Xu[106], Y. Xu[14b], Z. Xu[52], Z. Xu[14c], B. Yabsley[147], S. Yacoob[33a], Y. Yamaguchi[154], E. Yamashita[153], H. Yamauchi[157], T. Yamazaki[17a], Y. Yamazaki[85], J. Yan[62c], S. Yan[126], Z. Yan[25], H.J. Yang[62c,62d], H.T. Yang[62a], S. Yang[62a], T. Yang[64c], X. Yang[36], X. Yang[14a], Y. Yang[44], Y. Yang[62a], Z. Yang[62a], W-M. Yao[17a], Y.C. Yap[48], H. Ye[14c], H. Ye[55], J. Ye[14a], S. Ye[29], X. Ye[62a], Y. Yeh[96], I. Yeletskikh[38], B.K. Yeo[17b], M.R. Yexley[96], P. Yin[41], K. Yorita[168], S. Younas[27b], C.J.S. Young[36], C. Young[143], C. Yu[14a,14e,ai], Y. Yu[62a], M. Yuan[106], R. Yuan[62b], L. Yue[96], M. Zaazoua[62a], B. Zabinski[87], E. Zaid[52], Z.K. Zak[87], T. Zakareishvili[149b], N. Zakharchuk[34], S. Zambito[56], J.A. Zamora Saa[137d,137b], J. Zang[153], D. Zanzi[54], O. Zaplatilek[132], C. Zeitnitz[171], H. Zeng[14a], J.C. Zeng[162], D.T. Zenger Jr[26], O. Zenin[37], T. Ženiš[28a], S. Zenz[94], S. Zerradi[35a], D. Zerwas[66], M. Zhai[14a,14e], B. Zhang[14c],



JHEP05(2024)263

D.F. Zhang[139], J. Zhang[62b], J. Zhang[6], K. Zhang[14a,14e], L. Zhang[14c], P. Zhang[14a,14e], R. Zhang[170], S. Zhang[106], S. Zhang[44], T. Zhang[153], X. Zhang[62c], X. Zhang[62b], Y. Zhang[62c,5], Y. Zhang[96], Y. Zhang[14c], Z. Zhang[17a], Z. Zhang[66], H. Zhao[138], T. Zhao[62b], Y. Zhao[136], Z. Zhao[62a], A. Zhemchugov[38], J. Zheng[14c], K. Zheng[162], X. Zheng[62a], Z. Zheng[143], D. Zhong[162], B. Zhou[106], H. Zhou[7], N. Zhou[62c], Y. Zhou[14c], Y. Zhou[7], C.G. Zhu[62b], J. Zhu[106], Y. Zhu[62c], Y. Zhu[62a], X. Zhuang[14a], K. Zhukov[37], V. Zhulanov[37], N.I. Zimine[38], J. Zinsser[63b], M. Ziolkowski[141], L. Živković[15], A. Zoccoli[23b,23a], K. Zoch[61], T.G. Zorbas[139], O. Zormpa[46], W. Zou[41], L. Zwalinski[36]

[1] *Department of Physics, University of Adelaide, Adelaide; Australia*
[2] *Department of Physics, University of Alberta, Edmonton AB; Canada*
[3] [(a)] *Department of Physics, Ankara University, Ankara;* [(b)] *Division of Physics, TOBB University of Economics and Technology, Ankara; Türkiye*
[4] *LAPP, Université Savoie Mont Blanc, CNRS/IN2P3, Annecy; France*
[5] *APC, Université Paris Cité, CNRS/IN2P3, Paris; France*
[6] *High Energy Physics Division, Argonne National Laboratory, Argonne IL; United States of America*
[7] *Department of Physics, University of Arizona, Tucson AZ; United States of America*
[8] *Department of Physics, University of Texas at Arlington, Arlington TX; United States of America*
[9] *Physics Department, National and Kapodistrian University of Athens, Athens; Greece*
[10] *Physics Department, National Technical University of Athens, Zografou; Greece*
[11] *Department of Physics, University of Texas at Austin, Austin TX; United States of America*
[12] *Institute of Physics, Azerbaijan Academy of Sciences, Baku; Azerbaijan*
[13] *Institut de Física d'Altes Energies (IFAE), Barcelona Institute of Science and Technology, Barcelona; Spain*
[14] [(a)] *Institute of High Energy Physics, Chinese Academy of Sciences, Beijing;* [(b)] *Physics Department, Tsinghua University, Beijing;* [(c)] *Department of Physics, Nanjing University, Nanjing;* [(d)] *School of Science, Shenzhen Campus of Sun Yat-sen University;* [(e)] *University of Chinese Academy of Science (UCAS), Beijing; China*
[15] *Institute of Physics, University of Belgrade, Belgrade; Serbia*
[16] *Department for Physics and Technology, University of Bergen, Bergen; Norway*
[17] [(a)] *Physics Division, Lawrence Berkeley National Laboratory, Berkeley CA;* [(b)] *University of California, Berkeley CA; United States of America*
[18] *Institut für Physik, Humboldt Universität zu Berlin, Berlin; Germany*
[19] *Albert Einstein Center for Fundamental Physics and Laboratory for High Energy Physics, University of Bern, Bern; Switzerland*
[20] *School of Physics and Astronomy, University of Birmingham, Birmingham; United Kingdom*
[21] [(a)] *Department of Physics, Bogazici University, Istanbul;* [(b)] *Department of Physics Engineering, Gaziantep University, Gaziantep;* [(c)] *Department of Physics, Istanbul University, Istanbul; Türkiye*
[22] [(a)] *Facultad de Ciencias y Centro de Investigaciónes, Universidad Antonio Nariño, Bogotá;* [(b)] *Departamento de Física, Universidad Nacional de Colombia, Bogotá; Colombia*
[23] [(a)] *Dipartimento di Fisica e Astronomia A. Righi, Università di Bologna, Bologna;* [(b)] *INFN Sezione di Bologna; Italy*
[24] *Physikalisches Institut, Universität Bonn, Bonn; Germany*
[25] *Department of Physics, Boston University, Boston MA; United States of America*
[26] *Department of Physics, Brandeis University, Waltham MA; United States of America*
[27] [(a)] *Transilvania University of Brasov, Brasov;* [(b)] *Horia Hulubei National Institute of Physics and Nuclear Engineering, Bucharest;* [(c)] *Department of Physics, Alexandru Ioan Cuza University of Iasi, Iasi;* [(d)] *National Institute for Research and Development of Isotopic and Molecular Technologies, Physics Department, Cluj-Napoca;* [(e)] *National University of Science and Technology Politechnica, Bucharest;* [(f)] *West University in Timisoara, Timisoara;* [(g)] *Faculty of Physics, University of Bucharest, Bucharest; Romania*
[28] [(a)] *Faculty of Mathematics, Physics and Informatics, Comenius University, Bratislava;* [(b)] *Department of Subnuclear Physics, Institute of Experimental Physics of the Slovak Academy of Sciences, Kosice; Slovak Republic*

JHEP05(2024)263

[29] Physics Department, Brookhaven National Laboratory, Upton NY; United States of America
[30] Universidad de Buenos Aires, Facultad de Ciencias Exactas y Naturales, Departamento de Física, y CONICET, Instituto de Física de Buenos Aires (IFIBA), Buenos Aires; Argentina
[31] California State University, CA; United States of America
[32] Cavendish Laboratory, University of Cambridge, Cambridge; United Kingdom
[33] [(a)] Department of Physics, University of Cape Town, Cape Town;[(b)] iThemba Labs, Western Cape;[(c)] Department of Mechanical Engineering Science, University of Johannesburg, Johannesburg;[(d)] National Institute of Physics, University of the Philippines Diliman (Philippines);[(e)] University of South Africa, Department of Physics, Pretoria;[(f)] University of Zululand, KwaDlangezwa;[(g)] School of Physics, University of the Witwatersrand, Johannesburg; South Africa
[34] Department of Physics, Carleton University, Ottawa ON; Canada
[35] [(a)] Faculté des Sciences Ain Chock, Réseau Universitaire de Physique des Hautes Energies — Université Hassan II, Casablanca;[(b)] Faculté des Sciences, Université Ibn-Tofail, Kénitra;[(c)] Faculté des Sciences Semlalia, Université Cadi Ayyad, LPHEA-Marrakech;[(d)] LPMR, Faculté des Sciences, Université Mohamed Premier, Oujda;[(e)] Faculté des sciences, Université Mohammed V, Rabat;[(f)] Institute of Applied Physics, Mohammed VI Polytechnic University, Ben Guerir; Morocco
[36] CERN, Geneva; Switzerland
[37] Affiliated with an institute covered by a cooperation agreement with CERN
[38] Affiliated with an international laboratory covered by a cooperation agreement with CERN
[39] Enrico Fermi Institute, University of Chicago, Chicago IL; United States of America
[40] LPC, Université Clermont Auvergne, CNRS/IN2P3, Clermont-Ferrand; France
[41] Nevis Laboratory, Columbia University, Irvington NY; United States of America
[42] Niels Bohr Institute, University of Copenhagen, Copenhagen; Denmark
[43] [(a)] Dipartimento di Fisica, Università della Calabria, Rende;[(b)] INFN Gruppo Collegato di Cosenza, Laboratori Nazionali di Frascati; Italy
[44] Physics Department, Southern Methodist University, Dallas TX; United States of America
[45] Physics Department, University of Texas at Dallas, Richardson TX; United States of America
[46] National Centre for Scientific Research "Demokritos", Agia Paraskevi; Greece
[47] [(a)] Department of Physics, Stockholm University;[(b)] Oskar Klein Centre, Stockholm; Sweden
[48] Deutsches Elektronen-Synchrotron DESY, Hamburg and Zeuthen; Germany
[49] Fakultät Physik, Technische Universität Dortmund, Dortmund; Germany
[50] Institut für Kern- und Teilchenphysik, Technische Universität Dresden, Dresden; Germany
[51] Department of Physics, Duke University, Durham NC; United States of America
[52] SUPA — School of Physics and Astronomy, University of Edinburgh, Edinburgh; United Kingdom
[53] INFN e Laboratori Nazionali di Frascati, Frascati; Italy
[54] Physikalisches Institut, Albert-Ludwigs-Universität Freiburg, Freiburg; Germany
[55] II. Physikalisches Institut, Georg-August-Universität Göttingen, Göttingen; Germany
[56] Département de Physique Nucléaire et Corpusculaire, Université de Genève, Genève; Switzerland
[57] [(a)] Dipartimento di Fisica, Università di Genova, Genova;[(b)] INFN Sezione di Genova; Italy
[58] II. Physikalisches Institut, Justus-Liebig-Universität Giessen, Giessen; Germany
[59] SUPA — School of Physics and Astronomy, University of Glasgow, Glasgow; United Kingdom
[60] LPSC, Université Grenoble Alpes, CNRS/IN2P3, Grenoble INP, Grenoble; France
[61] Laboratory for Particle Physics and Cosmology, Harvard University, Cambridge MA; United States of America
[62] [(a)] Department of Modern Physics and State Key Laboratory of Particle Detection and Electronics, University of Science and Technology of China, Hefei;[(b)] Institute of Frontier and Interdisciplinary Science and Key Laboratory of Particle Physics and Particle Irradiation (MOE), Shandong University, Qingdao;[(c)] School of Physics and Astronomy, Shanghai Jiao Tong University, Key Laboratory for Particle Astrophysics and Cosmology (MOE), SKLPPC, Shanghai;[(d)] Tsung-Dao Lee Institute, Shanghai;[(e)] School of Physics and Microelectronics, Zhengzhou University; China
[63] [(a)] Kirchhoff-Institut für Physik, Ruprecht-Karls-Universität Heidelberg, Heidelberg;[(b)] Physikalisches Institut, Ruprecht-Karls-Universität Heidelberg, Heidelberg; Germany

JHEP05(2024)263

[64] [(a)] Department of Physics, Chinese University of Hong Kong, Shatin, N.T., Hong Kong;[(b)] Department of Physics, University of Hong Kong, Hong Kong;[(c)] Department of Physics and Institute for Advanced Study, Hong Kong University of Science and Technology, Clear Water Bay, Kowloon, Hong Kong; China
[65] Department of Physics, National Tsing Hua University, Hsinchu; Taiwan
[66] IJCLab, Université Paris-Saclay, CNRS/IN2P3, 91405, Orsay; France
[67] Centro Nacional de Microelectrónica (IMB-CNM-CSIC), Barcelona; Spain
[68] Department of Physics, Indiana University, Bloomington IN; United States of America
[69] [(a)] INFN Gruppo Collegato di Udine, Sezione di Trieste, Udine;[(b)] ICTP, Trieste;[(c)] Dipartimento Politecnico di Ingegneria e Architettura, Università di Udine, Udine; Italy
[70] [(a)] INFN Sezione di Lecce;[(b)] Dipartimento di Matematica e Fisica, Università del Salento, Lecce; Italy
[71] [(a)] INFN Sezione di Milano;[(b)] Dipartimento di Fisica, Università di Milano, Milano; Italy
[72] [(a)] INFN Sezione di Napoli;[(b)] Dipartimento di Fisica, Università di Napoli, Napoli; Italy
[73] [(a)] INFN Sezione di Pavia;[(b)] Dipartimento di Fisica, Università di Pavia, Pavia; Italy
[74] [(a)] INFN Sezione di Pisa;[(b)] Dipartimento di Fisica E. Fermi, Università di Pisa, Pisa; Italy
[75] [(a)] INFN Sezione di Roma;[(b)] Dipartimento di Fisica, Sapienza Università di Roma, Roma; Italy
[76] [(a)] INFN Sezione di Roma Tor Vergata;[(b)] Dipartimento di Fisica, Università di Roma Tor Vergata, Roma; Italy
[77] [(a)] INFN Sezione di Roma Tre;[(b)] Dipartimento di Matematica e Fisica, Università Roma Tre, Roma; Italy
[78] [(a)] INFN-TIFPA;[(b)] Università degli Studi di Trento, Trento; Italy
[79] Universität Innsbruck, Department of Astro and Particle Physics, Innsbruck; Austria
[80] University of Iowa, Iowa City IA; United States of America
[81] Department of Physics and Astronomy, Iowa State University, Ames IA; United States of America
[82] Istinye University, Sariyer, Istanbul; Türkiye
[83] [(a)] Departamento de Engenharia Elétrica, Universidade Federal de Juiz de Fora (UFJF), Juiz de Fora;[(b)] Universidade Federal do Rio De Janeiro COPPE/EE/IF, Rio de Janeiro;[(c)] Instituto de Física, Universidade de São Paulo, São Paulo;[(d)] Rio de Janeiro State University, Rio de Janeiro; Brazil
[84] KEK, High Energy Accelerator Research Organization, Tsukuba; Japan
[85] Graduate School of Science, Kobe University, Kobe; Japan
[86] [(a)] AGH University of Krakow, Faculty of Physics and Applied Computer Science, Krakow;[(b)] Marian Smoluchowski Institute of Physics, Jagiellonian University, Krakow; Poland
[87] Institute of Nuclear Physics Polish Academy of Sciences, Krakow; Poland
[88] Faculty of Science, Kyoto University, Kyoto; Japan
[89] Research Center for Advanced Particle Physics and Department of Physics, Kyushu University, Fukuoka; Japan
[90] Instituto de Física La Plata, Universidad Nacional de La Plata and CONICET, La Plata; Argentina
[91] Physics Department, Lancaster University, Lancaster; United Kingdom
[92] Oliver Lodge Laboratory, University of Liverpool, Liverpool; United Kingdom
[93] Department of Experimental Particle Physics, Jožef Stefan Institute and Department of Physics, University of Ljubljana, Ljubljana; Slovenia
[94] School of Physics and Astronomy, Queen Mary University of London, London; United Kingdom
[95] Department of Physics, Royal Holloway University of London, Egham; United Kingdom
[96] Department of Physics and Astronomy, University College London, London; United Kingdom
[97] Louisiana Tech University, Ruston LA; United States of America
[98] Fysiska institutionen, Lunds universitet, Lund; Sweden
[99] Departamento de Física Teorica C-15 and CIAFF, Universidad Autónoma de Madrid, Madrid; Spain
[100] Institut für Physik, Universität Mainz, Mainz; Germany
[101] School of Physics and Astronomy, University of Manchester, Manchester; United Kingdom
[102] CPPM, Aix-Marseille Université, CNRS/IN2P3, Marseille; France
[103] Department of Physics, University of Massachusetts, Amherst MA; United States of America
[104] Department of Physics, McGill University, Montreal QC; Canada
[105] School of Physics, University of Melbourne, Victoria; Australia
[106] Department of Physics, University of Michigan, Ann Arbor MI; United States of America
[107] Department of Physics and Astronomy, Michigan State University, East Lansing MI; United States of America

JHEP05(2024)263

[108] Group of Particle Physics, University of Montreal, Montreal QC; Canada
[109] Fakultät für Physik, Ludwig-Maximilians-Universität München, München; Germany
[110] Max-Planck-Institut für Physik (Werner-Heisenberg-Institut), München; Germany
[111] Graduate School of Science and Kobayashi-Maskawa Institute, Nagoya University, Nagoya; Japan
[112] Department of Physics and Astronomy, University of New Mexico, Albuquerque NM; United States of America
[113] Institute for Mathematics, Astrophysics and Particle Physics, Radboud University/Nikhef, Nijmegen; Netherlands
[114] Nikhef National Institute for Subatomic Physics and University of Amsterdam, Amsterdam; Netherlands
[115] Department of Physics, Northern Illinois University, DeKalb IL; United States of America
[116] [(a)] New York University Abu Dhabi, Abu Dhabi;[(b)] United Arab Emirates University, Al Ain; United Arab Emirates
[117] Department of Physics, New York University, New York NY; United States of America
[118] Ochanomizu University, Otsuka, Bunkyo-ku, Tokyo; Japan
[119] Ohio State University, Columbus OH; United States of America
[120] Homer L. Dodge Department of Physics and Astronomy, University of Oklahoma, Norman OK; United States of America
[121] Department of Physics, Oklahoma State University, Stillwater OK; United States of America
[122] Palacký University, Joint Laboratory of Optics, Olomouc; Czech Republic
[123] Institute for Fundamental Science, University of Oregon, Eugene, OR; United States of America
[124] Graduate School of Science, Osaka University, Osaka; Japan
[125] Department of Physics, University of Oslo, Oslo; Norway
[126] Department of Physics, Oxford University, Oxford; United Kingdom
[127] LPNHE, Sorbonne Université, Université Paris Cité, CNRS/IN2P3, Paris; France
[128] Department of Physics, University of Pennsylvania, Philadelphia PA; United States of America
[129] Department of Physics and Astronomy, University of Pittsburgh, Pittsburgh PA; United States of America
[130] [(a)] Laboratório de Instrumentação e Física Experimental de Partículas — LIP, Lisboa;[(b)] Departamento de Física, Faculdade de Ciências, Universidade de Lisboa, Lisboa;[(c)] Departamento de Física, Universidade de Coimbra, Coimbra;[(d)] Centro de Física Nuclear da Universidade de Lisboa, Lisboa;[(e)] Departamento de Física, Universidade do Minho, Braga;[(f)] Departamento de Física Teórica y del Cosmos, Universidad de Granada, Granada (Spain);[(g)] Departamento de Física, Instituto Superior Técnico, Universidade de Lisboa, Lisboa; Portugal
[131] Institute of Physics of the Czech Academy of Sciences, Prague; Czech Republic
[132] Czech Technical University in Prague, Prague; Czech Republic
[133] Charles University, Faculty of Mathematics and Physics, Prague; Czech Republic
[134] Particle Physics Department, Rutherford Appleton Laboratory, Didcot; United Kingdom
[135] IRFU, CEA, Université Paris-Saclay, Gif-sur-Yvette; France
[136] Santa Cruz Institute for Particle Physics, University of California Santa Cruz, Santa Cruz CA; United States of America
[137] [(a)] Departamento de Física, Pontificia Universidad Católica de Chile, Santiago;[(b)] Millennium Institute for Subatomic physics at high energy frontier (SAPHIR), Santiago;[(c)] Instituto de Investigación Multidisciplinario en Ciencia y Tecnología, y Departamento de Física, Universidad de La Serena;[(d)] Universidad Andres Bello, Department of Physics, Santiago;[(e)] Instituto de Alta Investigación, Universidad de Tarapacá, Arica;[(f)] Departamento de Física, Universidad Técnica Federico Santa María, Valparaíso; Chile
[138] Department of Physics, University of Washington, Seattle WA; United States of America
[139] Department of Physics and Astronomy, University of Sheffield, Sheffield; United Kingdom
[140] Department of Physics, Shinshu University, Nagano; Japan
[141] Department Physik, Universität Siegen, Siegen; Germany
[142] Department of Physics, Simon Fraser University, Burnaby BC; Canada
[143] SLAC National Accelerator Laboratory, Stanford CA; United States of America
[144] Department of Physics, Royal Institute of Technology, Stockholm; Sweden
[145] Departments of Physics and Astronomy, Stony Brook University, Stony Brook NY; United States of America

JHEP05(2024)263

[146] Department of Physics and Astronomy, University of Sussex, Brighton; United Kingdom
[147] School of Physics, University of Sydney, Sydney; Australia
[148] Institute of Physics, Academia Sinica, Taipei; Taiwan
[149] [(a)] E. Andronikashvili Institute of Physics, Iv. Javakhishvili Tbilisi State University, Tbilisi;[(b)] High Energy Physics Institute, Tbilisi State University, Tbilisi;[(c)] University of Georgia, Tbilisi; Georgia
[150] Department of Physics, Technion, Israel Institute of Technology, Haifa; Israel
[151] Raymond and Beverly Sackler School of Physics and Astronomy, Tel Aviv University, Tel Aviv; Israel
[152] Department of Physics, Aristotle University of Thessaloniki, Thessaloniki; Greece
[153] International Center for Elementary Particle Physics and Department of Physics, University of Tokyo, Tokyo; Japan
[154] Department of Physics, Tokyo Institute of Technology, Tokyo; Japan
[155] Department of Physics, University of Toronto, Toronto ON; Canada
[156] [(a)] TRIUMF, Vancouver BC;[(b)] Department of Physics and Astronomy, York University, Toronto ON; Canada
[157] Division of Physics and Tomonaga Center for the History of the Universe, Faculty of Pure and Applied Sciences, University of Tsukuba, Tsukuba; Japan
[158] Department of Physics and Astronomy, Tufts University, Medford MA; United States of America
[159] Department of Physics and Astronomy, University of California Irvine, Irvine CA; United States of America
[160] University of Sharjah, Sharjah; United Arab Emirates
[161] Department of Physics and Astronomy, University of Uppsala, Uppsala; Sweden
[162] Department of Physics, University of Illinois, Urbana IL; United States of America
[163] Instituto de Física Corpuscular (IFIC), Centro Mixto Universidad de Valencia — CSIC, Valencia; Spain
[164] Department of Physics, University of British Columbia, Vancouver BC; Canada
[165] Department of Physics and Astronomy, University of Victoria, Victoria BC; Canada
[166] Fakultät für Physik und Astronomie, Julius-Maximilians-Universität Würzburg, Würzburg; Germany
[167] Department of Physics, University of Warwick, Coventry; United Kingdom
[168] Waseda University, Tokyo; Japan
[169] Department of Particle Physics and Astrophysics, Weizmann Institute of Science, Rehovot; Israel
[170] Department of Physics, University of Wisconsin, Madison WI; United States of America
[171] Fakultät für Mathematik und Naturwissenschaften, Fachgruppe Physik, Bergische Universität Wuppertal, Wuppertal; Germany
[172] Department of Physics, Yale University, New Haven CT; United States of America

[a] Also Affiliated with an institute covered by a cooperation agreement with CERN
[b] Also at An-Najah National University, Nablus; Palestine
[c] Also at Borough of Manhattan Community College, City University of New York, New York NY; United States of America
[d] Also at Center for High Energy Physics, Peking University; China
[e] Also at Center for Interdisciplinary Research and Innovation (CIRI-AUTH), Thessaloniki; Greece
[f] Also at Centro Studi e Ricerche Enrico Fermi; Italy
[g] Also at CERN, Geneva; Switzerland
[h] Also at Département de Physique Nucléaire et Corpusculaire, Université de Genève, Genève; Switzerland
[i] Also at Departament de Fisica de la Universitat Autonoma de Barcelona, Barcelona; Spain
[j] Also at Department of Financial and Management Engineering, University of the Aegean, Chios; Greece
[k] Also at Department of Physics, Ben Gurion University of the Negev, Beer Sheva; Israel
[l] Also at Department of Physics, California State University, Sacramento; United States of America
[m] Also at Department of Physics, King's College London, London; United Kingdom
[n] Also at Department of Physics, Stanford University, Stanford CA; United States of America
[o] Also at Department of Physics, Stellenbosch University; South Africa
[p] Also at Department of Physics, University of Fribourg, Fribourg; Switzerland
[q] Also at Department of Physics, University of Thessaly; Greece
[r] Also at Department of Physics, Westmont College, Santa Barbara; United States of America
[s] Also at Hellenic Open University, Patras; Greece

JHEP05(2024)263

[t] Also at Institucio Catalana de Recerca i Estudis Avancats, ICREA, Barcelona; Spain
[u] Also at Institut für Experimentalphysik, Universität Hamburg, Hamburg; Germany
[v] Also at Institute for Nuclear Research and Nuclear Energy (INRNE) of the Bulgarian Academy of Sciences, Sofia; Bulgaria
[w] Also at Institute of Applied Physics, Mohammed VI Polytechnic University, Ben Guerir; Morocco
[x] Also at Institute of Particle Physics (IPP); Canada
[y] Also at Institute of Physics and Technology, Mongolian Academy of Sciences, Ulaanbaatar; Mongolia
[z] Also at Institute of Physics, Azerbaijan Academy of Sciences, Baku; Azerbaijan
[aa] Also at Institute of Theoretical Physics, Ilia State University, Tbilisi; Georgia
[ab] Also at L2IT, Université de Toulouse, CNRS/IN2P3, UPS, Toulouse; France
[ac] Also at Lawrence Livermore National Laboratory, Livermore; United States of America
[ad] Also at National Institute of Physics, University of the Philippines Diliman (Philippines); Philippines
[ae] Also at Technical University of Munich, Munich; Germany
[af] Also at The Collaborative Innovation Center of Quantum Matter (CICQM), Beijing; China
[ag] Also at TRIUMF, Vancouver BC; Canada
[ah] Also at Università di Napoli Parthenope, Napoli; Italy
[ai] Also at University of Chinese Academy of Sciences (UCAS), Beijing; China
[aj] Also at University of Colorado Boulder, Department of Physics, Colorado; United States of America
[ak] Also at Washington College, Chestertown, MD; United States of America
[al] Also at Yeditepe University, Physics Department, Istanbul; Türkiye
[*] Deceased

JHEP05(2024)263